
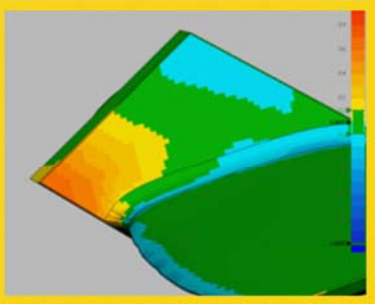


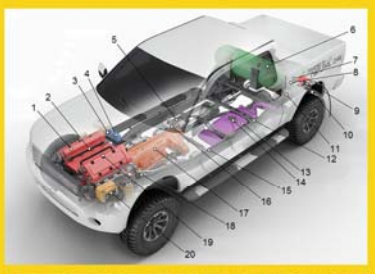

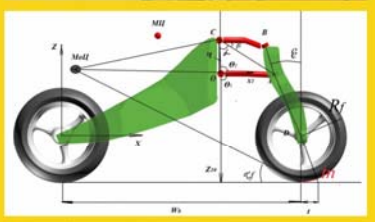


Technical University - Sofia
Faculty of Transport

SCIENTIFIC CONFERENCE
on Aeronautics, Automotive and
Railway Engineering and
Technologies

BulTrans-2019
PROCEEDINGS

Sponsored by:

Research & Development Sector

SIEMENS

АВТОМОТОР КОРПОРАЦИЯ

KNORR BREMSE

SOFIA AIRPORT

PEUGEOT София Франс Ауто

September 10-12, 2019
Sozopol, Bulgaria

http://bultrans.tu-sofia.bg

SCIENTIFIC COMMITTEE:

Chairman:
Prof. G. Mihov, Rector, TU-Sofia, Bulgaria

Members:
Prof. A. Ams, TU-Freiberg, Germany
Prof. A. Dimitrov, TU-Varna, Bulgaria
Prof. B. Belnikolovski, TU-Sofia, Bulgaria
Prof. D. Katsov, TU-Sofia, Branch Plovdiv, Bulgaria
Prof. D. Stamenković, University of Niš
Prof. D. Stoyanov, TU-Sofia, Bulgaria
Prof. E. Bratschitsch, University of Graz, Austria
Prof. F. Massouh, Arts et Metiers ParisTech, France
Prof. G. Descombes, CNAM, France
Prof. G. Kolarov, Hamburg University, Germany
Prof. G. Simic, Belgrade University, Serbia
Prof. H-H. Krause, UAS, Merseburg, Germany
Prof. I. Danilov, SSTU, Saratov, Russia
Prof. I. Kralov, TU-Sofia, Bulgaria
Prof. J. Majerčák, University of Žilina, Slovakia
Prof. K. Rotaru, Air Force Academy, Romania
Prof. K. Vesselinov, TU-Sofia, Bulgaria
Prof. L. Kunchev, TU-Sofia, Bulgaria
Prof. M. Karczewski, TU-Lodz, Poland
Prof. M. Sitarz, SUT-Katoviče, Poland
Prof. M. Svitek, TU-Prague, Czech Republic
Prof. N. Nenov, TU-Sofia, Bulgaria
Prof. P. Dimitrov, TU-Sofia, Bulgaria
Prof. P. Getsov, BAS, Bulgaria
Prof. R. Ivanov, University of Rouse, Bulgaria
Prof. R. Rusev, University of Rouse, Bulgaria
Prof. S. Medvedsky, University of Žilina, Slovakia
Prof. T. Evtimov, TU-Sofia, Bulgaria
Prof. V. Zhivkov, TU-Sofia, Bulgaria

ORGANIZING COMMITTEE:

Chairman:
Prof. M. Todorov, PhD, Dean, TU-Sofia, Bulgaria

Vice-Chairman:
Assoc. Prof. N. Nikolov, PhD

Members:
Prof. V. Stoilov, PhD
Assoc. Prof. Sv. Stoilova, DSc
Assoc. Prof. E. Dimitrov, PhD
Assoc. Prof. K. Velkov, PhD
Assoc. Prof. P. Punov, PhD
Assoc. Prof. P. Sinapov, PhD
Assoc. Prof. Ts. Stoyanov, PhD
Assoc. Prof. V. Tsonev, PhD

Secretariat:
Eng. Elena Pavlova, MSc
Assist. Prof. N. Pavlov, PhD
Assist. Prof. Ph. Michaylov

ПРОГРАМЕН КОМИТЕТ:

Председател:
чл.-кор. проф. Георги Михов, Ректор на ТУ-София

Членове:
проф. Алфонс Амс, TU-Фрайберг, Германия
проф. Ангел Димитров, ТУ-Варна
проф. Борис Белниколовски, ТУ-София
чл.-кор. проф. Венелин Живков, ТУ-София
проф. Георги Коларов, UAS-Хамбург, Германия
проф. Горан Симич, Университет Белград
проф. Димитър Кацов, ТУ-филиал Пловдив
проф. Димитър Стоянов, ТУ-София
проф. Душан Стаменкович, Университет в Ниш
проф. Емилия Брачич, UAS-Грац, Австрия
проф. Жорж Декомб, CNAM, Франция
проф. Иван Кралов, ТУ-София
проф. Игор Данилов, СГТУ, Саратов, Русия
проф. Йозеф Майерчак, UŽ-Жилина, Словакия
проф. Камен Веселинов, ТУ-София
проф. Константин Ротару, Академия на ВВС, Румъния
проф. Лило Кунчев, ТУ-София
проф. Марек Ситарж, SUT-Катовице, Полша
проф. Мачей Карчевски, ТУ-Лодз, Полша
проф. Мирослав Свитек, TU-Прага, Чехия
проф. Ненчо Ненов, ТУ-София
проф. Петър Гецов, ИКИ, БАН
проф. Петър Димитров, ТУ-София
проф. Росен Иванов, РУ-Русе
проф. Руси Русев, РУ-Русе
проф. Теодоси Евтимов, ТУ-София
проф. Фауаз Масу, Arts et Metiers ParisTech, Франция
проф. Х.-Х. Краузе, UAS-Мерзебург, Германия
проф. Щефан Медведски, UŽ-Жилина, Словакия

ОРГАНИЗАЦИОНЕН КОМИТЕТ:

Председател:
проф. д-р инж. Михаил Тодоров, Декан, ТУ-София

Зам.-председател:
доц. д-р инж. Николай Николов

Членове:
проф. д-р инж. Валери Стоилов
доц. дтн инж. Светла Стоилова
доц. д-р инж. Веселин Цонев
доц. д-р инж. Евгени Димитров
доц. д-р инж. Кирил Велков
доц. д-р инж. Петко Синапов
доц. д-р инж. Пламен Пунов
доц. д-р инж. Цветан Стоянов

Научни секретари:
маг. инж. Елена Павлова
гл. ас. д-р инж. Николай Павлов
ас. инж. Филип Михайлов

ТЕХНИЧЕСКИ УНИВЕРСИТЕТ - СОФИЯ
ФАКУЛТЕТ ПО ТРАНСПОРТА

НАУЧНА КОНФЕРЕНЦИЯ
С МЕЖДУНАРОДНО УЧАСТИЕ
по авиационна, автомобилна и железопътна техника и технологии

БулТранс-2019

СБОРНИК ДОКЛАДИ

10 - 12 септември 2019 г.
Морска почивна станция „Лазур“ в гр. Созопол

Редактор: доц. д-р инж. Николай Николов
Editor: Assoc. Prof. Nikolay Nikolov, PhD

Докладите в този сборник са публикувани след рецензиране от специалисти в съответната област.

The papers in this Proceedings are published after being reviewed by experts in the respective field.

ISSN 1313-955X

СЪДЪРЖАНИЕ / CONTENTS

ДОКЛАДИ, ПУБЛИКУВАНИ В / REPORTS PUBLISHED IN

IOP Conference Series: Materials Science and Engineering Volume 664 (2019)

https://iopscience.iop.org/issue/1757-899X/664/1

От секция: **Авиационна техника и технологии**
From section: **Aeronautics**

A. Kuzmin, Transonic flow hysteresis in divergent bent channels
DOI: https://doi.org/10.1088/1757-899X/664/1/012001

J. Hnidka and D. Rozehnal, Calculation of the maximum endurance of a small unmanned aerial vehicle in a hover
DOI: https://doi.org/10.1088/1757-899X/664/1/012002

O. A. Elsayed, Numerical study of a shock-wave boundary-layer interaction: compression ramp flow-fields
DOI: https://doi.org/10.1088/1757-899X/664/1/012003

K. Bouchaâla, M. F. Ghanameh, M. Faqir, M. Mada and E. Essadiqi, Prediction of the impact of friction's coefficient in cylindrical deep drawing for AA2090 Al-Li alloy using FEM and Taguchi approach
DOI: https://doi.org/10.1088/1757-899X/664/1/012004

D. T. Seyzinski, I. Georgiev, H. P. Panayotov and S. I. Penchev, Effective use of a helicopter with a Bambi bucket firefighting system in Bulgaria
DOI: https://doi.org/10.1088/1757-899X/664/1/012005

V. S. Serbezov, Assessment of the fuel efficiency of unmanned cargo aircraft, based on general aviation aircraft
DOI: https://doi.org/10.1088/1757-899X/664/1/012006

K. Georgiev and R. Nikolova, Noise sensitivity of a bio-inspired echolocation model
DOI: https://doi.org/10.1088/1757-899X/664/1/012007

От секция: **Автомобилна техника и технологии**
From section: **Automotive engineering**

Z. Dimitrova, Integration of the environomic energy services for mobility and household using electric vehicle with a range extender of solid oxide fuel cell
DOI: https://doi.org/10.1088/1757-899X/664/1/012008

Z. Dimitrova, Performance and economic analysis of an organic Rankine Cycle for hybrid electric vehicles
DOI: https://doi.org/10.1088/1757-899X/664/1/012009

От секция: **Динамика, якост и надеждност на транспортната техника**
From section: **Dynamics, Strength and Reliability of Vehicles**

От секция: **Двигатели с вътрешно горене**
From section: **Internal Combustion Engines**

От секция: **Железопътна техника и технологии**
From section: **Railway Engineering and Technologies**

От секция: **Мениджмънт и логистика в транспорта**
From section: **Transport Management and Logistics**

Effect of a vortex trapping cavity (VTC) on aerodynamic properties of a thick wind turbine airfoil

K Qaissi, O A Elsayed[1], M Faqir, E Essadiqi and M Fathi Ghanameh

International University of Rabat, School of aerospace engineering, LERMA Lab, Campus UIR Parc Technopolis, Rocade, Rabat-Sale, 11100 - Sala Al Jadida, Maroc

[1] E-mail: omer.almatbagi@uir.ac.ma

Abstract. Flow separates from the surface of an airfoil at high angles of attack when the boundary layer travels far enough against an adverse pressure gradient, the flow is then detached and appears in the form of vortices and eddies. For thick airfoils, the separation occurs at a relatively small angle of attack values. This is reflected on the amount of energy extracted by the wind turbine at the thick blade section. VTC was used to control and alleviate the effect flow separation. Trailing edge VTC effect on aerodynamic performance of NREL S835 wind turbines airfoil was investigated. Steady 2-D Navier-Stokes Equations with Roe-FDS flux type and a second order upwind flow discretization was used for flow simulation over NREL S835 airfoils, with and without cavity. Due to the cavity selected position immediate ahead of flow separation point a vortex was formed inside the cavity. However, the flow inside the cavity was characterized by a significant shedding downstream, which results in a drop-in lift and an increase in drag. In this paper, the results are reported in detail, compared and discussed.

1. Introduction

Boundary layer separation leads to an unsteady flow condition. The vortex formed then sheds downstream leaving space for another vortex to form and shed again in a periodic or chaotic cycle [1]. The unsteady vortex shedding results in a higher drag. To improve the flow, we speak of flow control.

Flow control is the act of introducing perturbations into the flow capable of changing the original flow development into an ideal [2]. Flow control devices were first introduced in the aviation field as a tool to improve the aerodynamic and environmental performance of the aircraft by drag reduction, noise reduction and lift enhancement among others. These flow control devices are being introduced and investigated on wind turbines with a focus on regulating the unsteady blade aerodynamics and vibrations.

Flow control devices are most commonly classified into passive and active based on their energy input. Passive flow control devices need no energy input but cannot be changed during the control process. Passive flow control devices include vortex generators, gurney's flap, bumps, cavity, etc. Meanwhile, the active flow control devices need an active actuator and an energy input. Active flow control devices include oscillations, flexible wall, suction, synthetic jet, etc. [2].

In aerodynamics, thin and streamlined airfoils are an answer to a better lift to drag ratio and hence, better performance and less perturbations. But with taking into considerations the design constraints of wind turbine blades, using thick airfoils can be beneficial structure wise. Aerodynamically, thick airfoils present a challenge considering that they are characterized by early flow separation even for a relatively small angles of attack.

Thick airfoil moving through a fluid experiences high drag. One way of controlling flow over thick airfoils is by using a VTC. A cavity is a properly shaped hole positioned along the span wise direction on the upper surface of the airfoil.

Rowley and Colonius and Murray [3] have investigated a rectangular cavities effect. Such cavity shapes haven't been previously considered or investigated on an airfoil. They focused on the method of modelling the flow. They were able to model he flow correctly, however the use of a rectangular cavity resulted in several vortices above the cavity. Lasagna et al [4], have shown that under certain flow conditions a circular vortex forms inside the cavity allowing for many investigations of a circular shaped cavity on an airfoil. The principle behind this flow control method is to create a kind of reservoir for the vortex, allowing for the recirculation region to be tamed under the dividing streamline. The flow, otherwise separated, is now forced to remain attached. One of the main issues encountered with using a cavity is how to maintain the vortex inside the cavity stable.

The idea was originally introduced somewhere in the last century, but can be tracked to 1961 with Ringleb [5]. However, the only proven successful implementations of the trapping vortex cavity for an aircraft are Kasper on the Kasper wing and the EKIP aircraft by L. Shchukin [6]. Kasper believed that the lift enhancement observed during experimental fly of his glider is due to the cavity but experimental tests aiming to verify Kasper's wing [7] showed the presence of vortex shedding and disapproved his high lift coefficient observation. For the EKIP aircraft, no publications are available to confirm its efficiency. For both cases, explanations of the difference between presented results versus the investigations tilted towards the disparity between real-life fly tests and wind tunnel experiments. Therefore, both the EKIP aircraft and Kasper's wing deserve to be quoted as attempts at verifying the efficiency of a VTC.

Researchers continued to investigate the effect of a circular vortex-trapping cavity by means of simulation and experiment. Some showed encouraging results in the field while others encouraged for more investigations of the position, shape and coupling the cavity with other active control devices. Olsman and Colonius [8] conducted simulation of the flow over a symmetrical airfoil with a cavity positioned near the leading edge at low Reynolds number and verified his results with an experimental one measured in a water tunnel. They found that the clean airfoil shows a laminar separation closer to half a chord line, hence the cavity is positioned prior to the separation. The flow of airfoil with cavity oscillates between the second shear layer mode and the first shear layer mode. These oscillations generate small vortices. Their results also reveal that at high angles of attack, the flow interacts with the cavity leading to smaller scale vortices and narrower wake compared to the airfoil without cavity. In the same year, Lasagna et al [4] investigated the effectiveness of a trapped vortex cell with and without the presence of suction. Different parameters had an influence on the quality of the flow, notably the range for the angle of the attack, Reynolds number and the suctions rate. Consequently, the cavity led to drag reduction only when the suction rate was high enough. They concluded that a circular cavity is ineffective in keeping the vortex trapped without the use of an active flow control tool in the form of a continuous suction. Donelli et. Al [1] numerically studied the effects of a cavity using different turbulence models. They declared that Prandlt-Bachelor model is efficient and quick for the study and design of a VTC. This model gives an accurate approximation of the flow velocity and pressure inside a vortex cavity. Using the previously mentioned model, the velocity contours show a trapped vortex under a separating layer. Experimentally, De Gregorio and Fraioli [9]; used particle image velocimetry to study the flow inside a VTC. They considered the effects of the flow velocity and the angle of attack for both airfoil cases with and without suction/injection. As a result of the experiment, they found that the cavity as a passive flow control tool is not enough to ensure a stable vortex inside the cavity. Moreover, the addition of a suction/injection system allows controlling the flow separation. More ambitious results showed flow reattachment for some specific blowing coefficient values. In the context, Mashud and Ferdous [10] measured the aerodynamics effects of a VTC on an airfoil at different angles and varying speeds, they showed relatively encouraging results. The separation point was delayed up to 8% chord length compared to the clean airfoil, which means that the cavity is able to control the flow separation and increase the lift. However, the vortex wasn't fully confined in the cavity with the presence

of shedding, indicating the needs for an active flow control. Experimentally, a PIV investigation of the flow behaviour of a VTC at an ultra-low-Reynolds number conducted by Shi et al [11] showed that the airfoil with a cavity had worse results compared to an airfoil without a cavity. They claim that, the vortex inside the cavity results in a reverse flow with a counter clockwise incoherent structure for all the investigated angles of attack.

More recently, Saeed et al [12] conducted simulations on a thick airfoil for four different turbulence models. They showed that the NRG k-ε is the best at predicting the flow behaviour. In addition, the simulation showed an increase both in lift and drag for the airfoil with the mid chord cavity compared to the reference Xfoil. The results were encouraging considering the Xfoil usually under predicts drag for low Reynolds numbers lower.

In the same context, a study of different passive flow control methods used to control stall in wind turbines by Chouldhry [13] showed encouraging results. It appears that at a lower angle of attack, the cavity can delay stall whereas for higher angles the intensity of the vortex is left unchanged.

The above-mentioned research survey re-emphasizes the importance of designing a low cost, efficient and practically applicable flow control approach. Various conclusions and results reported encourage a further numerical and experimental detailed research in this area. NREL airfoil family is known for being most adequate for wind turbine applications as they provide significant increases in an energy production [14]. Their high aerodynamics performance requires resolving or at least alleviating their flow separation problem occurring at a relatively low angles attack. VTC as a flow control approach was selected to improve the aerodynamic performance of NREL S835 airfoil used in a wind turbine mid-section blade. Feasibility, practical applicability and the relatively low operational cost made the VTC an attracting solution. In the present research a numerical simulation of NREL S835 airfoil with and without trailing edge VTC were investigated and detailed results were reported.

2. Numerical Setup

Simulations were carried-out over NREL S835 airfoil geometry with and without cavity. Inside the cavity, the streamlines are circular and closed; hence a circular shape for the cavity has been chosen with a sharp and chamfering sides at the leading and rear sides respectively.

Incompressible 2-D, Navier-Stokes equations were solved to simulate the flow. The flow governing equations for conservation of mass and momentum are cited below:

$$\frac{\partial \rho}{\partial t} + \nabla (\rho \vec{v}) = 0; \tag{1}$$

$$\frac{\partial}{\partial t}(\rho \vec{v}) + \nabla (\rho \vec{v} \vec{v}) = -\nabla p + \nabla (\bar{\bar{\tau}}) + \vec{F}, \tag{2}$$

where p, $\bar{\bar{\tau}}$, and $\vec{F}$ are the static pressure, the stress tensor, the gravitational body force and external body forces, respectively. The stress tensor $\bar{\bar{\tau}}$ can be written as:

$$\bar{\bar{\tau}} = \mu [(\nabla \vec{v} + \nabla \vec{v}^T) - \frac{2}{3} \nabla \vec{v} I], \tag{3}$$

where μ and I are the molecular viscosity and the unit tensor, respectively. Volume dilation is presented in the right-hand side of the equation. The Spalart-Allmaras turbulence model is effective for flows at a low Reynolds number and shows good results for boundary layers subject to adverse pressure gradients. In Spalart-Allmaras model, the viscous stress tensor τ_{ij} is related to the Reynolds stresses through the eddy viscosity μ_t, effectively modelling the momentum transfer by turbulent eddies, written as

$$\tau_{ij} = 2(\mu_l + \mu_t)(s_{ij} - 1/3\ \partial u_k/\partial x_k\ \delta_{ij}), \tag{4}$$

where δ_{ij} is the Kronecker delta and s_{ij} is the strain rate tensor defined as:

$$s_{ij} = ½(\partial u_i/\partial x_j + \partial u_j/\partial x_i). \tag{5}$$

The SA model utilizes one equation to solve the transport variable, $\tilde{\nu}$ is identical to the turbulent kinematic viscosity except in the near wall region. The transport equation for $\tilde{\nu}$ is:

$$\frac{\partial}{\partial t}(\rho\tilde{v}) + \frac{\partial}{\partial x_i}(\rho\tilde{v}u_i) = G_v + \frac{1}{\sigma\tilde{v}}[\frac{\partial}{\partial x_j}\left\{(\mu + \rho\tilde{v})\frac{\partial\tilde{v}}{\partial x_j}\right\} + C_{b2}\rho(\frac{\partial\check{v}}{\partial x_j})^2] - Y_v + S_{\tilde{v}}, \quad (6)$$

where G_v is the production of turbulent viscosity, and Y_v is the destruction of turbulent viscosity that occurs in the near-wall region due to wall blocking and viscous damping, $\sigma_{\tilde{v}}$ and C_{b2} are the constants and v is the molecular kinematic viscosity. $S_{\tilde{v}}$ is a user-defined source term.

NREL S835 airfoil for the mid-section of the blade with corresponding twist angles between 5° and 10° will be investigated in this research work. The NREL S835 airfoil without and with cavity is shown in figure 1 (a) and (b). The cavity has a radius to chord ratio of R/c = 0.035, As the flow separates near the trailing edge for low angles of incidence, the circular cavity centre was positioned at 60% in the chord wise direction.

Flow over NREL S835 airfoil reveals a laminar separation at 54% chord wise distance for a relatively low angles of attack. The design of the cavity with a sharp side and chamfered side was chosen according to the classical Kirchhoff hodograph-plane method [8]. While considering that both the density ρ and the dynamics viscosity μ are constant, the flow is governed by the ratio δ/L between the incoming boundary layer thickness δ and the cavity opening L. For lower Reynolds number $R_{e\delta}$, we have $\delta/L = 0.04$.

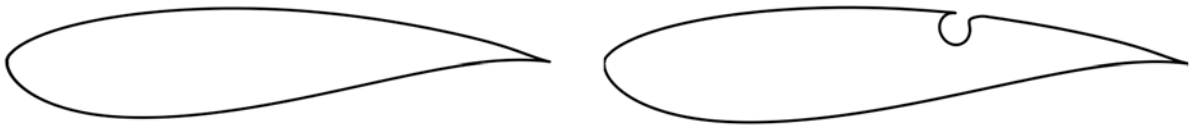

(a) (b)

Figure 1. Geometry of S835 airfoil (a) without cavity and (b) with the cavity.

Grids were generated around the airfoil using a C-mesh type domain as shown in figure 2 (a) and (b) for both airfoil cases. The domain length and width was 12.5 times the chord of the NREL S835 airfoil. The choice of the domain dimensions was such that the wall effects are negligible. Proper respective boundary conditions were implemented at the inlet, far field and airfoil.

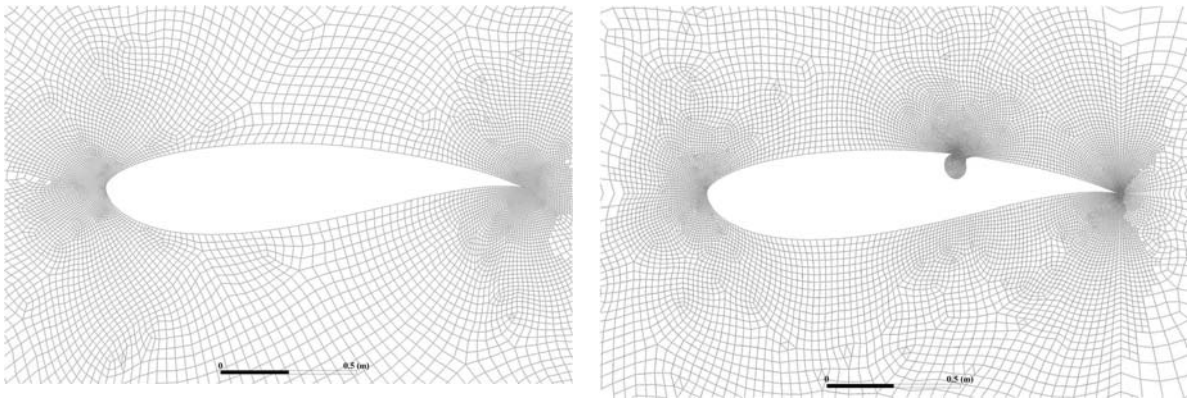

(a) (b)

Figure 2. (a) S835 clean airfoil mesh, (b) S835 airfoil with cavity mesh.

For the meshing, the NREL S835 airfoil was split into four blocks. Upon generation, the mesh was finer near the airfoil to enhance boundary layer flow resolution and coarser towards the edges of the domain. The convergence criteria are chosen to be 1.0e–6 for all simulations. The mesh for the NREL S835 airfoil without and with cavity consisted of 24035 and 37147 nodes respectively. To ensure that the results are grid independent grid resolution was varied between 5 and 7 and the domain length and width were varied between 10.5 chord 12.5 chord length respectively. With the variation of the grid resolution and the domain size, the results converged and were essentially grid independent.

3. Results

By comparing the obtained results collected from simulation of a clean NACA0015 airfoil on ANSYS Fluent to reference values of the same NACA0015 airfoil obtained by an experimental procedure lead by Sahin and Acir [14], we are able to validate the numerical solution procedure. We simulated a clean NACA0015 airfoil in a C-mesh using a laminar mode at a constant speed of 10 m/s for all angles. A comparison of the lift coefficient, for the clean NACA0015, obtained from literature's experimental investigation and from our simulation of the same model is presented in figure 3. We compared six angles of attack alpha ranging from 6 to 16 with a step of 2.

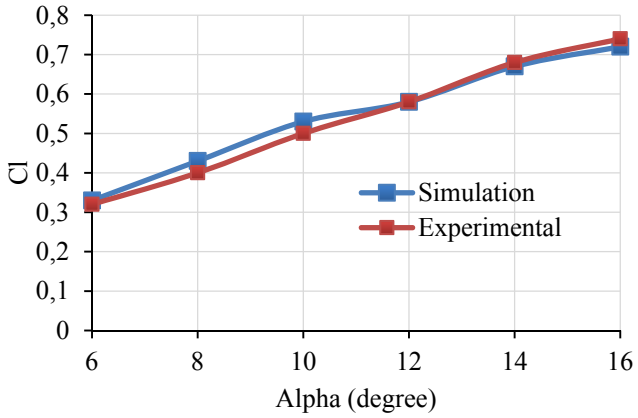

Figure 3. Lift coefficient.

Table 1 shows the solution that the error between the simulation we conducted and the experimental values obtained from literature [14] is considered minor and can be very small. The values are close, which validates our model.

Table 1. Lift coefficient comparison between our simulation and literature reference.

Alpha, deg	Cl for Clean airfoil literature reference	Cl for Clean airfoil simulation	Error, %
6	0.32	0.33	3.12
8	0.40	0.43	7.50
10	0.50	0.53	6.00
12	0.58	0.58	0.00
14	0.68	0.67	1.47
16	0.74	0.72	2.70

Over all, when compared to literature [14], we notice that the values of the lift coefficient and the drag coefficient of the clean NREL S835 airfoil are closely predicted and can be then used as a reference to validate our simulation on a clean NREL S835 airfoil.

The influence of the VTC on the aerodynamic properties of the flow has been investigated for a specified velocity and different angles of attack ranging from 4° to 12°. For all angles of attack, flow separation was observed, which occurs around 50% downstream in the chord wise direction. It moves towards the leading edge as the angle of attack increases and doesn't re-attach afterwards. For angles higher than 10^{o}, separation occurred so far upstream that the effect of the cavity became negligible compared to the airfoil without a cavity.

The clean NREL S835 airfoil pressure contours and pressure coefficient versus distance are shown in figures 4-6, for angle of attack of 5°. The lift created by the airfoil with cavity is expected to be higher than the lift of the clean airfoil for angles lower than 10^{o}, which can be observed from the areas enclosed by the pressure coefficient graphs. For the angles of attack higher that 10°, the influence of the cavity on the lift is negligible small.

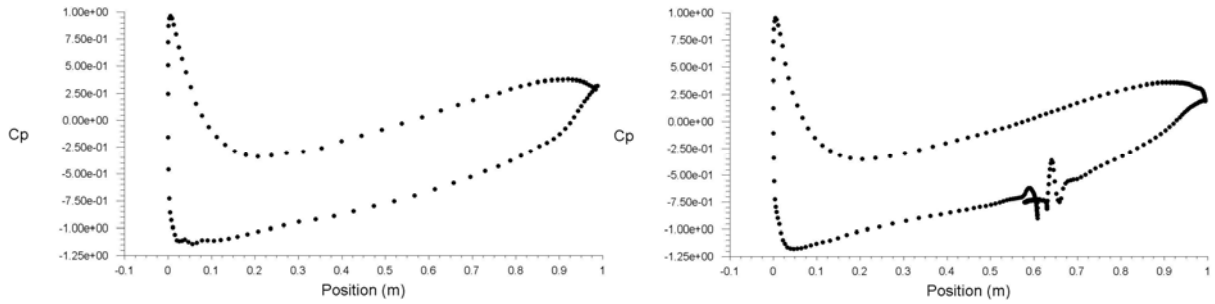

(a) (b)

Figure 4. Pressure coefficient versus distance over (a) clean airfoil (b) airfoil with VTC for angle of attack 5°.

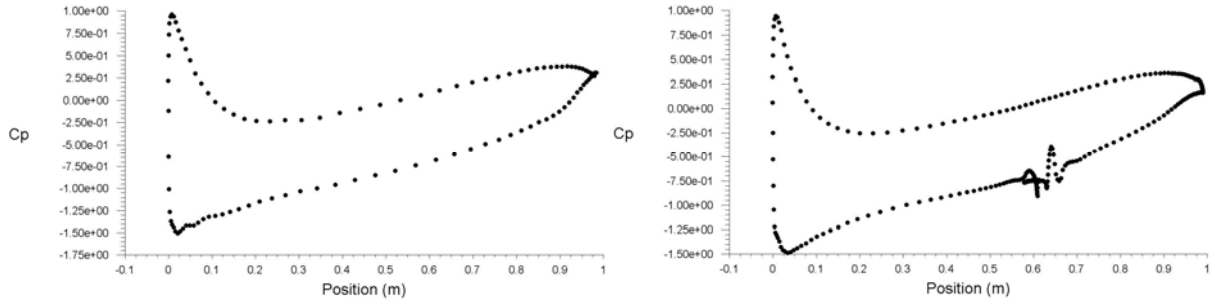

(a) (b)

Figure 5. Pressure coefficient versus distance over (a) clean airfoil (b) airfoil with VTC for angle of attack 8°.

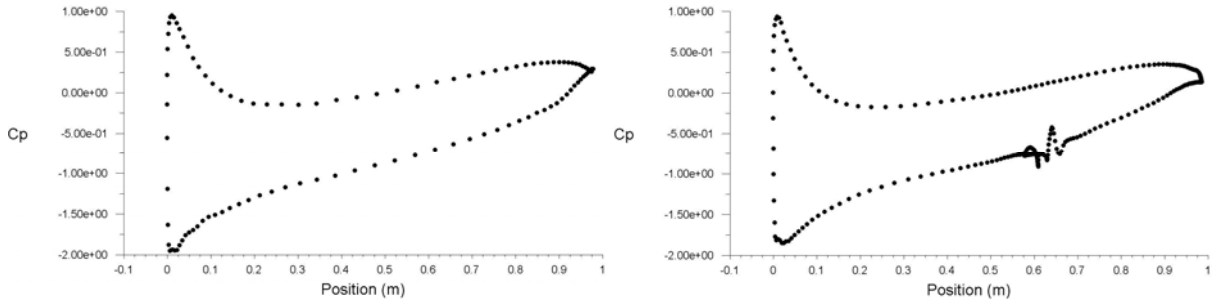

(a) (b)

Figure 6. Pressure coefficient versus distance over (a) clean airfoil (b) airfoil with VTC for angle of attack 10°.

Pressure contours and pathlines are shown here below in figures 7-9, for angle of attack of 6°. The cavity clearly contains a vortex and acts as a reservoir for it. The pathlines show that the vortex is actually circular with an inclination in the layers closer to the chamfered corner of the cavity. We observe a clear separating layer between the cavity and the outside stream. However, from the pressure contours, the cavity isn't able to fully contain the vortex inside with the clear appearance of shedding at the chamfered side of the cavity. The shedding becomes more significant as the angles of attack become higher.

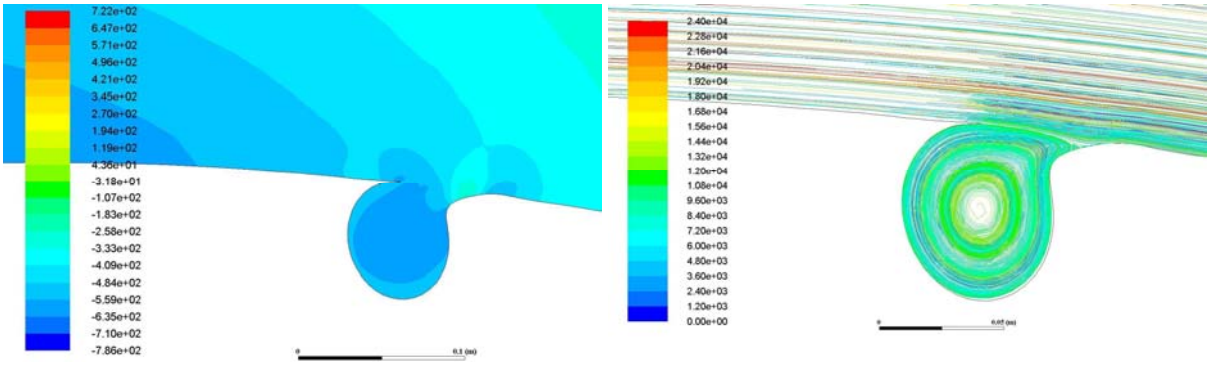

(a) (b)

Figure 7. (a) Pressure contours and (b) Pathlines inside the cavity for angle of attack 5°.

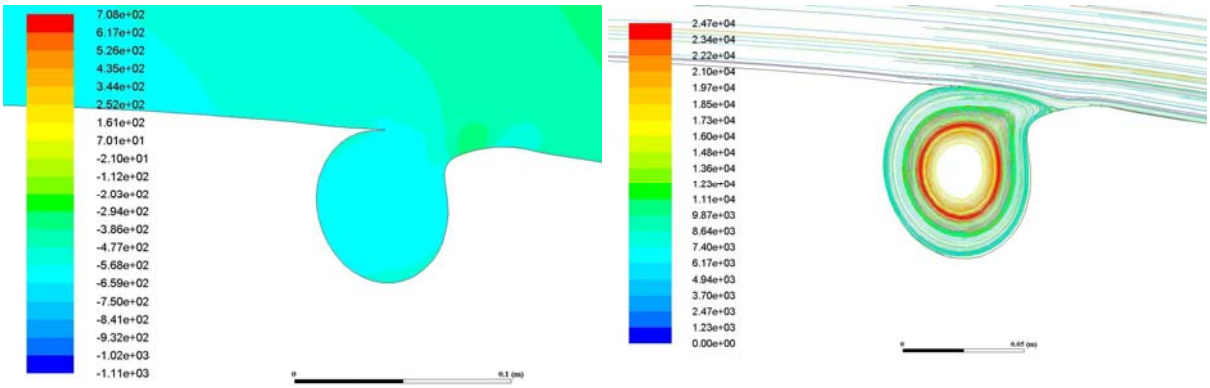

(a) (b)

Figure 8. (a) Pressure contours and (b) Pathlines inside the cavity for angle of attack 8°.

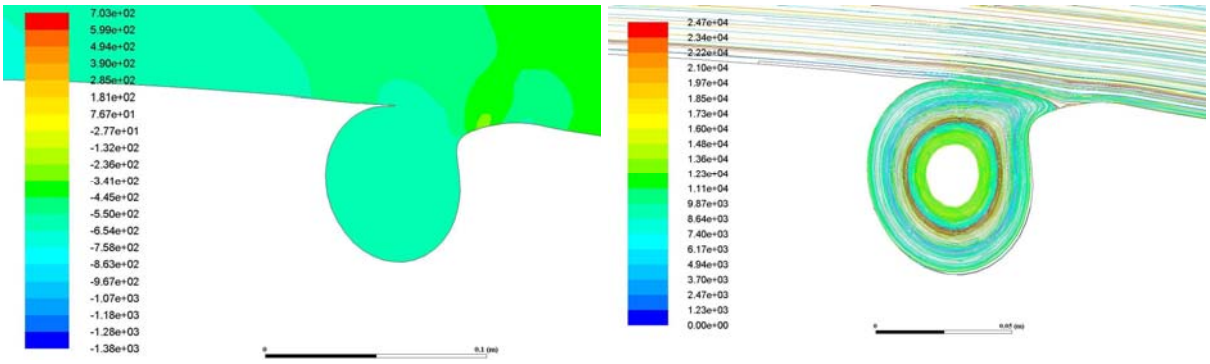

(a) (b)

Figure 9. (a) Pressure contours and (b) Pathlines inside the cavity for angle of attack 10°.

The increase of lift is noticeable for angles lower than 10° in figure 10. This is a clear evidence of the cavity capability of delaying the flow separation and allow for the generation of more lift. An increase of 8% of the lift can be noticed for the airfoil with a cavity compared to the airfoil without a cavity. After the angle of attack of 10°, we notice that the lift becomes lower because separation occurs far a head from the cavity, which make the cavity ineffective at those angles.

We observe that the drag increases as well in figure 11 from the airfoil without cavity to the airfoil with cavity. The shedding at the back of the cavity supports this increase in drag. With the increase in lift and increase in drag, the cavity as a passive flow control device might not be enough. The use of an active flow control device may lead to a decrease of the shedding and hence, a decrease of the drag.

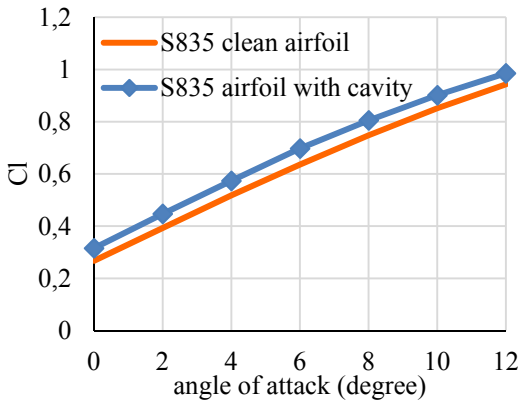

Figure 10. C_l versus Angle of attack graph for clean airfoil and airfoil with cavity.

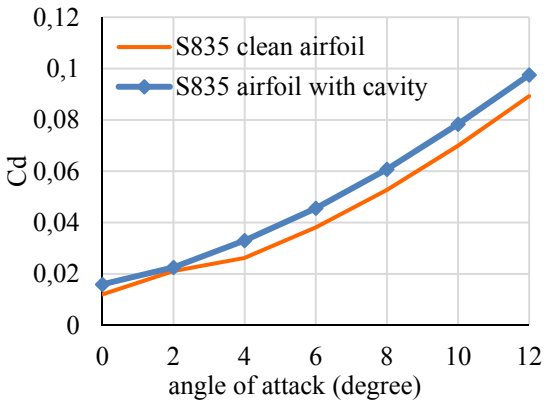

Figure 11. C_d versus Angle of attack graph for clean airfoil and airfoil with cavity.

4. Conclusion

From the simulation results of the flow over a wind turbine airfoil S835 belonging to the NREL airfoil family, with and without a vortex trapping cavity, it has been observed that the lift is increased by adding a VTC for angles lower than 12°. However, an increase in drag follows the increase in lift. The vortex is also not fully confined in the cavity with the appearance of shedding in the exit of the VTC, which supports the decrease of the aerodynamic characteristics. Overall, the results show that the cavity as a passive flow control device alone is unable to improve the flow. These first results are encouraging and call for more investigations of how to improve the flow by combining a cavity with a passive and/or active flow control technique.

References

[1] Donelli R., Iannelli P., Chernyshenko S., Iollo A and Zannetti L 2009 Flow models for a vortex cell *AIAA J.* **47(2)** 451–67

[2] Wang J and Feng L 2019 *Flow Control Techniques and Applications* (Cambridge University Press)

[3] Rowley C, Colonius T. and Murray R 2001 Dynamical models for control of cavity oscillations *7th AIAA/CEAS Aeroacoustics Conference and Exhibit* 2126

[4] Lasagna D, Donelli R, De Gregorio F and Iuso G 2011 Effects of a trapped vortex cell on a thick wing airfoil *Experiments in fluids* **51(5)** 1369–84

[5] Ringleb F 1961 Separation control by trapped vortices *Boundary Layer and Flow Control* **1** 265

[6] Savitsky A I et al 1995 *Method for Control of the Boundary Layer on the Aerodynamic Surface of an Aircraft, and the Aircraft Provided with the Boundary Layer Control System* (U.S. Patent No. 5,417,391)

[7] Kasper W 1974 *Aircraft Wing With Vortex Generation* (U.S. Patent No. 3,831,885)

[8] J Olsman W F and Colonius T 2011 Numerical simulation of flow over an airfoil with a cavity *AIAA J.* **49(1)** 143–9

[9] De Gregorio F and Fraioli G. 2008 Flow control on a high thickness airfoil by a trapped vortex cavity *14th International symposium on applications of laser techniques to fluid mechanics*

[10] Mashud M and Ferdous M 2012 Flow seperation control of thick airfoil by a trapped vortex *Int. J. Engineeirng & Technology* **12(6)** 1-4

[11] Shi S, New T H and Liu Y 2014 On the flow behaviour of a vortex-trapping cavity NACA0020 aerofoil at ultra-low Reynolds number *17th Int. Symp. Applications of Laser Techniques to Fluid Mechanics* (Lisbon, Portugal) 7–10

[12] Saeed F, Basha M and Al-Garni A Z 2013 Simulation of Flow around a Thick Airfoil with a Vortex Trapping Cavity *AIP conference proceedings*

[13] Choudhry A, Arjomandi M and Kelso R 2016 Methods to control dynamic stall for wind turbine applications *Renewable energy* **86** 26–37
[14] Mamadaminov U M 2015 Review of airfoil structures for wind turbine blades *Department of Electrical Engineering and Renewable Energy REE* 515

Initial analysis of an aircraft accident

K Maňas[1], J Hnidka and V Tříska

Department of Aircraft Technology, University of Defence in Brno, 602 00 Brno, Czech Republic

[1] E-mail: karel.manas@unob.cz

Abstract. The paper presents an initial analysis of the broken cardan joint of the helicopter Mi-171š, which is a part of a horizontal frontal suspension strut of a main gear. Based on the fractography of the fractured surface the main characteristics of the fracture are assessed. Instrumental hardness is used to assess the material properties of cardan joints manufactured by a Czech and a former Soviet Union manufacturer. Found characteristics are then used to determine the next steps in the investigation. The paper presents an initial analysis of the broken cardan joint of the helicopter Mi-171š, which is a part of a horizontal frontal suspension strut of a main gear. The cardan joint failed during landing, caused great damage to the helicopter and prompted this research. Based on the fractography of the fractured surface the main characteristics of the fracture are assessed. Instrumental hardness is used to assess the material properties of cardan joints manufactured by a Czech and a former Soviet Union manufacturer. Found characteristics are then used to determine the next steps in the investigation.

1. Introduction

The European air transport can be considered as one of the safest forms of travel, as demonstrated in [1]. However, the military aircraft are often deployed in much more challenging conditions than the civilian aircraft. The accident rate is therefore worse than in civilian sector, but still the safety margins are very small.

The paper describes a portion of the investigation after the serious incident, which occurred during the landing of a helicopter Mi-171š on a military airfield. As a helicopter contacted RWY, the left side of the main gear failed and broke off the helicopter. As a result of this incident, the helicopter landed on the side of its fuselage. Initial cause for this failure was the breakage of the cardan joint (sample marked as LOM-B), which is located on the frontal horizontal strut of the main gear. The main purpose of this element in the gear is to allow a "swinging" movement of the strut during a deformation of a damper and, therefore, reduce the impact of bending moments acting on the fuselage of the helicopter both in vertical and horizontal direction.

In the initial phases of the investigation, the investigation committee found out that the cardan joint was manufactured by a Czech manufacturer and not a former Soviet Union one. This led to a further investigation, which was to find the compliance of the Czech and former Soviet Union cardan joint. Unfortunately, no blueprints were available and the overall access to information about both cardan joints was very limited. However, a precautionary (and mandatory) check of all cardan joints on all Mi-171š was performed and it was found out that the initial signs of failure in form of cracks were observable on both Czech parts (sample LOM) and former Soviet Union parts (sample BS) – see figures 1 and 2.

The investigation roadmap is presented in the figure 3. The highlighted steps needed to be performed to assess the quality of the failed component and to determine the origins of the failure. Every step of the process up to the process analysis has to be performed by a special investigation team at the University. This paper further describes the roadmap of the investigation of aircraft accident/serious incident with limited access to the information about the failed component and the steps necessary to be performed to correctly identify the cause of the failure. The roadmap can help to keep the focus of the members of the investigation committee to the key steps of the investigation under immense pressure [2].

The investigation always starts with the accident and continues to the pre-accident period, in order to detail the complex interactions, which resulted into the accident [3]. Statistically, the human factor is the most likely cause of the accident and pilot's or ATCs errors, failures to comply with the procedures, indented sabotage/suicide, overload and other factors assessed in [4, 5] must be investigated. Flight conditions includes all unpredictable, or highly unlikely events, which could cause the accident, such as dual engine failure due to the bird strike of US Airways Flight 1549. Technical malfunction of aircraft's electrical/mechanical component is the second most likely cause for the aircraft accident and was the cause of the accident of the Mi-171š. Tests, which could determine the cause for the mechanical failure along with the determination of who caused the accident are presented. Before these tests, the preliminary assessment had to be performed as well.

Figure 1. Placement of the cardan joint on a fuselage.

Figure 2. Initial cracks of the cardan joint.

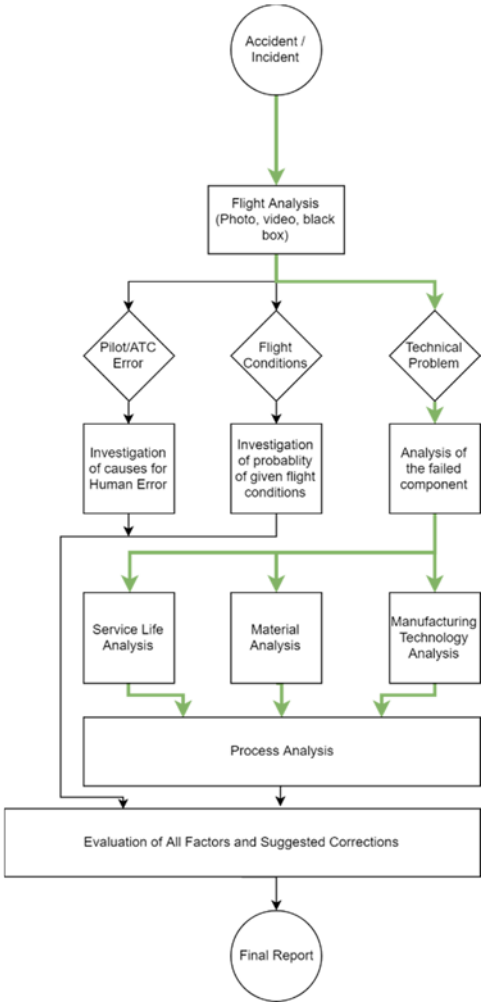

Figure 3. Flowchart of the accident investigation.

2. The preliminary assessment of the cardan joint of Mi-171š

The initial assessment was performed on cardan joints of snapped sample LOM-B, sample LOM, which showed signs of cracks, both manufactured by a Czech manufacturer and, also, a sample BS, which also showed signs of failure, manufactured by a former Soviet Union manufacturer. After preliminary assessment, i.e. visual fracture analysis of a failed cardan joint, it was found out that the fracture is not brittle, which is typical for an overloaded component. The investigation from the very first phases showed that the failure was most likely caused by the fatigue of the material of the cardan joint. After first assessment of the fracture with the opto-digital microscope it was obvious, that the fracture has indeed a fatigue-like nature similar to [6, 7], i.e. it was a result of process, during which the damage was cumulatively increased, caused by a cyclic load. Unfortunately, stress accumulated by fatigue or corrosion is often the cause for the mechanical malfunction of aircraft components, as showed in [8, 9]. The fatigue crack was created probably in regions marked as A and B on figure 4 and the continuous growth of the crack, which resulted in the final crack of the cardan joint (see regions marked as C on figure 4). With high likelihood the resulting fracture is ductile, with high level of line separation – see figure 5, region marked as D.

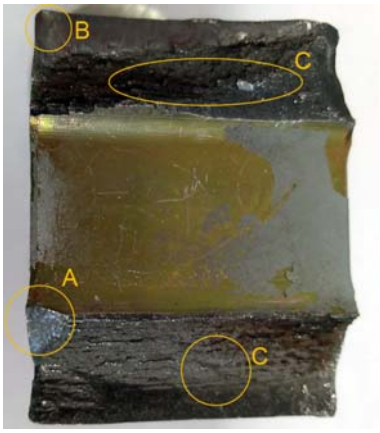

Figure 4. Macrogeometry of the fatigue fracture.

Figure 5. Detail of the ductile fatigue fracture.

Another initial parameter, which was chosen for preliminary assessment of basic material properties was instrumented indentation hardness, because all tested samples underwent surface coating. The instrumented indentation hardness was measured with a Zwick ZHU2.5 with Vickers indenter at a load of 490 N for 12 s, see table 1 [10].

Table 1. Results of the measurement of instrumented indentation hardness.

Samples Nr	h-kor. µm	HM_S N/mm^2	HM N/mm^2	W_{elast} Nmm	W_{plast} Nmm	η_{IT} %	C_{IT} %
BS	1.191	3736	2928	1.902	11.873	13.81	0.66
LOM	0.957	3604	2189	1.267	13.519	8.57	0.70
LOM-B	0.624	4197	3366	1.427	11.165	11.33	0.76

As figures 6 and 7 both clearly show, the values of measured instrumented indentation hardness are different for all three samples. This can point to difference in material or chemical or heat treatment. Furthermore, looking at the figure 7, it can be clearly seen the transition areas of indenting indenter between surface layer and the core material. There are noticeable differences between all samples, most apparent in this transition areas. These differences in transition areas can be used to identify failure to comply with technological process of surface coating [11].

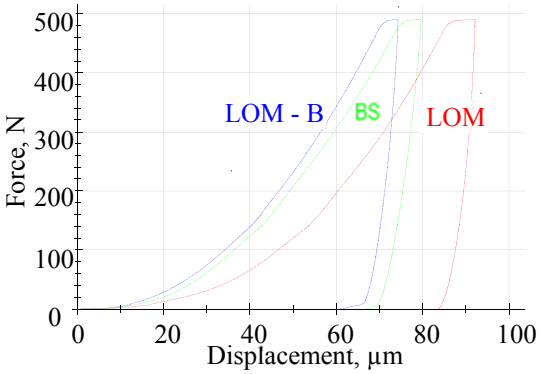

Figure 6. Measured displacement on indentation force

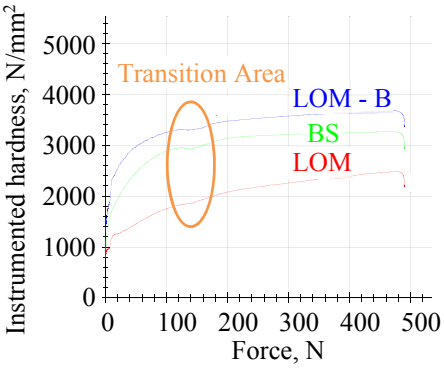

Figure 7. Measured instrumented hardness on indentation force

3. Methodology of the investigation of cardan joint of Mi-171š

Based on the result of the preliminary analysis, it was apparent, that the failure was a result of a long-term process. This further narrowed the investigation to three main points [12]:

- First, and most likely most important factor, which had to be checked, was the analysis of the service life of the helicopter, focusing predominantly on any changes during its service life. Dominant importance was that of the change of maximum take-off weight (MTOW), ratio between vertical and horizontal landings and, also, any changes of the character of rolling on runway (RWY) and its adjacent taxiways (TWY).
- Another important factor was the detailed material analysis and the geometrical analysis of both new and damaged cardan joint, with purpose of finding out the potential liability of the manufacturer, contracted repair centre and, also, mistakes in repairs and maintenance done on the military base level.
- Third and final process, which completed the assessment of the problem and helps to confirm or disregard the liability of different factors is the overall assessment of the failure. This phase is perhaps the most complicated, because to objectively assess a problem, it is necessary to determine the loads on the helicopter and assemble a computational program, which would allow to compute the estimated service life length corrected for fatigue and factors, which can contribute to shorter service life of the monitored cardan joint.

3.1. Service Life Analysis

Necessary factors to asses to determine the changes in the service life of the helicopter Mi-171š are:

- RWY (ratio between paved and unpaved RWYs used for landings);
- Landing type (ratio between landings/take-offs with and without forward velocity);
- Take-off weight and, also, landing weight (change caused by installation of ballistic defence, installation of more equipment, weapons, etc.);
- Nature, intensity and frequency of braking;
- Number of turns on TWY/RWY with no brakes;
- Ambient conditions (service on different locations, both geographically and climatically);
- Amount of toxic substances in surrounding air, namely substances increasing the corrosion rate (salt in seaside locations, dust, etc.);
- Impact of airport maintenance on the helicopter (e.g. service on airports with increased usage of de-icing fluids, etc.

It also might be necessary to assess the load on the suspension of the helicopter. This can be performed during flight, by installing the strain gauges on the suspension, or e.g. fibre optic sensors [13].

3.2. Material Analysis

The investigation after the serious incident required these tests:

3.2.1. Fractography – assessment (visual, macrofractography, microfractography) of the fractured surface. It was necessary to determine the fracture type and mechanism, which led to its existence (operating conditions) and determine:

- if the fracture is a result of a prior apparent plastic deformation, the fracture is ductile,
- if there is no apparent plastic deformation, the crack propagates across the crystallographic planes and the fracture is brittle,
- if there is a transient behaviour – the fracture changed from ductile to brittle, the fracture could be caused by a change of e.g. ambient temperatures.

3.2.2. Hardness Test

- It is a fast test, which can help to inform about mechanical properties of the metal components (ultimate strength, yield stress).

3.2.3. Chemical Composition Assessment

- Chemical Composition Assessment test can be used to find out and confirm the stock material used to manufacture the cardan joint and, also, to determine the possible liability of the elements contained in the material structure. The chemical composition showed that all cardan shafts were indeed manufactured from the same stock [14].

3.2.4. Macroscopy and Microscopy

- Both can be used to assess the material structure, find the structural failures and determine their causes and check the technological processes used to manufacture the cardan joints (e.g. heat treatment).

3.3. Analysis of the Manufacturing Technology

Analysis of the geometry of the cardan joint:

3.3.1. Geometry assessment consists from:

- assembly of a system, which would allow to input requirements for geometrical properties and assess the compliance of the measured part with the required geometry,
- methods and means to determine the true geometry of the cardan joint and final report.

3.3.2. The monitored geometrical properties are:

- Dimensions (angles) – numerically expressed value of dimensions (angles) in given units,
- shape and location of different functional surfaces and the relation between them,
- waviness – irregularities of the surface of random quasi-periodic shape with spacing considerably greater than surface roughness,
- surface roughness – deviation of the true surface from ideal surface with relatively small distance between irregularities. While all cardan joints measured showed same values of *Ra*, there were significant differences in roughness profiles. As demonstrated in [15], relying on purely 3D parameters can yield better results.

3.4. Process Analysis

Only after the impact of all aforementioned factors is assessed, the investigation can then focus on failures on different levels of maintenance/repairs at this order:

- methods of repair and maintenance at the military base,
- contracted repair centre,
- manufacturer of the aircraft.

Figure 8 shows the maintenance/repairs on different levels as arranged in the Czech armed forces. The design and operating requirements set by an aircraft manufacturer have to be checked as well. The figure 8 helps to narrow the investigation based on the results of the aforementioned analysis.

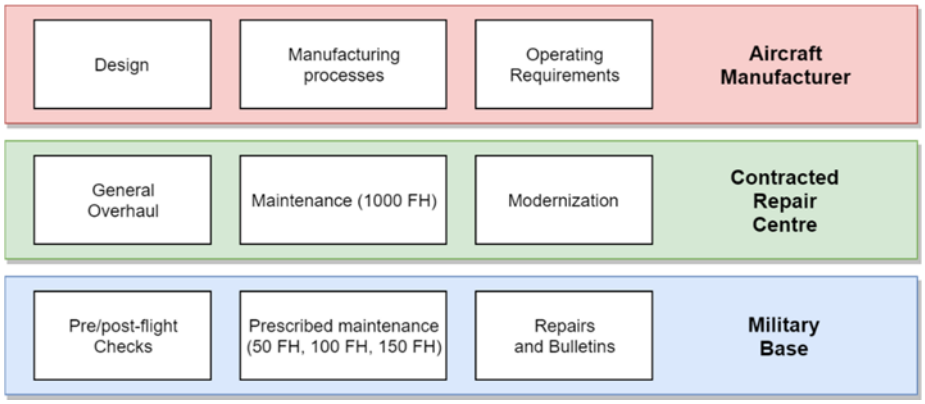

Figure 8. Measured displacement on indentation force

4. Conclusion

After each serious incident or accident an investigation is started, which main goal is to identify causes, which led to the incident or catastrophe. Another important goal of the investigation is to determine steps to prevent the incident from happening again. Typically, there is number of different factors, which are contributing to the failure and which need to be properly assessed. For this reason, the successful solution of the problem and correct determination of key causes requires a wide approach to the incident. The same factor must be assessed not only from different points of view, but also from different levels of view as well. Instinctively, due to the importance of the human factor in aviation catastrophes, the first detailed step of investigation is the confirmation of pilot's compliance with the flight procedures. Secondly, the investigation focuses on the aircraft design and its manufacturer. Despite the high standards, which the aircraft must meet to be certified for flight, mistakes can happen, and the design of a failed component is typically verified. Furthermore, the manufacturing process is checked, as well. The focus is on the quality of the stock, failure to comply with manufacturing and machining process required by the manufacturer, wrong choice of the manufacturing process, or underbuilding the component from the point of static or dynamic load, or, quite more often, fatigue. Heat and chemical treatment must be checked as well. Incorrect surface coating procedure can lead to corrosion due to operational or ambient factors.

The paper presents a method of investigating a failed component after a serious incident, which happened with Mi-171Š at the military base during landing. The method was created to quickly identify the causes, which led to the incident. Proposed method can safely and correctly show failure to comply with required processes and, furthermore, allows the investigation committee to focus on key steps during immense pressure.

Acknowledgment

This work was completed thanks to the successful cooperation within a project DZRO LETKONF "Podpora činnosti letectva AČR v lokálních konfliktech".

References

[1] Valdés R M A and Comendador F G 2011 Learning from accidents: Updates of the European regulation on the investigation and prevention of accidents and incidents in civil aviation *Transport Policy*

[2] Nixon J and Braithwaite R 2018 What do aircraft accident investigators do and what makes them good at it? Developing a competency framework for investigators using grounded theory *Safety Science*

[3] Barreto M M and Ribeiro S L O 2012 Aircraft accident investigation: the decision-making in initial action scenario *IEA 2012: 18th World congress on Ergonomics - Designing a sustainable future*

[4] Ergai A, Cohen T, Sharp J, Wiegmann D, Gramopadhye A and Shappell S 2016 Assessment of the Human Factors Analysis and Classification System (HFACS): Intra-rater and inter-rater reliability *Safety Science*
[5] Kharoufah H, Murray J, Baxter G and Wild G 2018 A Review of human factors causations in commercial air transport accidents and incidents: From to 2000-2016 *Progress in Aerospace Sciences*
[6] Li W Yan Q and Xue J 2015 Analysis of a crankshaft fatigue failure *Engineering Failure Analysis*
[7] Infante V Freitas M and Fonte M 2019 Failure Analysis of a crankshaft of a helicopter engine *Engineering Failure Analysis*
[8] Osman A and Yesil O 2013 Failure analysis of an aircraft nose landing gear piston rod end *Engineering Failure Analysis*
[9] Turan D, Karabayrak B, Baskut S and Dalkilic S 2017 Failure analysis of landing gears strut bearings *Engineering Failure Analysis*
[10] Oliver W C and Pharr G M 1992 An improved technique for determining hardness and elastic modulus using load and displacement sensing indentation experiments *Journal of Materials Research*
[11] Joska Z, Pospíchal M, Mrázková T and Sukáč J Mechanical properties of duplex system: ZrN coating on plasma nitrided stainless steel 2010 *Chemicke Listy* **104(15)** 322–5
[12] Failure Analysis - Industrial Case Studies: Failure of an Aircraft Towbar https://www.fose1. plymouth.ac.uk/fatiguefracture/tutorials/ FailureAnalysis/ Aircraft_Towbar/Towbar.htm (2019-01-30)
[13] Iele A et al. 2018 Load monitoring of aircraft landing gears using fiber optic sensors *Sensors and Actuators A: Physical*
[14] Maňas K, Hnidka J, Tříska V and Junas M 2019 Analysis of the damaged aircraft component after impact caused by harsh landing *7th International Conference on Military Technology 2019 (Brno: University of Defence)*
[15] Maňas K, Hnidka J and Tříska V 2019 Surface texture analysis of a joint sample by 2D and 3D surface roughness parameters *Engineering Mechanics* 247–51

Using drones in fire-fighting missions

V Radkov[1,3], V Aleksandrova[2] and A Guncheva[2]

[1] Faculty of Transport, Technical University – Sofia, 8 Kliment Ohridski Blvd., 1000 Sofia, Bulgaria

[2] National Defence College G. S. Rakovski, 82 Evlogi Georgiev Blvd., 1124 Sofia, Bulgaria

[3] E-mail: vradkov@tu-sofia.bg

Abstract: The present work outlines the possibilities of using remotely piloted aircraft systems (drones) to perform special missions related to fire-fighting process. The peculiarities of wildland fires and the requirements of the respective stages of combating them are considered. The advantages, disadvantages, and limitations of the commonly used aviation (air-tankers and helicopters) for fire-fighting have been analysed in detail. Consideration is given to the possibilities of using Drones to perform special tasks in fire extinguishing of wildfires. The advantages and the high economic efficiency of the drones are shown at the some stages of fire-fighting in highly intersected mountain areas. The main requirements that Drones have to meet for such missions are considered.

1. Introduction

Non-manned aircraft (with no human operator onboard or on the Earth) were intensively used at the end of World War II. These were the German-designed aircraft manufactured for military purposes and named V-1 and V-2. The first one was in fact, a cruise missile and the second one was a missile moving in a ballistic trajectory. Both vehicles, after their launch, are operated by onboard simple Gyrocompass based autopilot without additional external intervention. Those were the first aircraft to cover the current definition of Unmanned Aerial Vehicle (UAV).

In 1945, the US Air Force equipped retired aircrafts Boeing B-17 ("Flying Fortress") with a primitive radio-controlled system for remote directing the aircraft to hit enemy targets. The aircraft takes off with a crew, then at a certain stage of the flight control is taken by an accompanying airplane and the crew leaves the B-17 with parachutes. This is the first known use of remote-controlled aircraft, currently labelled Remote Piloted Aerial System (RPAS).

According to the Bulgarian Civil Aviation Act, "An unmanned aircraft is an aircraft which is intended to be operated independently or is remotely controlled without a pilot on board" [1]. Recently, both in Bulgaria and abroad, citizenship and broad use have been made of the term Drone has become popular and broadly used, which is generally referred to as RPAS.

Nowadays remote-controlled vehicles of various types and sizes are widely entering various civil sectors to perform a wide range of special missions - for example, to safeguard public order and national security as well as combating disasters, accidents, and breakdowns including forest fires.

In Southern European countries wildfires are the most natural threat to forests. In the period 2002 – 2011 the average annual number of forest fires throughout these countries exceeded 53000 according to European Commission statistics. The average annual burnt area on this one period was around 381000 hectares [2].

The purpose of this study was to analyse the impact of using RPAS to perform special missions related to combating forest fires in highly intersected areas.

2. Peculiarities of forest fires

It should be noted that wildland fires have the following features:

- they spread on large areas because there is a lot of vegetation on them;
- they spread rapidly due to the presence of winds that accelerate the process;
- in many cases, such fires are started in more than one place (for example, in the event of lightning or malicious human actions);
- often forest fires are in highly intersected areas that are difficult for firemen and related fire-fighting equipment to reach.

The use of aviation technologies has a place at all stages in the fight against forest fires, which are dealt with below.

2.1. Stages in forest firefighting

2.1.1. Stage "Fire reconnaissance". Before proceeding to fire extinguishing in a mountainous area, it is necessary to carry out fire reconnaissance to collect initial information about fire. Armed with this one preliminary information Fire-fighting manager will able to make an informed decision based on what method and with what technology to impact to the fire. So, it is necessary for the following information to be collected about:

- the type of fire and the peculiarities of the affected area;
- the fire spread rate;
- the most dangerous spread direction(s);
- the presence of obstacles to further distribution (rivers, lakes, rocky areas, etc.);
- a threat to distribution to individual buildings, settlements and other local infrastructure;
- a possibility to increase or weaken the fire due to the peculiarities of the local area and the type of vegetation on the distribution route;
- the presumed fire borders in the next few hours;
- possibilities for using mechanized means for fire localization and extinguishing;
- the presence of water sources and the possibility of their safe use, including the possibility of a safe approach of aviation equipment;
- the existence of obstacles to aviation within the bounds of the fire: electrical power lines, cabin lifts, ski lifts, etc.;
- safe places to concentrate human forces and fire-fighting equipment, places for hiding of people, to set up temporary medical centre(s), etc.

To obtain the preliminary information noted above, the drone must be equipped with a high-resolution video-camera, and it is also highly desirable to have a multi-spectral video-camera, or at least one operating in the infrared light range.

The drone's remote control system incorporates a GPS receiver, which allows the flight management centre (Fire manager) to obtain flight coordinates in real time, allowing him quickly delineate the boundaries of a fire and to calculate the area of this one.

When more than one fire is located, it is usually necessary to perform simultaneous (parallel) reconnaissance using additional drones (i.e. multi-drones reconnaissance).

Based on the carried out reconnaissance, the Fire manager develops a fire-fighting plan.

2.1.2. Stage "Fire Extinguishing". At this stage, the use of aviation technologies is based on the use of specialized airplanes or helicopters. The main tasks performed at this stage are:

- attacks on the fire - delivery of fire extinguishing agents (water or chemicals)
- spreading chemical agents to cause artificial rainfall, in the presence of suitable clouds;
- real-time monitoring of the results of the extinguishing;

- real-time monitoring of the fire spread rate and the main spread directions;
- real-time monitoring to trace if new fires are starting.

If new fires are detected, it is necessary to fire reconnaissance to be carried out for them, too.

2.1.3. Stage "Observation after fire extinguishing end". The main activity after fire suppression is required is real-time post-fire monitoring about the potential restart of fire on the same area(s). It should be noted that the duration of the observation is different depending on the risk degree of fire restart, which is a function of a large number of factors that are specific to each fire, but it usually lasts until there are rainfalls in the range as a minimum of 3 to 5 mm per hour.

3. Operation analysis of the use of traditional aircraft for fire-fighting

The use of aviation technology in fire suppression plays an auxiliary role, as the final extinguishing is always done by people.

However, in the case of fires in mountain areas, the use of specialized fire-fighting aircraft (i.e. fixed-wing aircraft/air-tanker) has the following advantages (strengths) and disadvantages (weaknesses) – table 1.

Table 1. Strengths and weaknesses of the air-tankers.

Strengths	Weakness
• fast and high-quality intelligence of the area of fire; • high operability for fire-extinguishing agents (water or chemicals) delivery; • the possibility of spreading chemical agents to cause artificial rainfall, in the presence of suitable clouds; • high efficiency of the extinguishing action (attacks) on the fire, which does not depend on the availability of road infrastructure; • speed and high flexibility to transport firefighters, equipment or medical personnel to the site of a fire, as well as the evacuation of victims; • high safety for the people while extinguishing operations are in progress	• restrictions of flights due to highly intersected mountain areas; • limited manoeuvrability (the impact with extinguishing agents is not so precise and effective); • the need for a take-off/landing airport (in many cases, this one is situated at a large distance from the fire); • in general, there is no possibility to use limited-sized water resources (lakes, rivers and small dams) located near the fire

Due to the weakness mentioned above of the fire-fighting aircrafts, as usual, the heavy helicopters are used in Bulgaria both for fire reconnaissance and fire-fighting. These large helicopters are military, i.e. meaning fire suppression efforts with these helicopters is limited to tank and bucket work (i.e. externally suspended water Bambi Bucket), and hauling cargo.

However, the use of fire-fighting helicopters has the following strengths and weaknesses in the case of fires in forest areas – table 2.

The flight restrictions mentioned above are necessary to ensure the needed reserve for longitudinal and transverse control, especially in the cases of a specific maximum take-off mass.

Apart from the above, the piloting in firefighting areas is associated with a lot of stressful work for the pilots, which requires limits to the duration of both a single mission and the length of flying in the helicopter for each pilot per day. In [3] it is shown that the US Army limits the duration of a single mission up to 2 hours, after which the crew has to be replaced by another.

4. Economic analyses of traditional aviation technologies for fire fighting

It should be noted that the currently used aviation technologies are costly and have low economic efficiency for the following reasons:

Table 2. Strengths and weaknesses of the fire-fighting helicopters.

Strengths	Weakness (Flight restrictions on/about)
• short mobilization time for the available helicopters after receiving a notification for a fire; • the need for a limited-size landing/take-off site that can be prepared relatively quickly if there is no suitable landing site; • more flexible manoeuvring capabilities, including low-speed movement and more precise fire extinguishing • the capability to "hover" over a fixed point (fireplace fire); • versatility - depending on the built-in or hanging equipment, the helicopter can be flexibly used to perform a variety of missions; • the capability to take water from nearby and small-sized water sources	• in case of limited visibility due to fog or strong smoke over the fire area; • the value of angle of Crane when executing manoeuvres at heights up to 50 m and at low flight speeds (from 120 up to 250 km/h); • flight in the event of the so-called "conventional jet" (convective column); • when performing hovering manoeuvre; • the speed of the wind (front, side, and rear winds) as well as when engines are started and stopped at take-off/landing as well as the in-flight mode

- the high initial acquisition value (from several million to several tens of millions USD/Euro);
- high operating costs;
- high technical maintenance/repair costs associated with the availability of suitable facilities and trained technical staff;
- high flight crew wages;
- high crew cost training and additional simulator training costs.
- costs for creating and maintaining a certified take-off/landing ground or feed paid as hangar costs in the absence of its own.

In [2] it is shown the average flight hourly cost was 1161 Euros under a contract of up to 5 fire-fighting helicopters and the average 900 flight hours per year. For the period 2001-2005 the new contract for wildland fire suppression was signed (for the same Tuscany region in Italy) covering 1600 flight hours per year, and the average flight hourly cost increased up to 1239 Euros.

The United States government spent approximately 150 million USD on helicopters for fire suppression during the year 2000. A considerable amount of this money was spent contracting large helicopters for use on large wildland fires. The United States government contract covered the rent of helicopters for wildland fire suppression. Helicopter operation costs are a function of the contracted daily availability rate and the hourly flight rate. Depending on the type and model of the helicopter, as well as the type of tasks performed, costs may vary. For example, in 2009 the USDA Forest Service signed a 120-day contract for an average type helicopter (Bell Huey) with a rental price of 5000 USD per day, plus 1546 USD paid for every hour in flight. In 2010, for the same type of rental contract, the price per day remained the same, but one hour flight price was doubled (the stated amounts do not include pilots' remuneration, insurance, and other costs) [4].

It is very important to indicate the need to prepare certified pilots capable of performing special missions. The pilot's training takes a lot of time and is expensive, and in this case, it is difficult to even estimate the costs as they depend on where the preparation takes place and for what type and model helicopter is concerned.

It should also be borne in mind that the training of pilots is specialized for the type and model of the helicopter, so that if the equipment is changed, the re-qualification of the new helicopter type is necessary, which, in addition to being expensive, also takes considerable time.

Similarly, there are difficulties in assessing the annual salary costs for the employed pilots.

Finally, the helicopter benefits are directly related to the amount of weight that the helicopter can carry. So as fire suppression tool the lifting capability of a helicopter at the fire is the main characteristic to the benefits this one can provide. It is important to keep in mind the lifting capability, (often referred to as helicopter performance), depends on the altitude and temperature of operation [5].

The presented above facts clearly show that the use of aviation equipment and helicopters in particular, though effective in fighting forest fires, is at the same time ineffective from a financial point of view.

5. Analysis of the use of RPAS (drones) for special missions related to forest fire-fighting

RPAS production and management technologies have already developed fast enough to allow these devices to combine all the benefits of helicopters with the absence of their inherent drawbacks and flight limitations. The only area of activity in which today's widely available RPASs are not competitive is the process of a direct impact on the fire (i.e. direct fire extinguishing). The latter results from the fact that the mass-used RPASs (excluding those for military purposes) have limited payload capacity, but nevertheless they have the following indisputable advantages, such as:

- low acquisition cost – from a few hundred to several thousand USD/Euro, including the specialized equipment – as usual, GPS receiver, video-camera(s), remote control equipment plus related software;
- huge fuel cost savings and high ecological effect;
- very low operating and technical maintenance expenses;
- no expenses for a specialized repair base as well as the relevant maintenance staff;
- no expenses to hire flight crews, as well as training/ongoing training costs;
- no expenses to own (or to rent) a certified take-off/landing ground and no hangar expenses;
- high readiness for use – within a few minutes of the disaster alert.

It is very important to point out the great effect of minimizing the fire intelligence time (i.e. fire reconnaissance stage) to reduce the damages (losses). As it was mentioned above, the preliminary information collection is obliged before start of fire extinguishing process. Looking at the curve in case of forest fire (figure 1), the damage-time function T_{lost} gives an exponential dynamic that diverges to infinity. It is easy to recognize if for any period of time Δt is reduced, the area burnt and thereby the damage caused is reduced exponentially. The smaller the area affected by the fire, the smaller the quantity of resources to extinguish it. Therefore, the application of any method that allows firefighting to begin earlier the intervention will result in an increase in efficiency of firefighting [6].

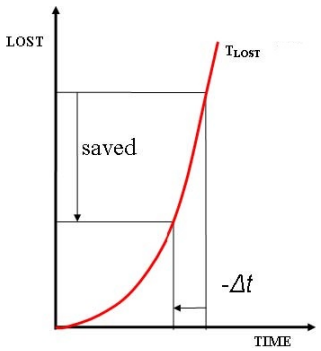

Figure 1. Damage-time function (a basic shape at uncontrolled forest fire).

So, as it was stated above the all expenses (including operational ones) are 3-4 or more orders of magnitude lower than those for aircraft or helicopters. So from economical point view about drones's cost, as well as all other related expenses have a high efficiency compared to traditionally used airplanes and helicopters. Nevertheless drones are able to perform with the same effectiveness and even better than airplanes and helicopters on all fire-fighting stages, except about the process of direct fire suppression.

In addition, figure 1 clearly shows the advantages of drones also have a direct economic effect on reducing the damages (losses) caused by fires.

Like any technology, currently RPASs have the following main disadvantages:

- the remote control is possible within the zone of Visual Line of Sight (VLOS);
- limited flight time due to limited power options;
- limited payload capacity;
- the need for a certified operator to manage and control the drone.

The limited payload capacity does not obstruct the use of RPASs in combating forest fires as long as the latter is not used to impact the fire but to solve all other tasks. Modern RPAS for professional use (except those for military application) has a payload of several kilograms to several tens of kilograms, which is enough to equip it with the necessary communication and video equipment.

The remote control of the RPAS for many reasons is implemented in the main range of VHF. It is known that the radio waves from this range travel according to the laws of geometric optics that require VLOS for dependable communication. The latter requirement greatly impedes the use of RPAS in heavily intersected areas because forest fires are characterized by a large area, rapid growth and frequent changes in the direction of the front. Overcoming this obstacle can be accomplished by:

- the use of a satellite communication channel;
- the use of a command/management channel and video-streaming channel to the command centre of Fire-manager by using a public cellular communication network – preferably a 3G/4G type.

Organizing and using a satellite communication channel is more complex and is also related to technical constraints, especially in mountain areas. On the other hand, the organization of a command channel and a video channel in real-time via a cellular network is easy to realize, given the very good coverage on the territory of Bulgaria. The modern 3G/4G networks offer high-speed communication that ensures the delivery of high-quality video streaming (real-time video streaming).

The flight time limitation exists due to the limited energy capabilities of modern rechargeable batteries. For most modern non-military RPAS flight time is as usual within 20-40 minutes. This time is extremely unsatisfactory in terms of the execution of forest firefighting tasks, which generally lasts for hours, and in some fires may continue for days. The possibility of solving this serious problem is the use of the so-called “hybrid drones”, which have an electrical generator onboard powered by a low-powered internal combustion engine. In-flight, the generator powers the electric motors and all other drone equipment and the battery is connected in parallel. In the case of engine failure, the drone uses the battery to return to its base. When using hybrid drones flight times are limited only by the amount of fuel that can be stored on-board as well as by the specific instantaneous fuel consumption of the generator.

The preparation of a certified RPAS operator can be done for a few days and is incomparably cheaper than the training of a pilot or even a helicopter technician. Also, a qualified operator after a brief training (even just a few hours) may learn to manage another RPAS type or model.

6. Conclusion

The present work outlines the possibilities of using remotely piloted aircraft systems (drones) to perform special missions related to fire-fighting process in highly intersected mountain areas. The peculiarities of wildland fires and the requirements of the respective stages of combating them are considered.

The analysis of the advantages, disadvantages and limitations of traditional aircrafts and above all of the helicopters in forest fire-fighting has been provided. As a result, the lower economic efficiency of old technologies has been justified.

The paper examines the strengths and weaknesses of RPAS (Drones) in the fight against forest fires and their higher efficiency has been justified. It is shown the advantages and the high economic efficiency of the drones at all stages of fire-fighting, except direct fire attack. The ways to avoid the RPAS weaknesses in the fire-fighting process in a highly intersected mountainous area have been shown too.

Drones are expected to act as the first response force of police and fire-fighting teams. These one forces will likely use small, highly manoeuvrable and low altitude (below 150 m) drones with beyond visual line of sight operation capabilities.

References

[1] *Civil Aviation Act* 1972 (State Gazette - Bulgaria, (Last Amendment – 2019)) **94**
[2] Marchi E, Neri F, Tesi E, Fabiano F and Brachetti Montorselli N 2014 Analysis of helicopter activities in forest fire-fighting *Croatian J. Forest Engineering: J. Theory and Application of Forestry Engineering* **35(2)** 233–43
[3] *The Utilization of Helicopters for Police Air Mobility* 1971 (U.S. Department of Justice, U.S. Government Printing Office, Washington D.C.)
[4] *Department of Natural Resources Helicopter Cost and Use* 2011 (Report 11-3 Joint Legislative Audit and Review Committee (JLARC), State of Washinton, January 5, 2011)
[5] Trethwey D Development of an index for quick comparison of helicopters and benefits 2007 *International J. of Wildland Fire* **16** 444–9
[6] Laszlo B, Agoston R and Xu Q 2017 Conceptual approach of measuring the professional and economic effectiveness of drone applications supporting forest fire management *8th Int. Conf. Fire Science and Fire Protection Engineering, Procedia Engineering* **211** 8–17

Преглед на грешките и нарушенията при изпълнение на техническо обслужване на самолети в четири организации

Красин Георгиев

Технически университет – София, бул.„Кл. Охридски“ №8, 1000 София, България

E-mail: krasin@tu-sofia.bg

Резюме. Целта на техническото обслужване е да гарантира летателната годност на самолетите, но при отказ в системата може да се получи обратен ефект и да се заложат опасности и отказни/предотказни състояния. Отказите на системата за техническо обслужване (ТО) реално се определят от грешки и нарушения на техниците и проверяващите и следователно трябва да се изследват с използване на теорията на човешкия фактор. В настоящата разработка се анализира опитът от прилагане на методика за разследване на събития MEDA в четири организации за техническо обслужване. Показано е, че броят на събитията със среден риск е свързан с броя на събитията с висок риск. Определени са основните причини за възникналите събития. Получените резултати са основа за управление на риска в организации за техническо обслужване.

1. Въведение

Техническото състояние на въздухоплавателните средства е основен фактор за недопускане на авиационни произшествия. Освен от летателно техническата експлоатация, то се определя от провежданото техническо обслужване (ТО). Изпълнението на техническо обслужване е задължително за поддържане на летателната годност на самолетите [1], но при отказ в системата може да се получи обратен ефект и да се заложат опасности и отказни/предотказни състояния [2, 3]. Отказите на системата за техническо обслужване реално се определят от грешки и нарушения на техниците и проверяващите [4] и следователно трябва да се изследват с използване на теорията на човешкия фактор.

Ефективността на техническото обслужване се определя от ефективността на работите по техническото обслужване, от спазването на сроковете за планирането им и от качеството на изпълнението им. За съдържанието и планирането на техническото обслужване отговарят производителят на самолета и организацията за поддържане на летателната годност към оператора [1, 5]. Изпълнението на техническото обслужване на транспортни самолети се извършва в специализирани организации, лицензирани по EASA Част 145 [1]. Качеството на работата на техниците и контролиращите е показателно за съвършенството на цялата организация за ТО – въпреки че те са конкретното звено, което взаимодейства с техниката, оценките показват, че само 10% до 20% от причините за грешка/нарушение са в тяхната сфера на пълномощия [4]. Останалите 80-90% от факторите, влияещи върху изпълнението на работите, се залагат от ръководството на компанията. За правилното протичане на процесите в такива

организации се въвеждат системи за управление на безопасността (SMS). Докладването и анализите на събития и откази на системата за техническо обслужване са важна част от SMS [6].

Човешкият фактор в авиацията е обект на дългогодишни изследвания, които първоначално са били насочени към летателния състав, но постепенно са разширени и приложени за подсистеми на авиационната транспортна система, в това число и системата за техническо обслужване [7-10]. Така наречената „Мръсна дузина“ систематизира причините за човешки грешки в 12 категории [10, 11]. Според една от основните теории на възникване на произшествия, моделът на Рийзън [8, 12], за настъпване на произшествие е необходим пробив едновременно на няколко бариери, в това число и в управлението на компанията и надзора над процесите. Конкретни методики за анализ, прилагащи този принцип за предотвратяване на произшествия, са HFACS-ME и MEDA [13-17]. За целта се предлагат номенклатури за типови грешки и фактори, които директно или индиректно са способствали за възникването на грешките. Най-често HFACS се прилага за ретроспективен анализ на авиационни произшествия и инциденти (авиационни събития с виок риск), свързани с техническото обслужване. MEDA цели ретроспективен анализ на технически проблеми и събития (особени ситуации), възникнали по време и непосредствено след техническо обслужване. Данни за честотата на поява на неблагоприятните фактори в самите организации за техническо обслужване на практика не се споделят.

В настоящата разработка се анализира опитът от прилагане на методиката MEDA в четри организации за техническо обслужване, лицензирани по EASA Част 145. При това се определят основните причини за възникналите събития и връзката между грешките с различно ниво на риск. Получените резултати са основа за управление на риска в организации за техническо обслужване.

2. Избрана система за разследване на грешки и нарушения

Изследваните организации използват системата MEDA, която е особено подходяща за идентифициране на опасности в организацията, като част от SMS. Освен това може да се комбинира с HFACS като допълваща структурата й в дълбочина [17].

Системата MEDA дава структуриран процес за разследване на грешки и нарушения при изпълнение на техническо обслужване [4, 16]. Буквално се превежда като „Помощ за решения при грешки в техническото обслужване“ (Maintenance Error Decision Aid). Проследява се причинно-следствената връзка за определени събития, които представляват смущения за нормалната експлоатация на самолетите, повреди на техниката или нараняване на персонала. Разглеждат се като ефекти от „откази“ на системата са техническо обслужване. Примерни извадки от стандартните номенклатури за идентифициране на отказите и събитията/ефектите по MEDA са дадени в таблица 1. За всеки отказ се анализират причините или неблагоприятните фактори, които са създали условия за появата му. Важно е да се определи не само какво е станало, но и защо. Типовите причини са развити в две нива. За илюстрация, категориите от първо ниво са дадени в таблица 2, където са дадени и примери от второ ниво.

Няколко паралелни грешки и множество последователни и паралелни причини може съвместно да са довели до настъпване на разглежданото събитие/ефект. Следователно MEDA може да се разглежда като формализирана реализация на модела на „швейцарското сирене“ на Рийзън [8] и може да бъде основа за съставяне на по-сложни логически модели.

3. Подход за преглед на грешките и нарушенията при техническо обслужване

Възможността за моделиране на всички възможни сценарии на спомагане, възникване и развитие на грешки при ТО според някои автори е ограничена [18]. При това се поставя основно ударение на систематизиране на причините за събитията. Голяма част от публикуваните изследвания се анализира разпределението на неблагобриятните фактори независимо един от друг. В такива случаи е възможно зависимостите между факторите да се разглеждат на ниво организация, а не на ниво индивидуални събития.

Таблица 1. Събития/ефекти и откази по MEDA. Подкатегориите от втори ред, означени с букви, са непълна извадка от оригиналната номенклатура [4].

Отказ на системата за ТО	Събитие / ефект
1. Неправилен монтаж *a*. Не е инсталирана част; *b*. Инсталирана е грешна част; *c*. Неправилно разполагане; ... ; *n*. Монтирана е негодна част	1. Нарушаване на летателната експлоатация *a*. Закъснение на полет; *b*. Отмяна на полет; *d*. Спиране на двигател в полет; *e*. Връщане от полет; *f*. Отклонение на полета; *g*. Пушек/пари/миризми; *h*. Други.
2. Неправилно обслужване *a*. Недостатъчно течност; *b*. Препълнено с течност; *c*. Неправилен вид течност; ... ; *f*. Не е деактивирана система/оборудване	
3. Неправилен ремонт (на компонент или конструкция) *a*. Неправилен; *b*. Неодобрен; *c*. Непълен	
4. Неправилна диагностика / тест/ проверка *a*. Не е открита неизправност; *b*. Нищо не е открито при диагностика; *c*. Нищо не е открито при проверка на работоспособност/ функционален тест; ... ; *i*. Справка с техническия дневник	4. Преработка на изпълнена работа
5. Повреда от външен предмет *a*. Забравени инструменти/части в самолета/двигателя; *b*. Отломки от перона; *c*. Отломки попадат в отворени системи	6. Проблем, открит при ТО 7. Проблем, открит в полет
6. Повреда на самолета/оборудването	2. Събитие повреда на самолета
7. Нараняване на персонала	3. Събитие нараняване на персонала
8. Неправилно управление на ТО *a*. Изпусната/закъсняла/неправилна регламентна работа; *b*. Интерпретация/прилагане/отпадане на списъка на минималното оборудване(MEL); ... ; *p*. Липса на оторизация/класификация/ сертификация за изпълнение на задачата	5. Управление на летателната годност

Таблица 2. Причини (съпътстващи фактори) [4].

Категория (Ниво 1)	Примерно уточнение (Ниво 2)
A. Информация	
B. Наземно оборудване / инструменти / защитно оборудване	**B1**. Необезопасено **B6**. Неправилно за задачата **B13**. Недостъпно (заето; прекалено далеч)
C. Проект / Конфигурация / части / оборудване / консумативи на самолета	
D. Работа / задача	
E. Знания / умения	**E2**. Познаване на задачата (бавно изпълнение; задачата е изпълнена в грешна последователност; задачата се изпълнява за първи път от техника) **E4**. Познаване на процесите в организацията (техникът е новопостъпил или на ново работно място; процесите не са документирани добре или не е наблегнато на тях при обучение; не се осигуряват необходимите части навреме)
F. Индивидуални фактори	**F3**. Притискане от времето (среда на постоянно бързане; изпълнение на множество задачи от един човек за ограничено време; повишаване на натоварването без увеличаване на персонала; прекалено наблягане на спазване на срока без правилно планиране; натиск за предсрочно приключване, за да се освободи перонът) **F5**. Самоувереност (Опасно отношение – усещане за неуязвимост, арогантност, прекомерна увереност)
G. Околна среда / съоръжения	
H. Организационни фактори	**H7**. Не е спазен работен процес/ процедура (пропусната проверка на работоспособност; не е използвано задължително защитно оборудване; не е поставен етикет „свалена част“) **H9**. Групова практика (норма) (повечето хора в организацията не следват въпросния процес или процедура; повечето хора в организацията изпълняват въпросната процедура, без да я документират)
I. Лидерство / надзор	**I6**. Степен на надзор (ръководство тип „висене над главата“; непрекъснато поставяне под съмнение на взетите решения; не се включват служителите във вземането на решения)
J. Комуникации	

Целта на настоящото изследване е да се определят най-често срещаните причини за грешки и нарушения на ниво организация. За да се ограничим до събития, свързани с летателната годност, първо се определя наличието на корелация между броя събития с различен риск. Анализите се ограничават до събития, показателни за риска за летателната годност.

3.1. Входни данни

Разглеждат се четири EASA част 145 организации за техническо обслужване на транспортни самолети от среден клас и съществен производствен капацитет (50 – 200 самолета годишно) за четиригодишен период. Означават се като База 1, База 2, База 3 и База 4. Характеризират се с един признак – ниво на разрастване на организацията, от нови, през развиващи се до установени организации (таблица 3).

Таблица 3. Характеристика на разглежданите бази за ТО.

Означение	Особености
База 1	Разрастваща се организация с опит
База 2	Новосъздадена организация
База 3	Леко разрастваща се организация
База 4	Установена организация с опит

За всяка организация е направена справка за броя обработени въздухоплавателни срадства по години от 2015 до 2018 включително (фигура 1). Извадени са списъци с констатираните нарушения/грешки, съдържащи дата на докладване, категоризацията на вида грешка по MEDA и нивото на риска по ICAO [6]. Аналогични списъци са извлечени за причините за грешките – дата на докладване, категоризация на причината по MEDA и нивото на риска по ICAO.

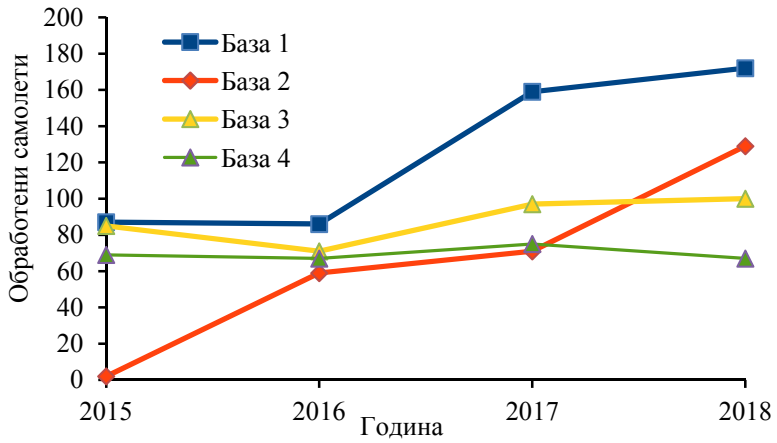

Фигура 1. Разпределение на обема работа по бази и по години.

3.2. Съпоставка на броя на събитията по ниво на риска

Проверката за връзка между броя на събитията с различен риск се извършва в следната последователност:

- определя се броят събития от нисък, среден и висок риск по години и по бази;
- определя се относителната честота на събитията, като се разделя броят събития на обработените самолети за съответната година и за съответната база;
- информацията за годините и базите се премахва;
- моделират се посредством линейна регресия следните зависимости: честота на високорискови към нискорискови събития; честота на високорискови към среднорискови събития и честота на среднорискови към нискорискови събития;

- анализират се коефициентът на детерминация R^2 (обяснената от модела дисперсия), коефициентите на регресия и вероятността да се отличават от нула по случайни причини (*p*-values или нива на значимост);
- визуализира се моделът и данните за трите разглеждани комбинации от събития.

За предварителната обработка на данните и визуализиране на резултатите се използва MS Excel. За статистически анализ е използван Python v3.6.8 и библиотеки Numpy v1.16.4 и Statsmodels v0.10.1.

3.3. Причини

За всяка от разглежданите бази за техническо обслужване се съставя списък с установените причини/фактори за грешки и нарушения, сортират се по честота и се определят най-често срещаните причини (факторите, регистрирани сумарно в 50% от случаите или индивидуално в 10%). Изчисляват се доверителни интервали за получените честоти, за да се установят статистически значимите разлики (с ниво на значимост 5%). Използван е интервал на Джефрис, който има Бейсов произход и равно вероятни опашки на разпределението [19].

4. Резултати от прегледа на събитията за четири организации за техническо обслужване

4.1. Връзка между събития с различно ниво на риска

Връзката между честотите x и y на събития с различен риск се представя чрез уравнение на линейна регресия

$$y = ax + b, \tag{1}$$

където a е наклон на кривата, b е свободен член или изместване. Наличието на статистически значими стойности на a е показателно за връзка между x и y. Статистическа значимост се приема, че има при p-стойност по малка 0.05. Мярка за силата на връзката е коефициентът на детерминация R^2. Регресионните модели са пресметнати за честотата на високорисковите събития спрямо честотата на среднорисковите (фигура 2а), високорисковите спрямо ниско-рисковите (фигура 2б) и среднорисковите спрямо нискорисковите (фигура 2в). Характеристиките на моделите са дадени в таблица 4.

Таблица 4. Коефициенти на уравненията на линейна регресия за честотата на събития с различен риск x и y.

x	y	a	p	b	p	R^2	Връзка
Среднорискови	Високорискови	0.086	0.018	-0.005	0.876	0.362	Да
Нискорискови	Високорискови	-0.004	0.925	0.072	0.038	0.001	Не
Среднорискови	Нискорискови	-0.119	0.661	0.938	0.001	0.015	Не

Вижда се, че статистически значима връзка има между високо- и среднорисковите честоти. Наличните данни не дават основание да се ползва честотата на нискорисковите събития за прогнозиране на високорискови събития. Затова по-нататък се ограничаваме до анализ на причините и факторите за грешки и нарушения, довели до събития със среден и висок риск.

4.2. Анализ на причините за човешки грешки и нарушения

Причините за човешки грешки и нарушения са анализирани в контекста на конкретни организации за техническо обслужване. Най-често срещаните причини по бази са представени в кодиран вид в таблица 5, като са използвани означенията, въведени в MEDA [4] (вж. таблица 2).

Основен фактор за грешки и нарушения е самоувереността на изпълнителите и контролиращите работата им (F5) – на първо място в три от организациите и на второ в четвъртата. Други важни фактори са неспазването на процедури (H7) и превръщането му в

групова практика (H9). Характерно за бързо разрастващата се организация е недостиг на време (F3), за новоразвиващата се е непознаване на процесите (E4) и неадекватен надзор (I6), а за установената с дългогодишен опит – самоувереност (F5) и проблеми с оборудването – необезопасено оборудване (B1), неправилен инструмент за задачата (B6), недостиг на оборудване (B13).

Таблица 5. Причини за човешки грешки, подредени по дялово участие по бази.

Организация Ранг	База 1 Бързо растяща	База 2 Нова	База 3 Растяща	База 4 Установена
Ранг 1	H7 (25.3%)	**F5** (31.1%)	**F5 (23.3%)**	**F5** (41.3%)
Ранг 2	**F5** (14.5%)	E4 (26.7%)	E4 (21.6%)	H7 (16.0%)
Ранг 3	H9 (10.0%)	I6 (17.8%)	H9 (17.2%)	E (10.7%)
Ранг 4	F3 (8.4%)	(H7)	H7 (12.9%)	(B1, B6, B13 – 19%)

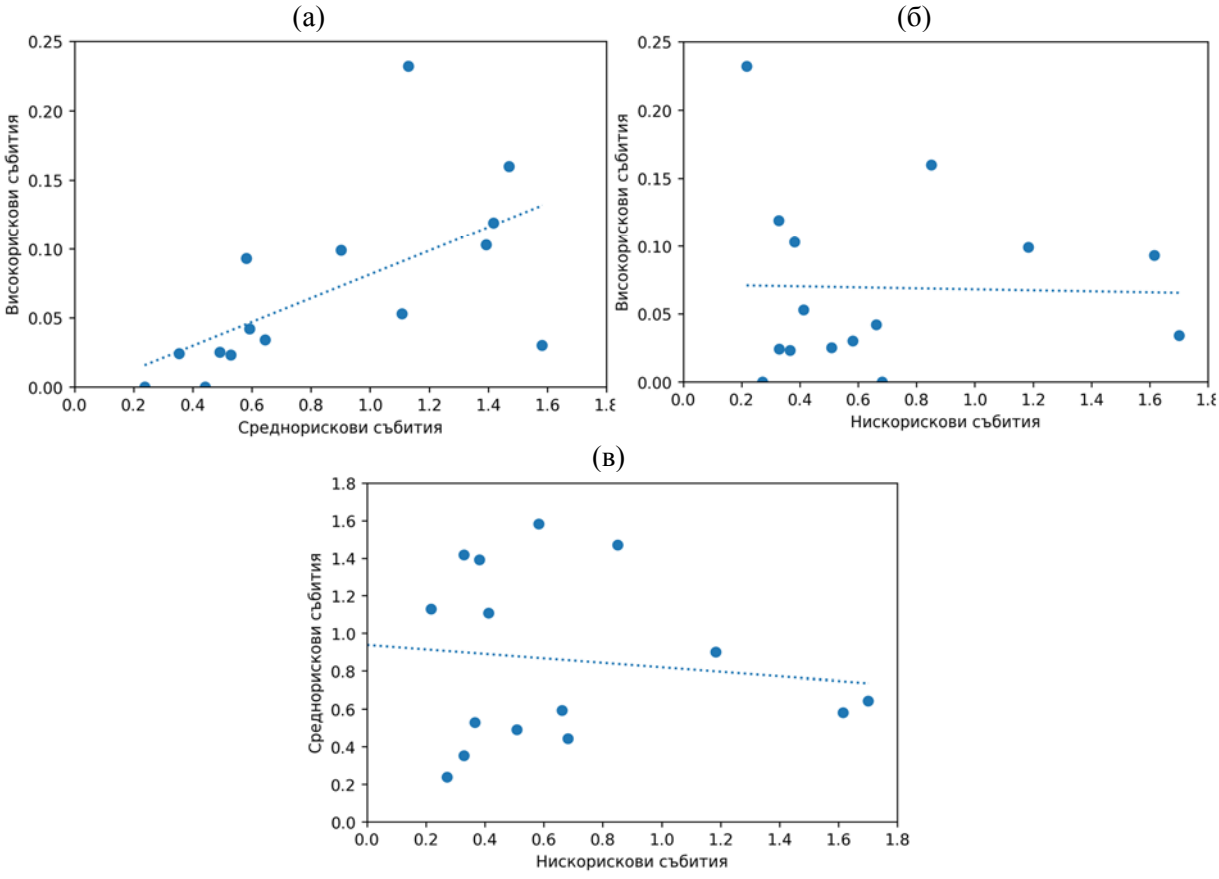

Фигура 2. Връзки между честотата на събития с различен риск:
(а) високорискови-среднорискови събития; (б) високорискови-нискорискови събития;
(в) среднорискови-нискорискови събития.

Честотите на фактор „Самоувереност“ по бази са показани на фигура 3. Разликите са статистически значими. Ясно се вижда, че този фактор е най-силно изразен при база 4, която е установена организация с опит, и най-слабо изразен при база 2, която е нова организация.

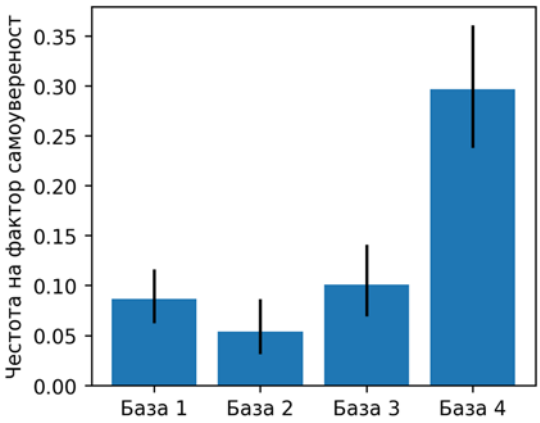

Фигура 3. Честота на фактор самоувереност.

5. Заключение

Направен е преглед на резултатите от прилагане на система за разследване на събития при техническо обслужване MEDA в четири организации за техническо обслужване. Установено е, че честотата на среднорисковите събития е свързана с честотата на високорисковите, докато при нискорисковите събития няма такава връзка. Определени са най-честите причини за събития с висок и среден риск, сред които са самоувереност, неспазване на процеси и процедури, непознаване на процесите в организацията. Също така е показано, че основните фактори варират според нивото на установеност на организацията, като за нова организация са характерни проблеми с упражняването на контрол, а за бързоразвиващите се – притискане от времето. При организацията с опит има значително по-голям дял на грешките, свързани със самоувереност.

Проучването може да се развие, като се увеличи броят на участващите организации и се изследват причинно-следствените връзки както на ниво организация, така и като последователности от събития. Направеното изследване на ниво причини и фактори за събития е основа за по-нататъшно моделиране на ефективността на различни мерки за управление на грешките и риска.

Литература

[1] Regulation (EU) No 1321/2014 on the continuing airworthiness of aircraft and aeronautical products, parts and appliances, and on the approval of organisations and personnel involved in these tasks OJ L 362/1 17.12.2014

[2] Reason J 1997 Approaches to controlling maintenance error *Proc. 11th Federal Aviation Administration Meeting on Human Factors Issues in Aircraft Maintenance and Inspection: Human error in aviation maintenance (Washington DC: Federal Aviation Administration/Office of Aviation Medicine)* 3–12

[3] Saleh J, Ray T A, Zhang K S and Churchwell J S 2019 Maintenance and inspection as risk factors in helicopter accidents: Analysis and recommendations *PloS One* **14**(2) e0211424

[4] Boeing 2013 *Maintenance Error Decision Aid (MEDA)© User's Guide* Maintenance Human Factors, Boeing Commercial Aviation Services

[5] EASA 2018 Annex I (Part-21) to Regulation (EU) No 748/2012 *Airworthiness and Environmental Certification, Easy Access Rules*

[6] ICAO Doc 9859 2018 *Safety Management Manual*, Fourth Edition, Quebec, Canada

[7] Index to FAA Office of Aerospace Medicine Reports: 1961 through 2017, FAA Office of Aerospace Medicine

[8] Reason J 1990 *Human Error* (New York: Cambridge University Press)

[9] Maddox M 2006 Human Factors, *Human Factors Guide for Aviation Maintenance and Inspection*, Chapter 1, FAA

[10] Dupont G 1997 The Dirty Dozen errors in aviation maintenance *Proc. 11th Federal Aviation Administration Meeting on Human Factors Issues in Aircraft Maintenance and Inspection: Human error in aviation maintenance (Washington DC: Federal Aviation Administration/Office of Aviation Medicine)* 45–49
[11] Mellema G M 2018 Application of Dupont's Dirty Dozen Framework to Commercial Aviation Maintenance Incidents *Dissertations and Theses (https://commons.erau.edu/edt/477)* **428**
[12] Reason J 1997 *Managing The Risks Of Organizational Accidents* (Ashgate, Aldershot)
[13] Shappell S and Weigmann D 2000 Human Factors Analysis and Classification System – HFACS. Office of Aviation Medicine Technical Report No. DOT/FAA/AM-00/7 (Civil Aeromedical Institute, Oklahoma City, OK 73125)
[14] Schimidt J, Lawson D 2001 Human factor analysis and classification system – maintenance extension (HFACS-ME) review of select NTSB maintenance mishaps: an update. Department of the Navy, US Government.
[15] Boeing 1994 Maintenance Error Decision Aid Seattle, WA: Boeing Commercial Airplane Group.
[16] Rankin W 2007 MEDA Investigation Process, *AERO Magazine* QTR 2.07 14–21
[17] Rankin W, Shappell S and Wiegmann D 2006 Error and Error Reporting Systems, *Human Factors Guide for Aviation Maintenance and Inspection*, Chapter 7, FAA
[18] Rashid HSJ, Place C S, Braithwaite G R 2013 Investigating the investigations: a retrospective study in the aviation maintenance error causation *Cogn Tech Work* **15** 171-188
[19] Brown L D, Cai T, Dasgupta A 2001 Interval Estimation for a Binomial Proportion *Statist. Sci.* **16(2)** 101–133

A review of errors and violations in maintenance performance in four aircraft maintenance organisations

Krasin Georgiev

TU-Sofia, Department of Aeronautics, 1756 Sofia, 8 Kl. Ohridski Blvd., Bulgaria

krasin@tu-sofia.bg

Abstract. The main purpose of aircraft maintenance is continuing airworthiness but failures of the maintenance system can bring an opposite effect by introducing new hazards and failure/potential failure conditions. Failures of the maintenance system are determined by errors and violations of the maintenance technicians and inspectors and should be studied accounting for the human factor theory. This research analysis the experience of applying a structured process MEDA for investigation of maintenance events in four maintenance organisations. It is shown that the number of medium risk events is related to the number of high risk events. The main causes for maintenance errors/violations are determined. These results are important for further development of effective risk control measures in the corresponding organisations.

Кинематичен анализ на предно окачване Multilink за мотоциклет

С И Хесапчиева[1], Г М Яначков и Д А Хлебарски

Технически университет – София, бул. „Кл. Охридски“ №8, 1000 София, България

[1] E-mail: six@tu-sofia.bg

Резюме. В публикацията са разгледани възможностите за използване на окачване тип Multilink като предно окачване на мотоциклет и реализирането на основните му геометрични характеристики. Направен е кинематичен анализ на поведението на окачването при работа. Разработен е математичен модел, с който се изследва промяната в базата на мотоциклета, рамото на устойчивост, ъгъла на вилката и траекторията, която описва колелото. В модела не се разглежда поведението при описване на крива. Изследвана е ефективността на системата против гмуркане при прилагане на спирачна сила само в предното колело.

1. Въведение

Системата на окачване на мотоциклета изпълнява две основни функции. Първата е да абсорбира неравностите на пътя, като по този начин изолира водача и пътника от протичащите колебания, осигурява плавност на движението, комфорт и безопасност. Втората е да гарантира достатъчно добра управляемост[1]. Най-често срещаният тип предно окачване на мотоциклет е телескопичната вилка. Въпреки предимствата си – простота на конструкцията, ниска цена и лесна поддръжка – предното окачване от този тип има съществени недостатъци [2]. Предното окачване трябва не само да се адаптира към увеличаването на скоростта и масата, но също така да удовлетворява изискванията за управляемост и устойчивост на движението. Окачването на мотоциклета има значение за подобряване на сцеплението и устойчивостта на движение на мотоциклета както при праволинейно движение, така и при описване на крива в завой.

За предно окачване на мотоциклетите са изпробвани разнообразни кинематични схеми. Някои доказват своята ефективност, други не, а трети са твърде скъпи и сложни. Многораменното окачване намира все по-широко приложение както в автомобилостроенето, така и при двуколесните машини, и е обект на задълбочени кинематични и динамични изследвания, както на съществуващи конструкции, така и на разнообразни кинематични схеми [1, 3-13].

Целта на публикацията е да се направи кинематичен анализ на многораменно окачване и влиянието му върху поведението на мотоциклета.

2. Кинематична схема на многораменното окачване

На фигура 1 е показана кинематична схема на предно окачване на мотоциклет тип Multilink. Предното колело 1 е окачено на предната вилка 2. Тя е свързана с рамата на мотоциклета 3 посредством четири носача. Рамената l_2 и l_4 оформят горния носач. Рамената l_1 и l_3 образуват долния носач.

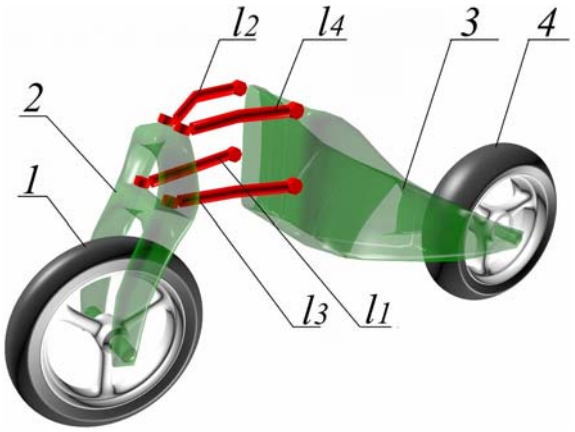

Фигура. 1 Кинематична схема на многораменно окачване. 1 – предно колело, 2 – вилка, 3 – рама, 4 – задно колело, l_1, l_2, l_3, l_4 – дължини на лостовете.

3. Кинематичен анализ

Свойствата управляемост и устойчивост на мотоциклета са силно повлияни от някои геометрични параметри, които зависят от конструкцията на предното окачване. Фигура 2 представя най-важните геометрични параметри на мотоциклета. Това са рамото на устойчивост t, проекцията на рамо на устойчивост t_n, ъгълът на надлъжен наклон на вилката ε и базата w_b [3]. Между тези параметри съществува следната зависимост [9]:

$$t = \frac{t_n}{cos\varepsilon} = R_f tan\varepsilon - \frac{d}{cos\varepsilon}, \quad (1)$$

където R_f е радиусът на предното колело, d – разстоянието от центъра предното колело до кормилната ос.

Задачата на кинематичния анализ е да се определят параметрите на лостовете, така че при деформация в окачването при преодоляване на неравност и в режим на интензивно спиране базата на мотоциклета и рамото на устойчивост да се изменят минимално.

Фигура 2 показва конструктивните параметри на четиризвенника (поглед отстрани): дължините на долните и горните рамена l_1 (OA) и l_2 (BC), разстоянията между точките на закрепване на рамената h_1 (CO) от страната на рамата и h_2 (AB) от към вилката и ъгълът между долното рамо и вертикалната равнина в средно положение Θ_1. С тези пет параметъра се определя напълно кинематиката на механизма. Промяната на който и да е от тях ще повлияе на цялостното поведение на геометричните параметри при хода на окачването. Конфигурациите на тези пет параметъра могат да бъдат изчислени за получаване на различно поведение на окачването.

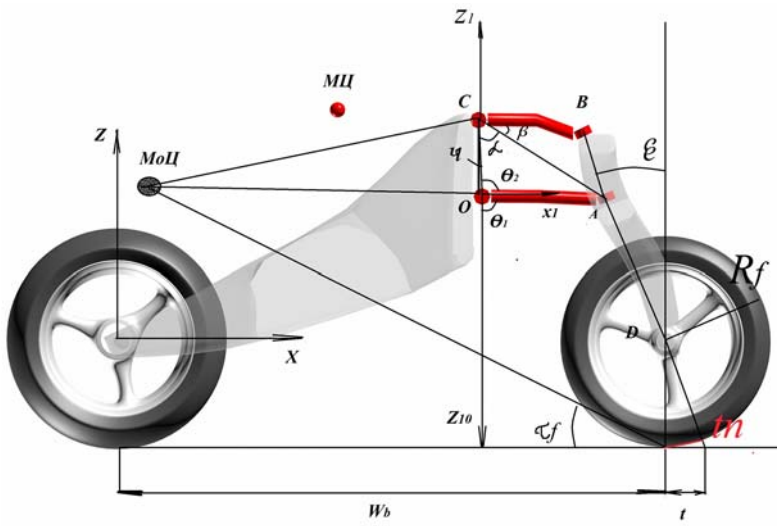

Фигура 2. Геометрични характеристики на мотоциклет и параметри на окачването.

Окачването е представено като равнинен механизъм. Броят степени на свобода се определя от формулата на Чебишев-Грюблер-Куцбах [14]

$$H = 6(n_b - 1) - 5n_r - 3n_s = 1, \quad (2)$$

където n_b е брой тела, n_r – брой цилиндрични шарнири, $3n_s$ – брой сферични шарнири.

Кинематичният анализ се извършва при условно неподвижно задно колело, при праволинейно движение (ъгълът на завъртане на кормилото е нула). Изследват се промените на геометричните параметри във функция на хода на окачването. Определя се и степента на гмуркане (Anti-dive). Изчислението се извършва с програмен продукт Матлаб. Въведена е подвижна координатна система Oz_1x_1, която е свързана с шарнира на долния лост в т. O.

Уравненията на геометричните ограничения се изразяват в декартовите координати на точките, както следва [8]:

$$(B_{x1} - C_{x1})^2 + (B_{z1} - C_{z1})^2 = {l_2}^2; \quad (3)$$

$$(\mathrm{A}_{x1} - \mathrm{O}_{x1})^2 + (\mathrm{A}_{z1} - \mathrm{O}_{z1})^2 = {l_1}^2, \quad (4)$$

където A, B, C, O са точките на закрепване на лостовете.

От фигура 2 могат да се определят моментните положения на точките от окачването [5]

$$\cos\Theta_1 = \frac{z_{1o} - z_{1a}}{l_1}; \quad (5)$$

$$\Theta_2 = \pi - \Theta_1; \quad (6)$$

$$\Theta_3 = \varphi + \beta + \alpha; \quad (7)$$

$$l_d^2 = h_2^2 + l_1^2 - 2h_2 l_1 \cos(\Theta_2 + \varphi); \quad (8)$$

$$l_d = \sqrt{h_2^2 + l_1^2 - 2h_2 l_1 \cos(\Theta_2 + \varphi)}; \quad (9)$$

$$sin\alpha = \frac{l_1}{l_d}\sin(\Theta_2 + \varphi); \quad (10)$$

$$h_1^2 = l_2^2 + l_d^2 - 2l_2 l_d \cos\beta; \quad (11)$$

$$\cos\beta = \frac{l_2^2 + l_d^2 - h_1^2}{2l_2 l_d}. \quad (12)$$

$$A_{x1} = l_1 \sin\Theta_1; \quad (13)$$

$$A_{z1} = -l_1 \cos\Theta_1; \quad (14)$$

$$C_{x1} = -h_2 \sin\varphi; \quad (15)$$

$$C_{z1} = h_2 \cos\varphi; \quad (16)$$

$$B_{x1} = C_{x1} + l_1 \sin\Theta_3; \quad (17)$$

$$B_{z1} = C_{z1} - l_1 \cos\Theta_3; \quad (18)$$

$$D_{x1} = A_{x1} + l_f \tan\varepsilon; \quad (19)$$

$$D_{z1} = A_{z1} + l_f \mathrm{atan}\varepsilon; \quad (20)$$

$$\tan\varepsilon = \frac{A_{x1} - B_{x1}}{B_{z1} - A_{z1}}. \quad (21)$$

Числените стойности и означенията на параметрите, използвани за модела са представени в таблици 1 и 2. За прототип е използван мотоциклет БМВ K1200R [15].

Таблица 1. Числените стойности и означенията на параметрите на мотоциклета.

Параметър	Означение	Стойност	Мерна единица
База	w_b	1571	mm
Наклон на вилката	ε	24	°
Рамо на устойчивост	t	112	mm
Offset	d	46	mm
Радиус на предното колело	R_f	300	mm
Височина на масов център	h_g	675	mm
Ход на окачването	z	70	mm

Таблица 2. Линейни и ъглови размери на елементи от окачването.

Дължина на долните лостове l_1, l_3, mm	230	235	240
Дължина на горните лостове l_2, l_4, mm	195	195	195
Разстояния между точките на закрепване на носачите от страната на рамата h_1, h_3, mm	190	190	190
Разстояния между точките на закрепване на носачите за вилката h_2, h_4, mm	160	160	160
Ъгъл между точките на закрепване φ, °	15	15	15
Ъгъл между долното рамо и вертикалната равнина в средно положение Θ_1,°	97.5	87.5	87.5
Разстояние от пътя до шарнира на лоста z_{1o} mm	635	635	635

4. Свойства на окачването при гмуркане

За произволна геометрия, ефективността на окачването против гмуркане не е постоянна в целия диапазон на хода на окачването. Това е така, защото положението на моментния център на въртене на лостовете (т. МоЦ, фигура 2) се променя при свиване на окачването, а с него и ъгълът τ_f, по който се преразпределят силите при спиране (фигура 2). Ъгъл τ_f се намира от следната зависимост [9]:

$$\tau_f = \text{atan}\frac{N_{tr}}{F_f}, \tag{22}$$

където F_f е спирачната сила в предното колело, N_{tr} –компонента на спирачната сила, породена от преразпределението на теглото.

Ефектът против гмуркане AD се определя по формулата [9]:

$$\text{AD} = F_f \tan\tau_f \frac{w_b}{h_g}. \tag{23}$$

5. Резултати

На фигури 3-7 са представени резултатите от изследването за целия диапазон на окачването. Показани са изменението на рамото на устойчивост, ъгълът на наклона на вилката, траекторията, която описва колелото и промяната на базата на мотоциклета.

От резултатите се вижда, че при промяна на дължината на долния лост, кривите остават със сходен характер. С увеличаване на дължината му без промяна в останалите размери се увеличава надлъжния наклон на вилката, а от там и рамото на устойчивост, но склонността към гмуркане нараства. Редуцирането на ъгъла и рамото на устойчивост водят до намаляване на устойчивостта, но се явява като благоприятен ефект в състезателните мотоциклети при описване на крива [8]. Най-важният критерий по отношение на степента на гмуркането е предпочитанието на водача и предназначението на мотоциклета. Твърде високата степен на т.нар. анти-дайв корекция понякога води до липса на усещане у водача за реакция на мотоциклета.

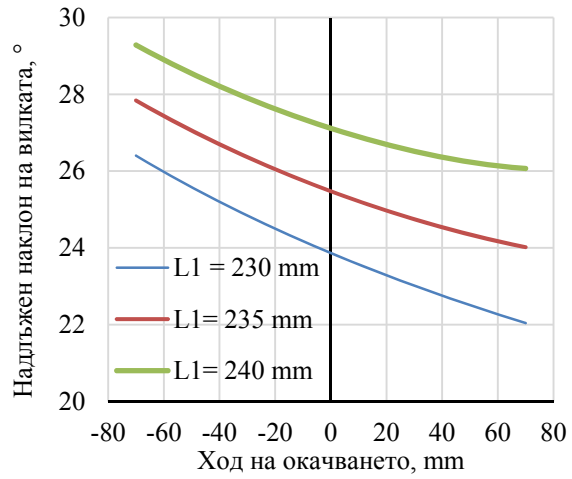

Фигура 3. Изменение на надлъжния наклон на вилката ε във функция на хода на окачването.

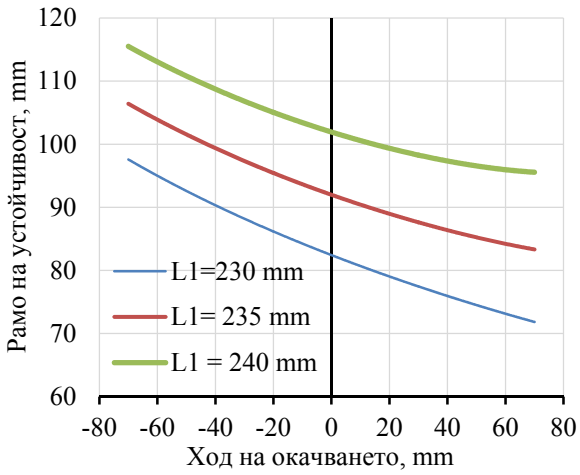

Фигура 4. Изменение на рамото на устойчивост във функция на хода на окачването.

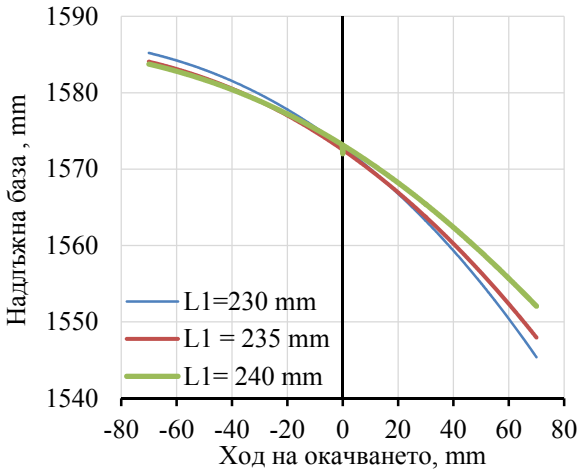

Фигура 5. Надлъжна база на мотоциклета във функция на хода на окачването.

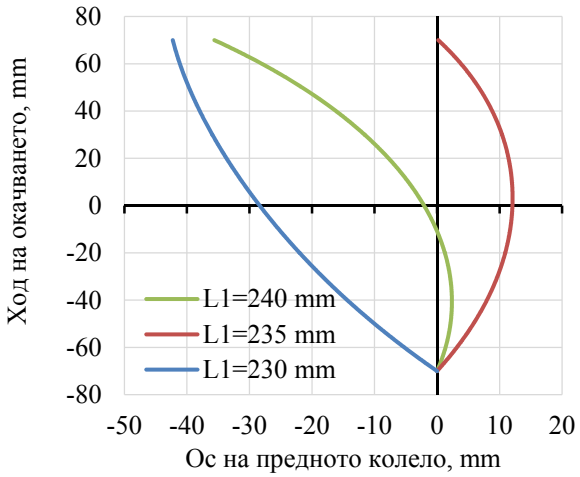

Фигура 6. Траектория на оста на предното колело във функция хода на окачването.

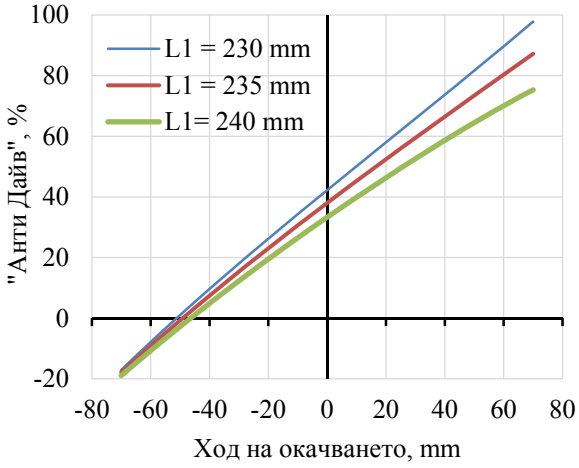

Фигура 7. Изменението на процентното отношение на съпротивлението при гмуркане.

6. Изводи

Многораменното окачване дава възможност за промяна на дължините и разположението на лостовете, с цел да се постигне желаното поведение мотоциклета.

При системата Multilink управлението и окачването са разделени. Системата може да осигури различна степен на „Anti-dive“ ефект, в зависимост от разположението и дължината на рамената. В сравнение с телескопичната вилка, при която законът на движението на центъра на колелото е линеен, при този тип окачване описаната траекторията е нелинейна крива.

В режим на спиране мотоциклетът, оборудван с многораменно окачване е по-устойчив. Рамото на устойчивост остава почти постоянно в целия диапазон на работа на окачването.

Базата на мотоциклета остава почти постоянна в целия диапазон на окачването. При оптимизиране на кинематиката на окачването може да се постигне дори повишаване на линейните размери на базата при свиване окачването [4].

Кинематичният анализ може да бъде използван за оптимизиране на окачването, якостен и динамичен анализ, които ще бъдат изследвани в следващи публикации.

Благодарности

Научните изследвания, резултатите от които са представени в настоящата публикация, са финансирани по договор № 192ПД0001-04 от Вътрешния конкурс на ТУ-София, 2019 г.

Литература

[1] Liu C 2017 *A Multibody Dynamics Model of a Motorcycle with a Multi-link Front Suspension* (Electronic Theses and Dissertations)
[2] Yanachkov G and Hesapchieva S 2017 Using Multilink type suspension as a front suspension for a motorcycle *FDIBA Conference*
[3] Ramírez C M, Tomás-Rodríguez M and Evangelou S A 2018 Dynamic analysis of double wishbone front suspension systems on sport motorcycles *Nonlinear Dynamics* **91(4)** 2347–68
[4] Ramírez C M, Tomas-Rodriguez M and Evangelou S A 2012 Dynamical analysis of a duolever suspension system *Proc. 2012 UKACC Int. Conf. on Control* 1106–1111
[5] Lange J 2015 Development of front suspension for an electric two-wheeled amphibious vehicle *Master of Science Thesis, Industrial Engineering and Management, Stockholm*
[6] Kanade A, Gadakh S, Jadhav P, Kadam V and Sudke D, 2019 Duolever suspension system in motorcycle, *Int. Res. J. Engineering and Technology (IRJET)* **06(4)**
[7] Mavroudakis B and Eberhard P 2006 Analysis of alternative front suspension systems for motorcycles *Vehicle system dynamics* **44(1)** 679–689
[8] Foale T 2006 Motorcycle handling and chassis design: the art and science *Tony Foale*
[9] Cossalter V 2006 Motorcycle Dynamics (Lulu.com)
[10] Watanabe Y and Sayers M W 2011 The effect of nonlinear suspension kinematics on the simulated pitching and cornering behavior of motorcycles *SAE Technical Paper 2011-01-0960*
[11] Minaker B P and Durfy B 2016 A multibody dynamic analysis of a motorcycle with a Multilink front suspension *Proc. Bicycle and Motorcycle Dynamics, Milwaukee, Wisconsin, USA*
[12] Gadola M, Chindamo D, Vitale F and Bonera E 2019 The design of a motorcycle featuring fully independent adjustability for front suspension and steering geometry *IOP Conf. Ser.: Materials Science and Engineering* **538(1)** 012064
[13] *Proc. Bicycle and Motorcycle Dynamics, Milwaukee, Wisconsin, USA,* 2016
[14] George R and Sidhant R 2018 Development of Kinematic Analysis Methods for Spatial Multi-link Road Vehicle Suspensions (*Master's thesis*).
[15] 2006 BMW K 1200 R (USA) Owner's Manual

Kinematic analysis of the Multilink front suspension for a motorcycle

S I Hesapchieva[1], G M Yanachkov, D A Hlebarski

Technical University – Sofia, 8 Kliment Ohridski Blvd., 1000 Sofia, Bulgaria

[1] E-mail: six@tu-sofia.bg

Abstract. The paper discusses the possibilities of using a Multilink suspension as a front suspension of a motorcycle and realizing its basic geometric characteristics. A kinematic analysis of the deformation behavior of the suspension was made. A mathematical model has been developed to investigate the change in the motorcycle base, the trail, the caster angle and the trajectory that describes the contact spot of the wheel. The model does not consider the behavior when driving in a curve. The result of the anti-dive effect when applying braking force only to the front wheel was investigated.

Оценка на жизнения цикъл на автомобили, използващи за гориво пропан-бутан и природен газ

Иван Евтимов[1], Росен Иванов и Христо Станчев

Русенски университет „Ангел Кънчев“, ул. „Студентска“ №8, Русе, България

[1] E-mail: ievtimov@uni-ruse.bg

Резюме. Оценка на жизнения цикъл на автомобили, използващи за гориво пропан-бутан и природен газ. В статията е направена оценка на жизнения цикъл на автомобили, използващи за гориво природен газ и газ пропан-бутан. Оценката е направена въз основа на съществуващите стандарти за жизнения цикъл на превозните средства по отношение на вложената първичната енергия и отделените вредни емисии, приведени към CO_2 (въглероден двуокис). Като база за сравнение са представени изследвания за целия жизнен цикъл на автомобили, използващи за гориво бензин. За да бъдат съпостави направените изследвания оценката е направена при еднаква маса на автомобилите и разход на гориво, отделящо при изгарянето си една и съща енергия. В подходящ вид са представени получените резултати и направени съответните изводи. Резултатите от това изследване биха могли да послужат като полезна информация, относно въздействието на различните горива върху околната среда, свързано с глобалното затопляне. Те не трябва да се разглеждат като абсолютно точна прогноза, а по-скоро като индикативна симулация, за да се покажат екологичните предимства на отделните горива.

1. Въведение

Автомобилите, използващи като горива природен газ (NG –natural gas) и газ пропан-бутан могат да се разделят на следните групи:

- специализирани автомобили (Dedicated vehicles);
- автомобили, работещи с два вида горива, с възможност за превключване работата на двигателя от един вид на друг (bi-fuel vehicles).
- автомобили, работещи с два вида горива, като едното се използва за подобряване процеса на горене (dual fuel vehicles).

Предимствата на природния газ като гориво за превозните средства е неговото изобилие и широко разпространената инфраструктура за разпределение. При изгарянето му се отделят по-малко вредни емисии – до 30% намаление на емисиите на парникови газове (GHG) за лекотоварните автомобили и до 23% намаление за средни до тежкотоварни автомобили, в сравнение с конвенционалните автомобили [1, 2].

В [3] се оценяват вредните емисии в отработилите газове на горивата бензин и природен газ на лекотоварни автомобили. Посочва се, че природният газ отделя приблизително 6÷11% по-ниски нива на вредни емисии в сравнение с бензина през целия жизнен цикъл на горивата.

Голяма част от вредните емисии, отделяни през жизнения цикъл на природния газ са предимно резултат от изтичането му по време на производствения цикъл [4]. Общо през целия жизнен цикъл загубите от изтичане на природен газ се движи в границите от 0.2 до 17.3%, но

агенцията за опазване на околната среда (EPA – Environmental Protection Agency) регламентира 1,5% загуби [5, 6].

Дали природният газ, използван като гориво в автомобилите или електрическите централи, има по-ниски емисии на парникови газове от жизнения цикъл от въглищата и петрола, зависи от степента на изтичане по време на извличането и транспортирането му, реалният потенциал на глобалното затопляне на природния газ, ефективността на преобразуване на енергия и други фактори. Установено е, че загубите от природен газ трябва да се поддържат под 3.2%, за да могат електрическите централи, използващи като гориво природен газ да имат по-ниски емисии за жизнения цикъл, отколкото въглищните електрически централи за кратки срокове поне от 20 години. Използването на природен газ в превозните средства ще доведе до определени ползи, ако загубите от природен газ бъдат неповече от 1 до 1.6% в сравнение с дизеловото гориво и бензина. Разбира се, съществуват съвременни технологии за намаляване на голяма част от изтичащия метан, но внедряването им е ограничено основно от политически и икономически причини [7].

Всичко досега, изложено в изследванията в тази насока, е с неясни и непълни заключения относно оценката на влиянието на различните видове горива върху отделяните въглеродни емисии през жизнения им цикъл. Това се дължи на различните методи на изследвания с доста широк интервал на изменение на стойностите на определени параметри при отделните етапи на жизнения цикъл.

2. Изложение

2.1. Методология за оценка на жизнения цикъл

През последните години оценката на жизнения цикъл се превърна в основен инструмент в научните изследвания с цел да се изследва целият жизнен цикъл на даден продукт по отношение неговото устойчиво развитие [8]. Оценката обхваща всички процеси, свързани с функционирането на даден продукт – от добива на суровини за производството, използването и рециклирането му. Резултатите от това изследване не трябва да се разглеждат като абсолютно точна прогноза, а по-скоро индикативна симулация, за да се осветлят положителните и отрицателните страни на различните видове горива върху отработените емисии и отражението им върху глобалното затопляне.

За тази оценка е подходящо да се използват по-високите стойности на топлината на изгаряне, тъй като тя отразява истинското енергийно съдържание на горивата, основано на принципа на запазване на енергията (таблица 1).

При направеното изследване са приети следните условия: еднакви маси на автомобилите, използващи горивата бензин, природен газ и пропан-бутан; разход на гориво (бензин) на бензиновия автомобил – 7.6 l/100 km; разход на природен газ при еквивалентното количество енергия – 4.43 kg/100 km; разход на пропан-бутан при еквивалентното количество енергия – 10.2 l/100km; пробег за жизнения цикъл на превозните средства – 290 000 km; разход на енергия за производство на превозните средство – 11 900 kWh [1]; отделени CO_2 емисии от изгарянето на бензин – 240.82 g/kWh; природен газ – 183.96 g/kWh; газ пропан-бутан – 214.48 g/kWh [9]; КПД при производството на LPG – 94% [10]; КПД при производството на природен газ – 91% [10]; КПД при производството на бензин – 89.1% [10]; загуби при изтичане на природен газ – 1.5% [6]; загуби при втечняване на природния газ – 8% [11].

Оценката на жизнения цикъл на автомобилите, работещи с различни горива обикновено включва въздействия, свързани с производството на суровини, транспортиране, рафиниране, дистрибуция и разход на гориво за превозни средства. Някои от етапите на процеса са изключени от анализа поради значително големите отклонения на определени параметри. Например транспортиране на горивото и изградените съоръжения за производството, транспортиране и съхранение. На фигури 1 и 2 са показани общите етапи на жизнения цикъл на различните горива, включително производство и рециклиране на превозните средства [11-16].

Въглеродните емисии, отделяни от автомобилите при всеки вид използвано гориво се изчислява на базата на целия жизнен цикъл, който включва емисии от производството на автомобила, производството на горивата и съответните суровини, и изгарянето на горивата през време на жизнения цикъл на автомобилите.

Пропан-бутанът се разглежда като съвместен продукт на горива, получени от петрол или природен газ, което дава основание да се разпределят отделените емисии при производството на природен газ и рафиниране на суров нефт. Този подход намалява тежестта на вредните емисии от природния газ и споделя емисиите с пропан-бутан.

Въздействието на природния газ върху глобалното затопляне се приема, съгласно оценката на IPCC – Intergovernmental Panel on Climate Change, с потенциал за глобално затопляне (global warming potential – GWP) 25 [17].

Таблица 1. Физико-механични свойства на автомобилните горива.

Параметри	Бензин	Втечнен нефтен газ	Природен газ
Химична формула	C_8H_{17}	$C_3H_8 + C_4H_{10}$	CH_4
Топлина на изгаряне, (LHV–HHV), MJ/kg	43.45÷46.54	47÷50	45.86÷59.84 49÷55*
Енергийна плътност, (LHV–HHV), MJ/l	31.16÷34.90	23÷26	$(35.22÷39.05).10^{-3}$
Относителна плътност при 20 °C, kg/l	0.72÷0.76	0.50÷0.58	$0.7166.10^{-3}$ 0.4218*
Температура на самовъзпламеняване, °C	228÷471	365÷470	632
Октаново число (RON)	91÷98	94÷112	135
Молекулярна маса, g/mol	102÷107	44÷58	16.04
Стехиометрично съотношение	14.96	15.4	17.2
Температура на кипене, °C	80÷225	–42÷–0.5	–161.58

* течна фаза

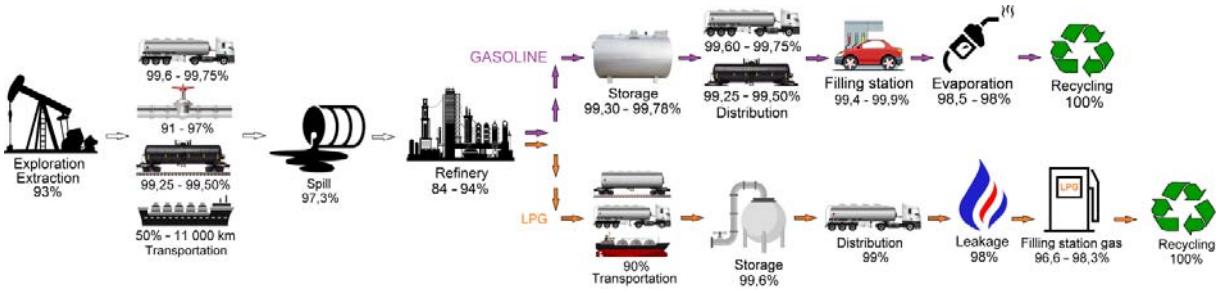

Фигура. 1. Етапи от жизнения цикъл при производството на бензин и LPG.

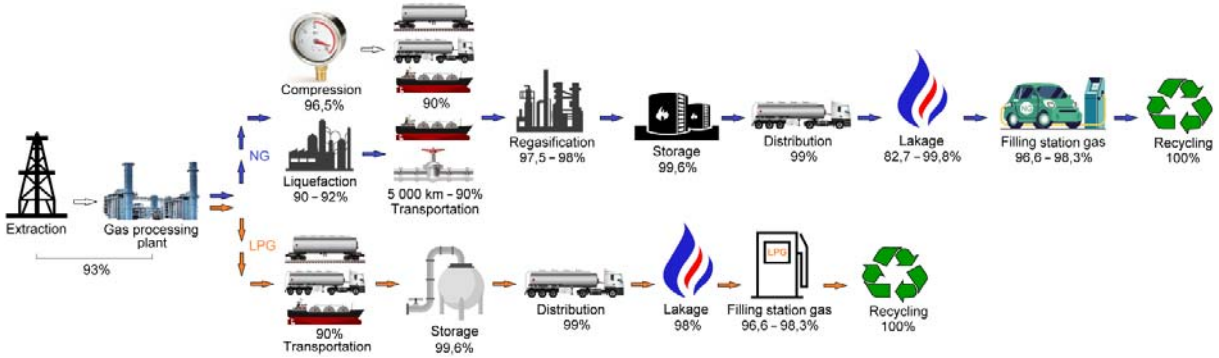

Фигура. 2. Етапи от жизнения цикъл при производството на NG и LPG.

2.2. Специализирани автомобили (Dedicated vehicles)

Специализираните автомобили са разработени специално да използват като гориво природен газ (CNG – compressed natural gas). Автомобилите с гориво природен газ (NGVs – natural gas vehicles) все повече подобряват експлоатационните си свойства по отношение на безопасност. При изминаване на дълги разстояния е за предпочитане да се използва втечненият природен газ (LNG – liquefied natural gas). В света повече от 22 милиона автомобили се движат на природен газ, като 10% от тях са в Европа. Устройството на специализиран автомобил работещ с природен газ е показано на фигури 3 и 4.

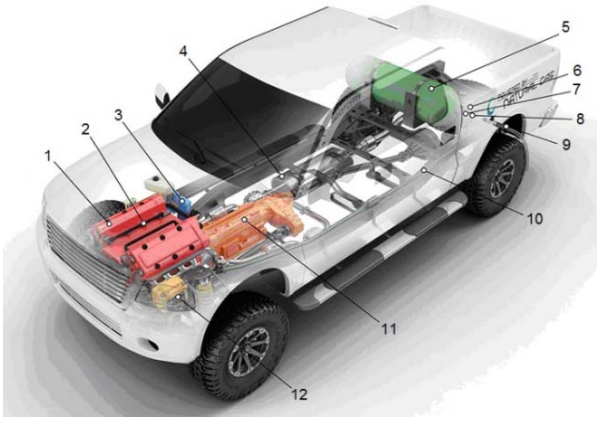

Фигура 3. Устройство на специално разработен лек автомобил за работа с CNG:
1 – ДВГ; 2 – инжекционна система за пръскане на гориво; 3 – електронен контролен модул; 4 – ауспухна система; 5 – контейнер за гориво; 6 – ръчно включване и изключване на горивото; 7 – регулатор за високо налягане; 8 – филтър; 9 – зареждане с гориво; 0 – горивен тръбопровод; 11 – трансмисия; 12 – акумулаторна батерия.

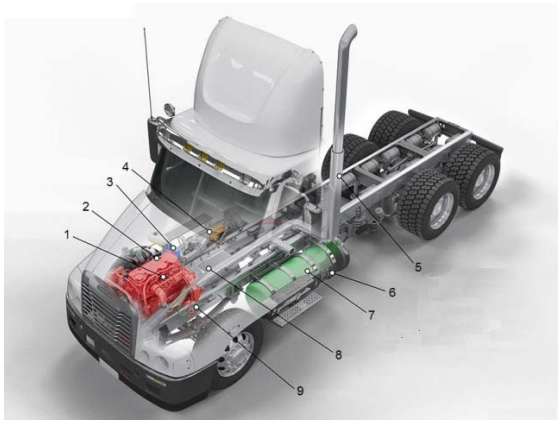

Фигура 4. Устройство на специално разработен товарен автомобил за работа с LNG:
1 – инжекционна система за пръскане на гориво; 2 – ДВГ; 3 – електронен контролен модул; 4 – акумулаторна батерия; 5 – ауспухна система; 6 – горивен филтър; 7 – контейнер за гориво; 8 – трансмисия ; 9 – горивен тръбопровод.

2.3. Автомобили, работещи с два вида горива, с възможност за превключване работата на двигателя от един вид на друг (bi-fuel vehicles)

Тези превозни средства използват два вида гориво. Едното е бензин или дизелово гориво, а другото – природен газ, втечнен нефтен газ (liquefied petroleum gas – LPG) наречен още пропан-бутан или водород. Двете горива се съхраняват в отделни резервоари и имат възможност за превключване от едното към другото гориво, ръчно или автоматично (фигура 5).

2.4. Автомобили, работещи с два вида горива, като едното се използва за подобряване процеса на горене (dual fuel vehicles)

Използването на два вида с цел подобряване процеса на горене намира приложение най-вече при тежкотоварните автомобили [18, 19]. Те притежават горивни системи, работещи с природен газ, но използват дизелово гориво за подобряване процеса на горене. При работа едновременно на двете горива, природният газ се въвежда при ниско налягане и се смесва с всмукателния въздух. Дизеловото гориво се вкарва директно в горивната камера в края на хода компресия и се използва за запалване на слаба смес от природен газ и въздух. По този начин се подобряват характеристиките на двигателя и се повишава ефективността от използването на природен газ в сравнение с традиционните двигатели, работещи само с природен газ. Тъй като въздухът и природния газ са предварително смесени в цилиндъра, тези двигатели имат много общи черти с искровото

запалване Обикновено двата вида горива се използват при отношение 60/40% в полза на природния газ. По-високи съотношения са възможни само чрез конструктивни подобрения на двигателя. При необходимост тези двигатели могат да работят само с дизелово гориво.

Като гориво в много случаи се използва LNG (поради неговата по-голяма енергийна плътност от тази на CNG), особено подходящ за товарни автомобили от 7 и 8 клас (Heavy trucks), със собствена маса над 11 794 kg при превоз на товари на дълги разстояния.

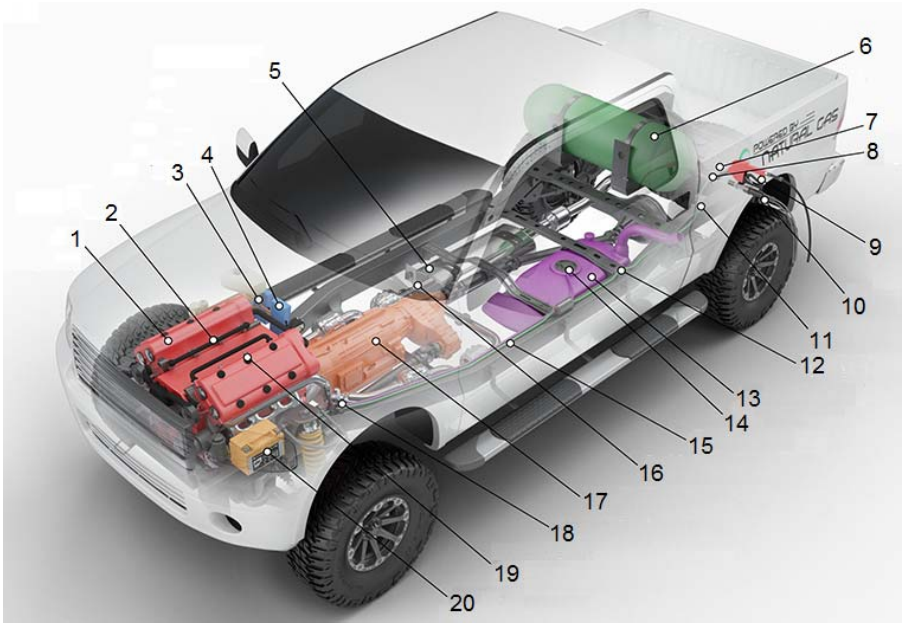

Фигура 5. Устройство на автомобил, работещ с два вида горива, с възможност за превключване работата на двигателя от един вид на друг (bi-fuel vehicles):

1 – ДВГ; 2 – инжекционна система (природен газ); 3 – електронен контролен модул(бензин); 4 – електронен контролен модул (природен газ); 5 – ауспухна система; 6 – контейнер за природен газ; 7 – ръчно включване и изключване на горивото; 8 – регулатор за високо налягане; 9 – зареждане с гориво (бензин); 10 – зареждане с гориво (природен газ); 11 – филтър за гориво (природен газ); 12 – горивен тръбопровод (природен газ); 13 – резервоар за гориво (бензин); 14 – помпа за гориво (бензин); 15 – горивен тръбопровод (бензин); 16 – превключвател за избор на гориво; 17 – трансмисия; 18 – сензор (натурален газ); 19 – инжекционна система (бензин); 20 – акумулаторна батерия

2.5. Природен газ (NG)

Извлечен от земните находища, природният газ представлява смес от няколко газа и съдържание на вода. А като гориво в транспортните средства се състои основно от метан. Въпреки че в добивания от находищата природен газ също се съдържа основно метан, в състава му може да има още етан, пропан, бутан, водни пари, сероводород, въглероден двуокис, азот, хелий и пясък. Много от тези компоненти при преработването на природния газ трябва да бъдат отстранени за да се повиши ефективността при транспортирането му, най-вече по магистрални газопроводи.

Природният газ, съдържащ 98% метан, при втечняване заема 0.17% от обема на същото количество в газообразно състояние. Процесът на втечняване включва пречистване чрез отделяне на определени компоненти като например прах, въглероден диоксид, сероводород, хелий, вода и тежки въглеводороди, които биха причинили затруднения при превръщането на газа в течност. Температурата на охлаждане е приблизително –162 °C. Енергийната плътност на втечнения природен газ е 2.4 пъти по-висока от тази на сгъстения. По-лек е от въздуха и при изпускане в атмосферата „отлита” във въздушното пространство. Спрямо другите видове горива

за двигатели с вътрешно горене (ДВГ), природният газ има най-висока детонационна устойчивост при горене. Октановото му число е между 105÷110 единици, което позволява да се повиши степента на сгъстяване на ДВГ и да се подобри горивната им икономичност. По-пълно изгаря при смесването му с въздуха, поради еднаквите им агрегатни състояния.

При бензиновите двигатели природният газ може да замени 100% бензина.

Освен изкопаемият природен газ намира приложение и възобновяемият природен газ (RNG – renewable natural gas). Произвежда се от органични суровини от селското стопанство, хранително-вкусовата промишленост и от отпадъци), известен също като биометан. Той е химически идентичен с изкопаемия природен газ, но при изгарянето си дава далеч по-малко емисии парникови газове. Смесването на относително малки количества RNG с изкопаем природен газ осигурява намаляване на емисиите на парникови газове през жизнения цикъл.

Основният недостатък на природния газ като гориво за ДВГ е ниската му обемна концентрация на енергия. Поради тази причина се налага да се осигури достатъчен запас от гориво, което може да се реализира по следните начини:

- чрез сгъстяване до високо налягане до 20÷22 MPa;
- чрез втечняваме на природния газ до минус 162 °C;
- чрез получаване на метанол от природния газ.

Най-широко приложение е намерил първият начин – сгъстяване до 20÷22 MPa в специални контейнери, изработени от легирана стомана или от леки сплави с усилена конструкция от метални нишки.

2.6. Втечнен нефтен газ (LPG)

При автомобилите, работещи с LPG се използват следните горивни системи:

- система с конверсия чрез изпарител и смесител;
- система за впръскване на горивото с газови инжекционни.

Първата система доминира от десетилетия и все още намира широко приложение. Това са така наречените обикновени газови уредби. Втората система е най-популярна през последните години, поради по-добро управление на горивния процес в цилиндрите на двигателя.

Втечненият нефтен газ (Liquefied Petroleum Gas – LPG) е съвместен продукт от производството на природен газ, производството и рафинирането на суров нефт. Пропан-бутанът се отделя от суровия нефт и природен газ по време на извличането им. Природният газ съдържа главно метан, но и други вещества, сред които и по-тежки въглеводороди, т.е. включително C_3 и C_4. Подготовката му за транспорт изисква отстраняването на LPG фракцията – дегазиране. Също така се получават допълнителни количества LPG при стабилизиране на суров нефт при извличането му, като част от подготовката на нефта за транспорт. Счита се, че в световен мащаб около 60% пропан-бутан се получава по този начин. Останалите 40% пропан-бутан се получават по време на рафинирането на нефт. В зависимост от вида суров нефт, той може да съдържа от 1 до 4% фракция на пропан-бутан [20].

LPG е газообразен при нормални температури и атмосферно налягане, а се доставя втечнен под налягане в стоманени бутилки. Съотношението между обемите на изпарения газ и втечнения газ варира в зависимост от състава, налягането и температурата, но обикновено е около 250:1. Налягането, при което LPG се втечнява, (налягане на наситените пари), също варира в зависимост от състава и температурата, като е около 0.22 MPa за чист бутан при 20 °C, и около 2.2 MPa за чист пропан при 55 °C.

Пропан-бутанът няма да създаде опасност за околната среда, ако бъде освободен като течност или пара във водата или почвата. Ако се разлее в голямо количество, единствените щети върху околната среда, които могат да се появят, е замръзване на всеки организъм или растителен живот в непосредствена близост. Все още не са регистрирани дългосрочни последици вследствие на разлив на газ пропан – бутан, дори при големи количествата. Единствено големи щети могат да възникнат, ако след разлива, парите биват възпламенени.

Основна разлика между конвенционалните горива и LPG е съхранението, тъй като LPG е газообразен при стайна температура и атмосферно налягане. По този начин са необходими резервоари за съхранение под налягане както в бензиностанциите, така и в превозните средства. Поради конструкцията, устойчива на налягане, резервоарите за втечнен нефтен газ са малко по-скъпи, по-тежки и изискват повече пространство от бензиновите или дизеловите резервоари.

2.7. Математичен модел за оценка на жизнения цикъл на автомобили, използващи горива бензин, природен газ и втечнен нефтен газ по отношение на първичната енергия, необходима за производството и експлоатацията им

Първичната енергия за жизнения цикъл на автомобилите при използване на различни горива, може да се представи със следния математичен модел

$$E_P = \frac{1}{\eta_T} \sum_{i=1}^{n} \frac{\alpha_i}{\eta_i} \left(E_{MV} + E_{PF} + E_{C(L)F} + E_{L(E)} \right), \text{kWh}, \tag{1}$$

където α_i е процентният дял на електрическата енергия, произведена от различните видове електроцентрали, спрямо общо произведената енергия; η_T – КПД при пренос на електрическа енергия; η_i – КПД на електроцентралите, с отчитане цикъла на производство и транспортиране на горивата им ; E_{MV} – енергията, необходима за производство и рециклирането на превозните средства, kWh; E_{PF} – енергията, необходима за производство на горивото, kWh; $E_{C(L)F}$ – енергията, необходима за компресиране или втечняване на горивото, kWh; $E_{L(E)}$ – енергията, изгубена вследствие изтичане или изпарение на горивото, kWh.

2.8. Математичен модел за оценка на жизнения цикъл на автомобили, използващи горива бензин, природен газ и втечнен нефтен газ по отношение на отделените вредни емисии, приведени към въглероден двуокис

Отделените CO_2 емисии за жизнения цикъл на горивата и превозните средства, могат да се представят със следния математичен модел

$$CO_2\, emissions = c\, E_{MV} + 10^{-2} c \left(1 - \eta_F\right) k_F\, Q\, L + 10^{-2} c_F\, k_F\, Q L + c_{GWP}\, Q_L =$$

$$= c\, E_{EM} + 10^{-2}\, k_F\, Q L \left[c\left(1 - \eta_F\right) + c_F \right] + c_{GWP}\, Q_L, \text{ kg} \tag{2}$$

където c е емисионният фактор при производство на електрическа енергия, kg CO_2/kWh; η_F – КПД при производството на горивото; k_F – калоричността на горивото, kWh/kg или kWh/l; Q – разходът на гориво, l/100 km или kg/100 km; L – пробегът на автомобила за жизнения цикъл, km; c_F – емисионният фактор при изгаряне на горивото, kg CO_2/kWh; c_{GWP} – потенциал на глобалното затопляне; Q_L – изтекло гориво, kg.

3. Резултати от изследването

При изследването е прието за изработването шасито на автомобила да се изразходва 11 900 kWh енергия [12]. Като цяло жизненият цикъл на автомобил с бензин, произведен и задвижван в България, се нуждае от приблизително 309 750 kWh първична енергия. Около 86.5% от енергията на жизнения цикъл се изразходва за движение. Този процент зависи от енергията за производство на автомобили в съответната държава, а последната зависи от енергийния микс. Енергията за експлоатация се променя незначително в различните страни и основно зависи от загубите в процеса на производство на гориво. Други етапи от жизнения цикъл на CV, като производството на превозни средства и ремонт на части, транспорт на продукцията и др., Консумират по-малко енергия – 13.5% от жизнения цикъл или приблизително 42 000 kWh.

Разходът на природен газ при еквивалентното количество енергия съответстващо на 7.6 l/100 km бензин е 4.43 kg/100 km. За целия жизнен цикъл ще се изразходват общо 12 847 kg. При емисионен фактор 183.96 g/kWh, общо през време на експлоатацията на автомобила ще се отделят 39 280 kg CO_2 емисии.

Разходът на LPG при еквивалентното количество енергия, съответстващо на 7.6 l/100 km бензин е 10.2 l/100 km. За целия жизнен цикъл са изразходени 29 580 литра LPG. При приет емисионен фактор на горивото 214.48 g/kWh, се получа общо количество CO_2 емисии за жизнения цикъл 45 820 kg.

При природния газ възниква променлива и несигурна част на емисиите на парникови газове, поради изтичане на метан в атмосферата през жизнения му цикъл. В [6] се посочва (въз основа на 26 публикации за периода 2012÷2015 г.) ,че загубите на метан от изтичане в атмосферата варират в твърде широки граници (от 0.2% до 17.3%). По-високите стойности вероятно. по-широки доверителни интервали при изследването. Въпреки това Агенцията за защита на околната среда (EPA – Environmental Protection Agency) заключават, че степента на загуба на изтичане на природен газ за САЩ е 1.5%. Следователно влиянието на тези загуби върху глобалното затопляне за жизнения цикъл на автомобила приведени към CO_2 с потенциал за затопляне на атмосферата 25, съгласно доклад за оценка на Междуправителствения комитет по изменение на климата (IPCC – Intergovernmental Panel on Climate Change) биха повишили отделените CO_2 емисии с 4 820 kg CO_2 емисии.

За жизненият цикъл на бензиновия автомобил, произведен и експлоатиран в България, се нуждае от 309 750 kWh първична енергия (фигура 6а). Около 86.5% от енергията на жизнения цикъл се изразходва за движение. Този процент зависи от енергията за производство на автомобила в съответната държава, а последната зависи от енергийния микс.

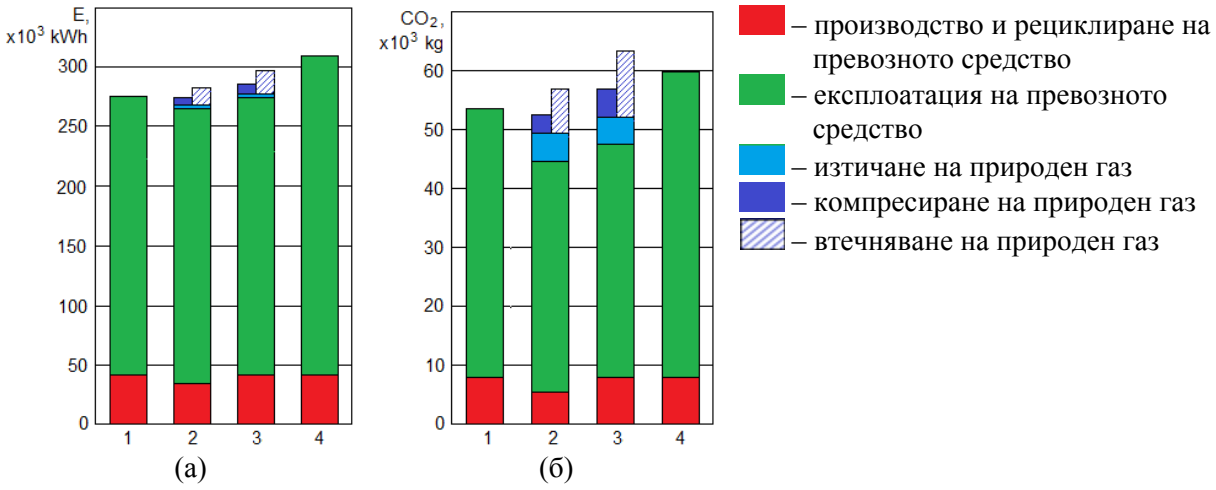

Фигура 6. Първична енергия (а) и CO_2 емисии (б) на превозни средства с различни горива за жизнения им цикъл:
1 – автомобил, произведен и експлоатиран в България, ползващ гориво LPG;
2 – автомобил, произведен и експлоатиран с енергийния микс на EU-28, ползващ гориво NG;
3 – автомобил, произведен и експлоатиран в България, ползващ гориво NG;
4 – автомобил, произведен и експлоатиран в България, ползващ гориво бензин.

Енергията за движение, се променя незначително в различните страни и основно зависи от загубите в процеса на производство на гориво. Други етапи от жизнения цикъл на бензиновия автомобил, като производство на превозното средство и ремонт на части, транспорт на производството и др., консумират по-малко енергия – 13.5% от енергийния цикъл на живота или около 42 000 kWh. При автомобили 3, произведен и експлоатиран в България, използващ гориво природен газ, първичната енергия е в границите от 285 690 до 295 310 kWh, в зависимост от агрегатното състояние на природния газ – компресиран или втечнен. При автомобил 2, произведен и експлоатиран с енергийния микс на EU-28, първичната енергия би се движила в границите от 274 920 до 283 030 kWh, по-малко с 3.9÷4.4%. За автомобил 1, използващ гориво LPG, произведен и експлоатиран в България, първичната енергия за жизнения му цикъл е 274 390 kWh.

Разликата в първичната енергия на автомобилите, ползващи различни горива, се дължи на различните разходи на енергия за производство на горивата и средния микс при производство на електрическа енергия.

Емисиите парникови газове (приведени в еквивалент на CO_2), генерирани по време на целия жизнен цикъл на конвенционалните автомобил с гориво бензин, произведен и експлоатиран в България, е 59 750 kg (фигура 6б). При приетите условия за оценка на жизнения цикъл, за различните европейски страни, тези емисии биха се колебали около тази стойност в зависимост от ефективността при производството на горивото и енергийния микс на страната.

Общо отделените CO_2 емисии за автомобила произведен и експлоатиран у нас при използване на CNG са 57 060 kg, а при използване на LNG – 63 490 kg. За същия автомобил с осреднени данни за емисионния фактор при производство на електрическа енергия 447 g/kWh са както следва: при използване на CNG – 52 770 kg, а с LNG – 57 070 kg. Съществено влияние върху тези емисии оказва изтичането на природен газ в атмосферата и отделените емисии при втечняването му. В процентно отношение, спрямо емисиите по време на експлоатацията, са както следва: 12% CO_2 емисии от изтичане на природен газ в атмосферата и 19÷21% при втечняване. Последните зависят основно от емисионния фактор при производството на електрическа енергия. Възможност за намаляване на тези емисии е използване на възобновяема енергия.

Отделените CO_2 емисии при използване на LPG за жизнения цикъл са 53 780 kg, с 10% по-малко отколкото конвенционалния автомобил с гориво бензин.

В табл. 2 са показани числените резултати за енергийните разходи и отделените емисии CO_2 за разглежданите автомобили, отнесени за единица път – 1 km.

Таблица 2. Енергия и емисии CO_2 за 1 km.

Превозно средство	E, kWh/km	CO_2, g/km
1	0.946	186
2	0.948÷0.976	182÷197
3	0.985÷1.018	197÷219
4	1.068	206

4. Заключение

Въз основа на направеното изследване, могат да се направят следните по-важни извода:

1. По отношение на първичната енергия, необходима за производството на автомобилите и съответните горива, най-енергоемки са автомобилите с бензиново гориво, приблизително 11÷12% по-голяма от автомобилите, използващи гориво пропан-бутан. Тази разлика се дължи на технологията на производство на различните горива и енергийния микс на страните, в които се произвеждат и експлоатират.

2. Най-ефективни, по отношение на въглеродните емисии са автомобилите, използващи гориво пропан-бутан – 186 g/km.

3. Производството и експлоатацията на природния газ са свързани с изтичането му в атмосферата, което се отразява с 12% на вредните емисии за целия жизнен цикъл при приетите условия на изследването. Допълнително се отделят немалко емисии при неговото компресиране и втечняване, което в действителност намалява в голяма степен предимствата му като екологично гориво.

4. Вредните емисии на автомобилите с гориво природен газ може до голяма степен да се намалят чрез подобряване технологиите на производство, транспортиране и съхранение на природния газ със значително повишаване делът на възобновяемата енергия в енергийния микс на страната.

Благодарности

Авторите изказват своята благодарност на фонд „Научни изследвания“ на Русенския университет, проект 2019-ФТ-01, за финансовата подкрепа.

Литература

[1] Learn about the environmental and economic benefits of natural gas vehicles (https://www.socalgas.com/for-your-business/natural-gas-vehicles/benefits, 10/10/2019)

[2] Bielaczyc P, Szczotka A and Woodburn J 2016 A comparison of exhaust emissions from vehicles fuelled with petrol, LPG and CNG *IOP Conf. Ser.: Materials Science and Engineering* **148(1)** 012060

[3] Natural Gas Vehicle Emissions **(***Alternative Fuels Data Center*. U.S. Department of Energy. *https://www.afdc.energy.gov/vehicles/natural_gas_emissions.html)*

[4] Tollefson J 2013 Methane leaks erode green credentials of natural gas *Nature News* **493(7430)** 12

[5] McKain K, Down A, Raciti S M, Budney J, Hutyra L R, Floerchinger C, ... and Phillips N 2015 Methane emissions from natural gas infrastructure and use in the urban region of Boston, Massachusetts *Proc. National Academy of Sciences* **112(7)** 1941–6

[6] Value Chain Methane Loss Update Review of Publicly Available Studies *(November 2015, ConocoPhillips, http://static.conocophillips.com/files/resources/methanestudies112015.pdf)*

[7] Environmental Impacts of Natural Gas *(Union of Concerned Scientists, https://www.ucsusa.org/clean-energy/coal-and-other-fossil-fuels/environmental-impacts-of-natural-gas)*

[8] IS0 14040/44:2006. Environmental management – Life cycle assessment.

[9] DECC D 2016 UK government GHG conversion factors for company reporting. London *(UK: DECC, DEFRA)*

[10] Peng T, Zhou S, Yuan Z and Ou X 2017 Life cycle greenhouse gas analysis of multiple vehicle fuel pathways in China *Sustainability* **9(12)** 2183

[11] Liquified natural gas (LNG) *(https://petrowiki.org/Liquified_natural_gas_(LNG), 10/10/2019)*

[12] Abdelmajeed M A, Onsa M H and Rabah A A 2009 Management of evaporation losses of gasoline's storage tanks *Sudan. Eng. Soc. J.* **55(52)** 39–45

[13] Magaril E 2015 Reducing gasoline loss from evaporation by the introduction of a surface-active fuel additive *Urban Transport XXI. WIT Transactions on The Built Environment* **146** 233–242

[14] Kimeu J M 2012 Development of optimum energy use model for a petrol station *(Master's thesis, University of Nairobi)* p. 78

[15] Oil Tanker Spill Statistics 2018 (Itopf, Promoting Effective Spill Response *https://www.itopf.org/knowledge-resources/data-statistics/statistics/)*

[16] Unnasch S and Goyal L 2017 Life Cycle Analysis of LPG Transportation Fuels under the Californian LCFS *(LCA.8103.177.2017, October 24, 2017)*

[17] Методика за определяне интензитета на емисиите на парникови газове от целия жизнен цикъл на горивата и енергията от небиологичен произход в транспорта *(Министерство на околната среда и водите на Република България, 2017)* стр. 36

[18] Weaver C S and Turner S H 1994 Dual fuel natural gas/diesel engines: technology, performance, and emissions *(SAE Technical Paper No. 940548)* p. 18

[19] Weaver C S and Turner S H 1994 Dual fuel natural gas/diesel engines: technology, performance, and emissions *(SAE Technical Paper No. 940548)*

[20] Paczuski M, Marchwiany M, Puławski R, Pankowski A, Kurpiel K and Przedlacki M 2016 Liquefied Petroleum Gas (LPG) as a Fuel for Internal Combustion Engines (*Alternative Fuels, Technical and Environmental Conditions. IntechOpen*) 105–136

Life cycle assessment of vehicles, using LPG and NG

Ivan Evtimov[1], Rosen Ivanov and Hristo Stanchev

University of Ruse

[1] E-mail: ievtimov@uni-ruse.bg

Abstract. The paper presents a life cycle assessment of vehicles using gas fuel. The assessment is done on the basis of used primary energy and generated emissions in CO_2 equivalent. A comparison with conventional gasoline vehicle is done. The investigation is done at equal car mass and fuel consumption, which give the same energy from burning process. The results are presented in appropriate form. The results from the investigation can be used as useful information concerning environment impact of the different types of fuel and as an indicative simulation.

Graph-analytical method for analysis of vehicle-pedestrian forward projection impact accidents with forward and transverse post-impact motion of pedestrian body on uneven road with gradient

Danail Hlebarski

Department of Combustion Engines, Automobile Engineering and Transport, Faculty of Transport, Technical University of Sofia, 8 St. Kliment Ohridski Blvd., Sofia 1000, Bulgaria

E-mail: dhlebarski@tu-sofia.bg

Abstract. This paper discusses the reconstruction of vehicle-pedestrian impact accidents of the type of forward projection. It proposes a graph-analytical method capable of determining the vehicle-pedestrian point of impact and the impact speed of vehicle. The method is based on the widely adopted in the literature assumption that movement of pedestrian's body after impact can be approximated by movement of its mass point and takes into account the pedestrian's body throw distance. Known methods take into account only the longitudinal gradient of the road with constant pedestrian-road friction and straightforward motion of the pedestrian's body after impact. In contrast to them, the proposed method determines also the transverse motion of the pedestrian's body after impact and the variations of pedestrian-road friction. An application of the method is illustrated by reconstructing a vehicle-pedestrian forward projection impact accident.

1. Introduction

Factors, like the shape and speed of the vehicle and the height, stance and speed of the body relative to the vehicle at the instant of collision, determine the vehicle-pedestrian impact [1].

Ravani et al. [2] showed that pedestrian motion is determined by the relative geometric configuration and speed of the vehicle and pedestrian at impact and that injury patterns are dependent on the subsequent trajectory type. The impacts by the vehicle front are the most common (67%), sidewipes occur about 18% of the time and pedestrian impact by the rear of vehicles is rare (2%). The remainder were front corner impacts.

Amount of 80 % of the front collisions belong to one of five basic trajectory categories, widely adopted in the literature [1]:

- wrap projection,
- forward projection,
- somersault,
- roof vault,
- fender vault.

Pedestrian/vehicle geometry and respective velocities at the time of impact determine the specific configuration.

[3] give the next description of these categories. Pedestrian wrap projection is a collision in which the impacting vehicle is decelerating at the moment of collision and the pedestrian centre of gravity is above the leading edge of the vehicle, as depicted in figure 1. The front of the vehicle strikes the legs and thigh/pelvic areas (primary impact) and this is followed by secondary impact of head and/or shoulder with the vehicle. After this, continued interaction with the vehicle or a flight phase may occur, or a combination of both, followed by ground impact(s) and slide, roll, and bounce to rest.

Forward projection is a collision in which the pedestrian's centre of gravity is within the primary impact zone. The pedestrian is accelerated in the direction of vehicle's motion and projected forward rather than upward. This typically occurs where an adult is struck by a minivan, bus or a truck, a small adult is struck by a large SUV or a child is struck by a passenger car, van, truck or an SUV, as illustrated in figure 2.

Figure 1. Pedestrian wrap projection [3, 4].

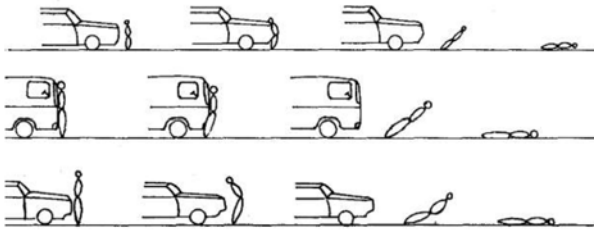

Figure 2. Pedestrian forward projection [3, 4].

When the pedestrian collides with the vehicle near the front corner of a braking and non-braking vehicle, this is a fender vault collision. The pedestrian is deflected to one side without secondary impact of the upper body with the vehicle front, see figure 3. The transverse speed of the pedestrian may be sufficient to prevent head contact while the body rotates on the bonnet.

Somersault occurs at higher impact velocities with car braking. Due to the increased impact velocity, the pedestrian is projected into the air and rotates after impact. These types of pedestrian kinematic can result in the secondary contact with the vehicle, as shown in figure 4.

Figure 3. Fender vault collision [3, 4].

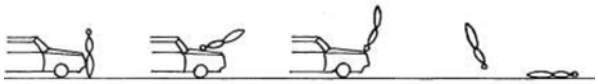

Figure 4. Somersault [3, 4].

Roof vault is a collision in which after the first impact the pedestrian slides from the hood to the windshield and further to the roof of the vehicle, figure 5. Depending on the vehicle behaviour (braking or not braking), the pedestrian can have multiple contacts with the vehicle before hitting the road. This type of impact usually happens at high impact velocities or in cases of not braking vehicle.

Figure 5. Roof vault [3, 4].

It is seen that the somersault and roof vault are special cases of wrap projection, and the fender vault is an uncompleted wrap projection. Finally, there are three collision categories: wrap projection, forward projection, and sideswipe.

There is a considerable amount of works correlating vehicle-pedestrian accidents for low profile vehicles (e.g. passenger cars), resulting a wrap projection pedestrian trajectory. However, there is a limited amount of works concerning high profile automobiles (e.g. cargo/passenger vans, SUVs, large trucks, etc.) versus pedestrian collisions, which typically result in a forward projection pedestrian trajectory.

In this article, we analyse the front collisions.

In vehicle-pedestrian collision accidents reconstruction, the most important parameter to analyse is the vehicle collision velocity [5] because it is correlated with pedestrian injury and fatality potential. The vehicle collision velocity may be determined by tire marks from the road, if they exist. If there are no tire marks, such parameters like pedestrian injuries, vehicle post-accident deformations, simultaneously taking into account vehicle characteristics, etc., are used. These results have been statistically investigated and various forms of models are developed [5]. The difficulty when using them is the necessity of data about the conditions the accident passed.

Mostly used parameter in determining vehicle collision speed is the pedestrian's throw distance – the distance along the road between the location of the pedestrian-vehicle contact and pedestrian's centre of gravity rest position [6].

The models to analyse vehicle-pedestrian impacts are of three types: theoretical, based on laws of mechanics, empirical and hybrid. The results of theoretical models are reliable, but these models need a big quantity of input parameters. The empirical models consist of a regression formula connecting the vehicle impact speed with pedestrian throw distance and do not need such amount of data, but are applicable with sufficient accuracy only in well-defined scenarios. The hybrid models combine the theoretical and the empirical models.

To describe the vehicle-pedestrian impact mathematically, the following assumptions are made in the models, as described in [7]:

- the car-pedestrian impact is symmetric so all events happen in a single plane;
- the initial velocity of the pedestrian is zero;
- after launch the pedestrian is considered as a mass point;
- the ground is flat;
- the pedestrian-ground friction is constant;
- the air resistance is neglected.

As seen from above, the impact model of wrap projection considers pedestrian movement during three consequent phases: 1) vehicle-pedestrian impact, including wrap over the bonnet and restitution, 2) flight, and 3) slide/roll/bounce to rest.

The forward projection model also considers three distinct phases: 1) impact, 2) fall-over, and 3) slide/roll/bounce to rest, see figure 6 [8]. The total throw distance of the pedestrian S_{total} is the sum of the distances travelled in each phase: S_{impact}, $S_{fall-over}$, and $S_{slide/roll/bounce}$:

$$S_{total} = S_{impact} + S_{fall-over} + S_{slide/roll/bounce}. \quad (1)$$

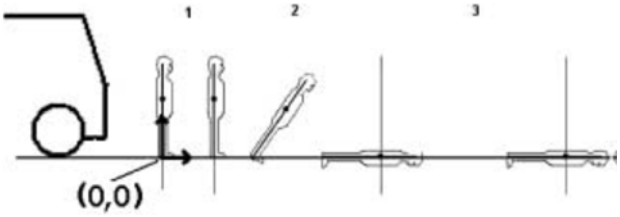

Figure 6. Schematic of the forward projection sequence, showing the system origin [8].

From analyses of the trajectory of forward projection tests in [9] it is seen, that at the beginning there is a small take-off angle. So, in the present paper the throw distance is considered consisting of three phases: 1) vehicle-pedestrian impact, including wrap over the bonnet and restitution, 2) flight, and 3) slide/roll/bounce to rest.

2. Method

First of all, the parameters of road plane have to be determined. That is why, a Cartesian coordinate system *Oxyz* is introduced, the axis *Ox* positive to the front, the axis *Oy* positive to the left and the axis *Oz* positive to the top of the vehicle, standing on a horizontal plane.

The road plane may be inclined longitudinally at an angle of road gradient α and laterally at a transverse slope angle β. The coordinates of the normal vector $\boldsymbol{N}$ of the road plane may be derived by two rotations, see figure 7: about the axis *Oy* through an angle of road gradient α, and about the new axis *Ox′* through an angle γ. Finally, the axis *Oz″* coincides the normal vector $\boldsymbol{N}$. The rotation matrices M_α about the axis *Oy* and M_γ about the axis *Ox′* are [10].

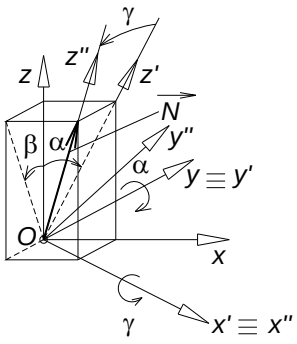

Figure 7. Coordinates of the normal vector *N* of the road plane.

$$M_\alpha = \begin{bmatrix} \cos\alpha & 0 & \sin\alpha \\ 0 & 1 & 0 \\ -\sin\alpha & 0 & \cos\alpha \end{bmatrix}; \tag{2}$$

$$M_\gamma = \begin{bmatrix} 1 & 0 & 0 \\ 0 & \cos\gamma & -\sin\gamma \\ 0 & \sin\gamma & \cos\gamma \end{bmatrix}, \tag{3}$$

where

$$\tan\gamma = \tan\beta\cos\alpha. \tag{4}$$

The rotation matrix about the axis *Oy* followed by rotation about the axis *Ox′* is

$$M_{\gamma\alpha} = M_\gamma M_\alpha = \begin{bmatrix} \cos\alpha & 0 & \sin\alpha \\ \sin\gamma\,\sin\alpha & \cos\gamma & -\sin\gamma\,\cos\alpha \\ -\cos\gamma\,\sin\alpha & \sin\gamma & \cos\gamma\,\cos\alpha \end{bmatrix}. \tag{5}$$

With initial coordinates of the normal unit vector $\boldsymbol{N}$ of the road plane

$$\boldsymbol{N_0} = [0; \quad 0; \quad 1], \tag{6}$$

its coordinates of an inclined plane are

$$\boldsymbol{N} = \begin{bmatrix} \sin\alpha \\ -\sin\gamma\,\cos\alpha \\ \cos\gamma\,\cos\alpha \end{bmatrix}. \tag{7}$$

Then, the general form of the equation of the road plane is [10]

$$\sin\alpha\, x - \sin\gamma\,\cos\alpha\, y + \cos\gamma\,\cos\alpha\, z = 0. \tag{8}$$

Next, we assume that the pedestrian body moves in a vertical plane, declined from the direction of the road at angle δ as shown at figure 8.

The initial coordinates of the normal unit vector $\boldsymbol{N_P}$ of the plane of motion of the pedestrian body are

$$\boldsymbol{N_{P0}} = [0; \quad 1; \quad 0]. \tag{9}$$

The coordinates of the normal unit vector $\boldsymbol{N_P}$ of the plane of motion of the pedestrian body after rotation through an angle δ are

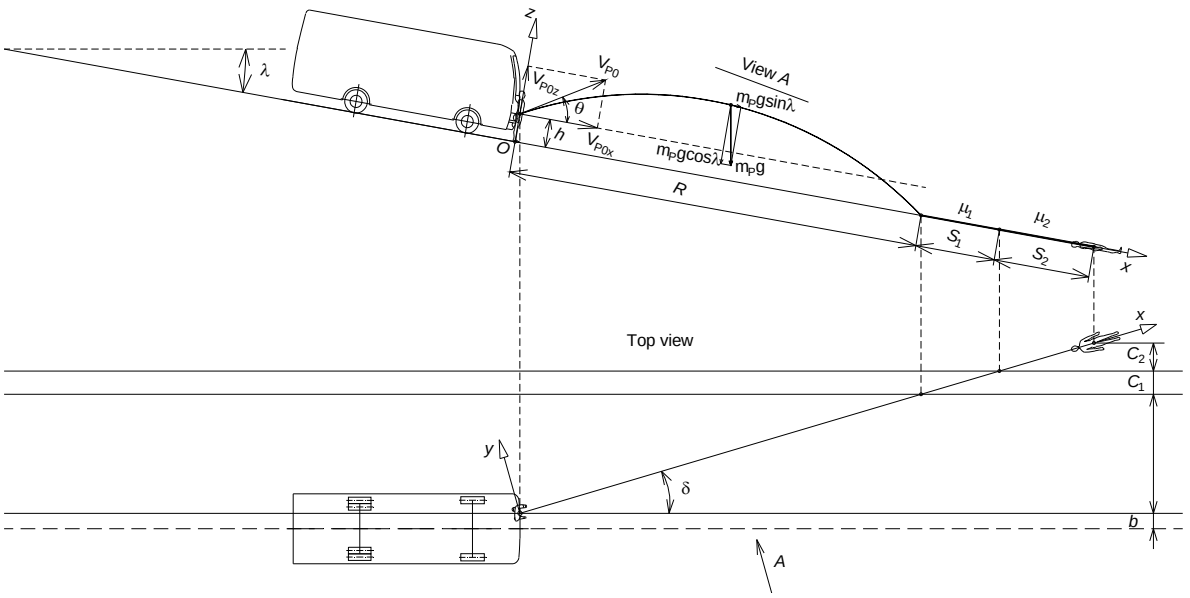

Figure 8. Side and top view at a vehicle-pedestrian accident.

$$\boldsymbol{N_P} = \begin{bmatrix} -\sin\delta \\ \cos\delta \\ 0 \end{bmatrix}. \tag{10}$$

The general form of the equation of the vertical plane of pedestrian movement is

$$-\sin\delta\, x + \cos\delta\, y + 0\, z = 0. \tag{11}$$

Because the road plane is inclined longitudinally at an angle α and laterally at an angle β, the line of intersection between the road plane (8) and the vertical plane of pedestrian movement (11) is the vertical projection of the pedestrian trajectory onto the road plane.

The equation of the line of intersection between the road plane (8) and the plane (11) is

$$\begin{cases} \sin\alpha\, x - \sin\gamma\, \cos\alpha\, y + \cos\gamma\, \cos\alpha\, z = 0 \\ -\sin\delta\, x + \cos\delta\, y + 0\, z = 0 \end{cases} \tag{12}$$

The coordinates of the vector $\boldsymbol{a}$ parallel to the line (12) are

$$\boldsymbol{a} = \boldsymbol{N} \times \boldsymbol{N_P}. \tag{13}$$

After performing the vector product, we have

$$\boldsymbol{a} = a_x \boldsymbol{i} + a_y \boldsymbol{j} + a_z \boldsymbol{k} =$$

$$= \cos\delta\, \cos\gamma\, \cos\alpha\, \boldsymbol{i} + \sin\delta\, \cos\gamma\, \cos\alpha\, \boldsymbol{j} + (\sin\delta\, \sin\gamma\, \cos\alpha - \cos\delta\, \sin\alpha)\boldsymbol{k}, \tag{14}$$

where a_x, a_y and a_z are the coordinates of the vector $\boldsymbol{a}$, and $\boldsymbol{i}$, $\boldsymbol{j}$ and $\boldsymbol{k}$ are the unit vectors respectively of axes *Ox*, *Oy* and *Oz* of the Cartesian coordinate system *Oxyz*.

The angle of inclination of the vector **a** about the horizontal level is

$$\lambda = \arctan \frac{a_z}{\sqrt{a_x^2 + a_y^2}}. \tag{15}$$

Now, let the initial launch angle be θ, Figure 8. The vector of initial velocity of launch of the pedestrian body, $\boldsymbol{v_{P0}}$, can be expressed in the coordinate system *Oxz* as follows:

$$\boldsymbol{v_{P0}} = v_{P0} \cos\theta\, \boldsymbol{i} + v_{P0} \sin\theta\, \boldsymbol{k}. \tag{16}$$

At any time t, the components of the velocity are

$$\frac{\mathrm{d}x}{\mathrm{d}t} = v_{Px}; \frac{dz}{dt} = v_{Pz}. \tag{17}$$

Neglecting the air resistance and following the Newton's 2nd Law, the next equations of motion of the pedestrian body during projection process can be written:

$$m_P \frac{\mathrm{d}v_{Px}}{\mathrm{d}t} = m_P\, g\, \sin\lambda; m_P \frac{\mathrm{d}v_{Pz}}{\mathrm{d}t} = -m_P\, g\, \cos\lambda. \tag{18}$$

Here, m_P is the mass of the pedestrian, and $g = 9.81$ m/s^2 is the acceleration due to gravity.

The equations (18) are completed with the initial conditions

$$t = 0; x(0) = 0; v_{Px}(0) = v_{P0}\cos\theta; \mathrm{z}(0) = h; v_{Pz}(0) = v_{P0}\sin\theta, \tag{19}$$

where h is the distance from the pedestrian centre of gravity to the ground in meters.

After integration and imposing the initial conditions, the velocity of the pedestrian body is

$$\begin{aligned} v_{Px} &= g\,\sin\lambda t + v_{P0}\cos\theta\,; \\ v_{Pz} &= -g\,\cos\lambda t + v_{P0}\sin\theta\,. \end{aligned} \tag{20}$$

Carrying out a second integration and imposing the initial conditions, the position coordinates of the pedestrian body centre of gravity are

$$\begin{aligned} x &= g\sin\lambda\frac{t^2}{2} + v_{P0}\cos\theta\, t; \\ z &= -g\cos\lambda\frac{t^2}{2} + v_{P0}\sin\theta\, t + h. \end{aligned} \tag{21}$$

The pedestrian body impacts the ground at impact time t_R after flying the distance R. Substituting $z(t_R) = 0$, the impact time t_R is derived from the second equation of (21):

$$t_R = \frac{-v_{P0}\sin\theta \pm \sqrt{v_{P0}^2\sin^2\theta + 2gh\cos\lambda}}{-g\cos\lambda}. \tag{22}$$

From the first equation of (21) we have the flying distance:

$$R = g\sin\lambda\frac{t_R^2}{2} + v_{P0}\cos\theta\, t_R. \tag{23}$$

Let's assume there are some road distances the pedestrian body slides/rolls/bounces to rest after impacting the road: S_1, S_2, etc., every of them with a drag resistance coefficient μ_1, μ_2, etc., of the pedestrian body.

The pedestrian body speed in the *x* direction after the impact with the ground is [7]

$$v'_{PxR} = v_{PxR} + I_1 v_{PzR}, \tag{24}$$

where the pedestrian body speed in the *x* direction at the end of the projectile trajectory is v_{PxR}, in the *z* direction is v_{PzR}, and the I_1 is the impulse ratio at ground impact of the pedestrian, typically equal to the drag resistance coefficient μ_1 over the distance S_1. After substituting (20), we have [7]

$$v'_{PxR} = v_{P0}(\cos\theta + \mu_1\sin\theta) - g(\mu_1\cos\lambda - \sin\lambda)t_R. \tag{25}$$

Finally, the distance travelled by the pedestrian body after impact with the ground is

$$S_g = S_1 + S_2 + \cdots = \frac{v'^2_{PxR} - v^2_{Px1}}{2g(\mu_1\cos\lambda - \sin\lambda)} + \frac{v^2_{Px1} - v^2_{Px2}}{2g(\mu_2\cos\lambda - \sin\lambda)} + \cdots, \tag{26}$$

where S_1, S_2, etc., are road distances, each of them with drag resistance coefficient μ_1, μ_2, etc., see figure 1.

Respectively, the speed of the pedestrian body at the beginning of sliding phase is

$$v'_{PxR} = \sqrt{2g(\mu_1 \cos\lambda - \sin\lambda)S_1 + 2g(\mu_2 \cos\lambda - \sin\lambda)S_2 + \cdots} \quad (27)$$

The time of sliding phase is

$$t_g = t_1 + t_2 + \cdots = \frac{v'_{PxR} - v_{Px1}}{g(\mu_1 \cos\lambda - \sin\lambda)} + \frac{v_{Px1} - v_{Px2}}{g(\mu_2 \cos\lambda - \sin\lambda)} + \cdots. \quad (28)$$

The total throw time is

$$t_T = t_R + t_g, \quad (29)$$

and the total throw distance is

$$S_T = R + S_g. \quad (30)$$

Note, than the angles used in formulae above are in positive directions about the coordinate axes as shown at the figures. If the directions of the angles are opposite, they have to be rewritten with negative signs.

3. Application of the model

To applicate the model, a reconstruction of a forward projection impact accident is performed.

A bus travelling with a speed V_A = 60 km/h =16.67 m/s, on a road with longitudinal gradient in ascent i_α = 7 % (according the coordinate system, angle $\alpha = -0.07\ rad = -4$ degrees) and with a transverse slope of descending from the middle of road to right side i_β = 2.5 % (according the coordinate system, angle $\beta = 0.25\ rad = 1.43$ degrees), struck by its front side a pedestrian. After the impact, the pedestrian moved forward and to the right and stopped on the grass aside, on the right side of the way as shown on figure 9.

So, the pedestrian body final position and the vehicle impact speed are known, the coordinates of vehicle-pedestrian impact are to be found.

The input parameters are: lateral coordinate of point of impact on the asphalt road y_a = 1.95 m; lateral coordinate of pedestrian's center of mass on the grass is y_g = 0.6 m.

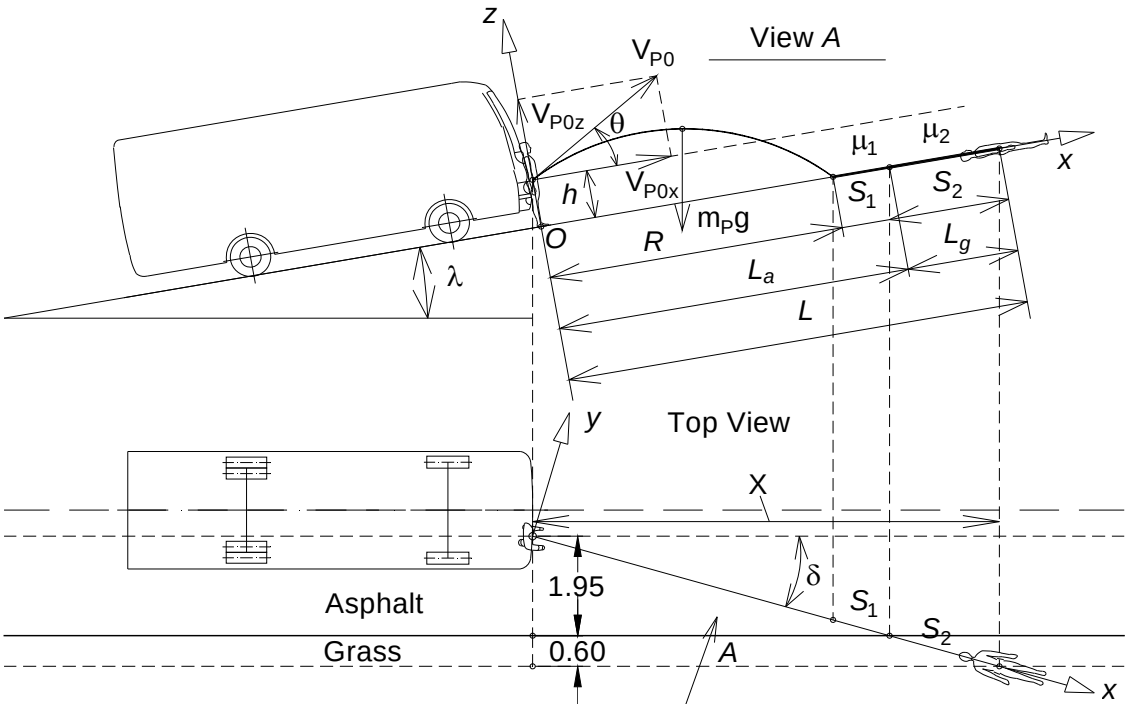

Figure 9. Side and top view at a reconstructed vehicle-pedestrian accident.

The problem is we do not know the distances S_1, S_2, etc., of sliding/rolling/bouncing of the pedestrian body. That is why, the first parameter to be calculated is the flying distance R.

The procedure of computation is the next.

1. At first, the angle , see (4), is

$$\gamma = \arctan(\tan\beta\ \cos\alpha) = \arctan(\tan 1.43°\cos(-4°)) = 0.025 \text{ rad} = 1.43 \text{ degrees}. \quad (31)$$

2. Then, with a beginning at some distance, say 40 m, and an end at 10 m, by a step of 1 m, a massive of distances from the point of contact to the pedestrian body final position, measured along the way, is created:

$$X = [40;\ 39; 38; \ldots; 10]\ . \quad (32)$$

3. For every point X_i of the massive, the angle δ_i is

$$\delta_i = \arctan\frac{y_a + y_g}{X_i}. \quad (33)$$

4. For every point X_i of the massive, the lengths along the asphalt L_{ai} and the grass L_{gi}, and the sum of them L_i in meters are

$$L_{ai} = \frac{y_a}{\sin\delta_i}; \quad (34)$$

$$L_{gi} = \frac{y_g}{\sin\delta_i}; \quad (35)$$

$$L_i = L_{ai} + L_{gi}. \quad (36)$$

5. For every point X_i of the massive, the coordinates of the unit vector **a**, see (14), are

$$a_{xi} = \cos\delta_i\ \cos\gamma\ \cos\alpha; \quad (37)$$

$$a_{yi} = \sin\delta_i\ \cos\gamma\ \cos\alpha; \quad (38)$$

$$a_{zi} = \sin\delta_i\ \sin\gamma\ \cos\alpha - \cos\delta_i\ \sin\alpha. \quad (39)$$

6. For every point X_i of the massive, the angle of inclination of the vector **a** about the horizontal level, see (15), is

$$\lambda_i = \arctan\frac{a_{zi}}{\sqrt{a_{xi}^2 + a_{yi}^2}}. \quad (40)$$

7. For every point X_i of massive, the value of the speed of the vehicle along the plane of pedestrian projection process is

$$V_{P0x\,i} = V_a\cos\delta_i. \quad (41)$$

8. For every point X_i of the massive, the initial velocity of launch of the pedestrian body is

$$v_{P0\,i} = v_{P0x\,i}\cos\theta. \quad (42)$$

9. For every point X_i of the massive, the impact time t_{Ri} is

$$t_{Ri} = \frac{-v_{P0\,i}\sin\theta \pm \sqrt{v_{P0\,i}^2\sin^2\theta + 2gh\cos\lambda_i}}{-g\cos\lambda_i}. \quad (43)$$

10. For every point X_i of the massive, the flying distance is

$$R_i = g\sin\lambda_i\frac{t_{Ri}^2}{2} + v_{P0\,i}\cos\theta\ t_{Ri}. \quad (44)$$

11. For every point X_i of the massive, an analysis has to be made.

a) If the flying distance $R_i < L_{ai}$ (from step 4), the pedestrian centre of mass impacted the asphalt road and the remain part, $S_{1\,i}$ of sliding/rolling/bouncing the asphalt is

$$S_{1\,i} = L_{ai} - R_i. \tag{45}$$

b) If the distance of flying $R_i \geq L_{ai}$ (from step 4), the pedestrian centre of mass impacted the grass and the remain part, $S_{2\,i}$ of sliding/rolling/bouncing the grass is

$$S_{2\,i} = L_i - R_i. \tag{46}$$

12. For every point X_i of massive, the value of the speed of the pedestrian body at the beginning of sliding/rolling/bouncing phase is

$$v'_{PxR\,i} = \sqrt{2g(\mu_1 \cos\lambda_i - \sin\lambda_i)S_{1\,i} + 2g(\mu_2 \cos\lambda_i - \sin\lambda_i)S_{2\,i}}. \tag{47}$$

13. For every point X_i of massive, the initial velocity of launch of the pedestrian body, calculated by the sliding phases, is

$$v'_{P0\,i} = \frac{v'_{PxR\,i} + g(\mu_{1(2)}\cos\lambda_i - \sin\lambda_i)t_{R\,i}}{\cos\theta + \mu_{1(2)}\sin\theta}, \tag{48}$$

where in the case 11 a) μ_1 is used, and in case 11 b) μ_2 is used.

14. For every point X_i of massive, the horizontal component of the initial velocity of launch of the pedestrian body, calculated by the sliding phases, is

$$V'_{P0x\,i} = v'_{P0\,i}\cos\theta. \tag{49}$$

15. For every point X_i of massive, the speed of the vehicle at the at the instant of collision, calculated by the sliding phases, is

$$V'_{A\,i} = V'_{P0x\,i}/\cos\delta_i. \tag{50}$$

16. Finally, a graph of speeds of the vehicle V_A and $V'_{A\,i}$ is used to determine the instant of collision, figure 10.

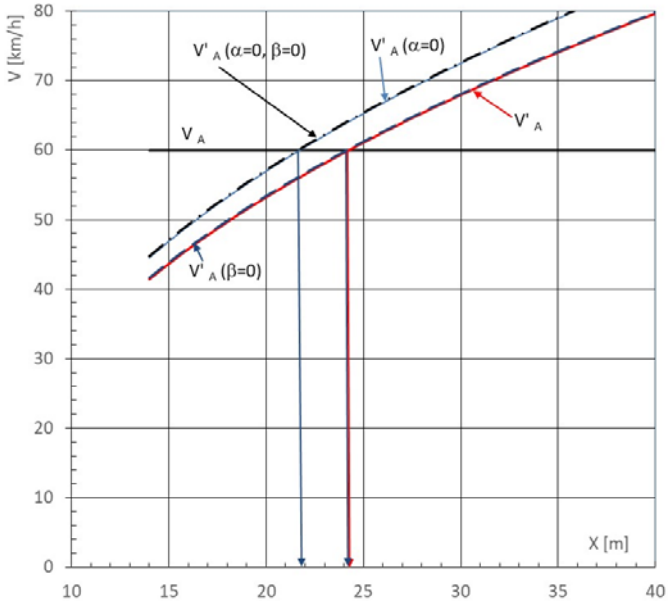

Figure 10. Graph of speeds of a reconstructed vehicle-pedestrian accident.

On the graph, the results $V'_{A\,i}$ for a road with ascent longitudinal gradient i_α = 7 % and with a transverse slope of descending from the middle of road to right side i_β = 2.5 % are compared with the results when $\alpha = 0$, or $\beta = 0$, and both $\alpha = 0$, and $\beta = 0$. It is seen, that the influence of the transverse slope is little and the results in the same longitudinal gradient are almost identical.

The horizontal coordinates X of the points of intersection of line of vehicle speed V_A with the line $V'_{A\,i}$ determine the point of impact. So, for a road with ascent longitudinal gradient i_α = 7 % and with a transverse slope of descending from the middle of road to right side i_β = 2.5 % it is 24.3 m; when only $\beta = 0$, the coordinate is 24.2 m, and when only $\alpha = 0$ and both $\alpha = 0$, and $\beta = 0$, the coordinate is 21.8 m. The difference between 21.8 m and 24.3 m is 2.5 m, which value in some cases may be very important.

4. Conclusions

In this paper, an algorithm has been presented for reconstruction of vehicle-pedestrian impact accidents of the type of forward projection. The graph-analytical method proposed is capable of determining the vehicle-pedestrian point of impact with known impact speed of vehicle. Known methods take into account only the longitudinal gradient of the road with constant pedestrian-road friction and straightforward motion of the pedestrian's body after impact. In contrast to them, the presented method determines also the transverse motion of the pedestrian's body after impact and the variations of pedestrian-road friction.

An application of the method is illustrated by reconstructing a vehicle-pedestrian forward projection impact accident.

From the results, it is concluded, that the longitudinal gradient of the road influences the position of point of impact more, than the transverse road slope.

References

[1] Simms C and Wood D 2009 *Pedestrian and Cyclist Impact. A Biomechanical Perspective* (ed. Springer Science + Business Media, B.V.)
[2] Ravani B, Brougham D and Mason R T 1981 Pedestrian post-impact kinematics and injury patterns *Society of Automotive Engineers Conference* 137–8
[3] Bastien C, Orlowski M and Bhagwani M 2017 Validation of a finite element human model throw distance in a pedestrian accident scenarios *11th European LS-DYNA Conf., Salzburg, Austria*
[4] Karapetkov S 2005 *Automotive expertise* (TU-Sofia Academic Publishing House, in Bulgarian)
[5] Han I 2013 Fuzzy Estimation of vehicle speed in pedestrian collision accidents *Int. J. Automotive Technology* **14(3)** 385−93
[6] Han I and Brach R M 2001 *Throw Model for Frontal Pedestrian Collisions* (SAE Paper 2001-01-0898)
[7] Batista M 2008 A Simple throw model for frontal vehicle-pedestrian collisions *Promet – Traffic&Transportation* **20(6)** 357–68
[8] Wood D P, Simms C K and Walsh D G 2005 Vehicle-pedestrian collisions: Validated models for pedestrian impact and projection *Proc. IMechE*. **219** Part D: J. Automobile Engineering, 183–195
[9] Fugger T F Jr., Randles B C, Wobrock J L and Eubanks J J 2002 *Pedestrian throw kinematics in forward projection collisions* (SAE Paper No. 2002-01-0019)
[10] Vygodskiy M Ya 1975 *Handbook of Higher Mathematics* (M, Science, in Russian)

Approach for reverse engineering of complex geometry components

Yavor Sofronov[1], Mihail Zagorski, Georgi Todorov and Todor Gavrilov

Lab. CAD/CAM/CAE in Industry, Technical University – Sofia, 8 Kl. Ohridski Blvd., 1797 Sofia, Bulgaria

[1] E-mail: ysofronov@tu-sofia.bg

Abstract: This paper study present an approach for part recognition, process known as "Reverse engineering" using turbine blade component as an example. It has a complex geometrical shape and it's produced from specific material, who should work under high thermodynamical stress. To fulfil the task different 3D scanning technologies were evaluated and as a result the laser triangulation was used for geometry acquisition. Geometry creation in mesh to CAD software was explained step by step. Elemental analysis with Energy-dispersive X-ray spectroscopy (EDX) for material characterization was used. The result from presented approach for reverse engineering is a solid CAD model with defined material, capable for production.

1. Introduction

The development of the computer technologies over the last few decades leads to radical changes on a global scale, digitizing the world. At the threshold of the so-called Industry 4.0, a number of professions, including the engineering sciences, are changing dynamically. A mechanical engineer is more often working with a variety of software products – a modern designer knows at least a few CAD products, the analysts are using variety of CAE solutions, as well as technologists – increasingly intuitive CAM software. The basis of all these technologies is the 3D model. The reverse engineering does not stay on a side of these processes too. Reverse Engineering is a process of reworking and reconstructing the principles and the mechanisms, that are used to create a specific object, i.e. when a specialist (designer, analyst or technologist) has at his disposal a final product, but not its documentation, it is necessary to create a digital model of the product, in order to be able to implement it for processing in CAD, CAM or CAE software [1-3].

In mechanical engineering, the reverse engineering or the reconstruction typically consists of accurately recreating the geometry of an object and assigning properties that match its working parameters and characteristics [4].

The reconstruction process begins with the digitization of geometry. When a complex geometry object is under study, several basic non-contact 3D image creation methods are used, merged under the name 3D scanning. One of these methods is the so called photogrammetry, which uses a camera shots from different angles of the subject, and subsequently, by the use of specialized software, a three-dimensional image as a cloud of points is reached.

Two other basic methods for 3D scanning are LiDAR scanners and scanners with laser triangulation. The common feature is that both types of scanners use a laser light to capture the geometry of the object. Differences between these methods are how the distance between the scanner and a given surface is measured. In the table 1 is shown a comparison between the three methods [5].

Table 1. Comparison of 3D scanning methods.

	Photogrammetry	LiDAR	Laser Triangulation
Sensitivity to the type of lighting	High	Low	Low
Texture reproduction capability	High	Low	Low
Accuracy for the purposes of mechanical engineering	Low	Low	High
Software and equipment prices	Relatively low	High	High
Scanning ability for small objects	Average	Low	High
Scanning ability for large objects	High	High	Relatively low
Generating point cloud timing	Fast	Fast	Slow
Level of detail	Average	Average	High
High qualification of the staff	No	Yes	Yes
Subsequent software processing timing	Slow	Relatively fast	Relatively fast

1.1. Purpose of the development

The aim of the present work is to develop a methodology for reconstruction a complex geometry part with high accuracy requirements.

2. Methodology of work

For the reconstruction of a small size part with high accuracy requirements, a laser triangulation scanner is the most suitable choice. The principle of work of a laser triangulation scanner is shown on figure 1 [6].

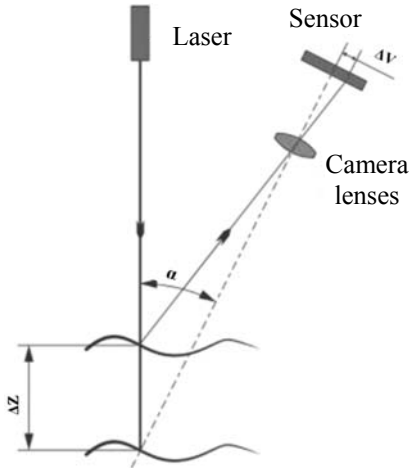

Figure 1. Principle of work of a laser triangulation scanner.

During the scanning process a point cloud is created. The number of points in the cloud sometimes exceed several million points which is making the cloud really difficult for future processing.

After the point cloud is created and cleared from the noises, a polygonal mesh (usually composed of triangles) based on the cloud is generated. This step is necessary because the polygonal mesh is easier for processing. In figure 2 [7] a scheme of the process is shown.

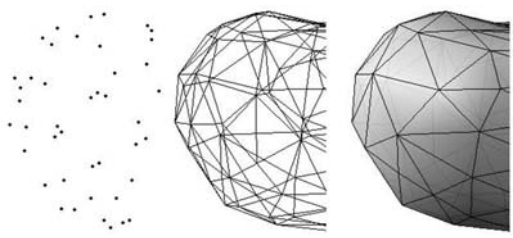

Figure 2. Generating a mesh from a cloud of points.

The next stage is related to construction of a surface model on the polygonal mesh, its subsequent transformation into a solid model and the placing of radii, fillets, inclines, etc. The last step is the selection of identical material or such one with the required characteristics. After the product reconstruction cycle is completed, its model can be used for various engineering purposes, as example creating a technical documentation, developing a manufacturing technology, calculating engineering analyses in order to optimize construction, and more. In figure 3 a summary of the process methodology for part reconstruction is shown.

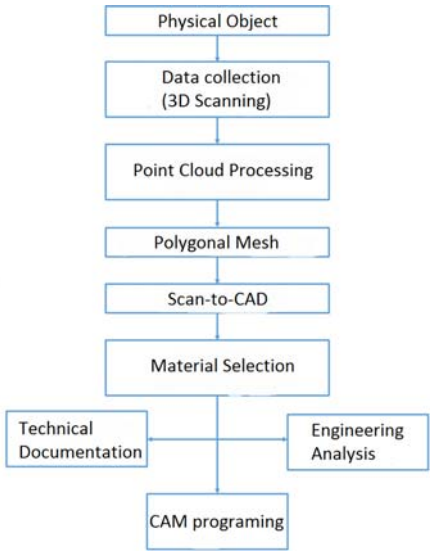

Figure 3. Methodology of the reconstruction process.

Figure 4. 6-axis coordinate-measurement machine Romer Absolute Arm.

3. 3D scanning

The 3D scanning of the part – turbine blade was performed using a 6-axis ROMER Absolute Arm, portable coordinate measuring machine and a laser triangulation scanner, model 7320SI, similar to that shown in figure 4. The scanning, the generation of the mesh and the comparison were performed using the software solution 3D Reshaper.

For the purpose of this study, a scanning accuracy of 0.05 mm is required and achieved.

After the scanning process is done (figure 5), a point cloud of about 1400000 points was obtained.

The next step is cleaning the point cloud and generate a polygonal mesh – figure 6.

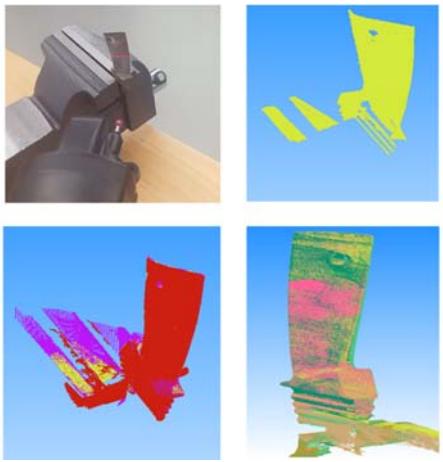

Figure 5. Stepwise scanning of the turbine blade.

Figure 6. Final appearance of the mesh.

4. Creating a solid CAD model on a computer mesh (Scan-to-CAD)

The creation of a solid CAD model from a polygonal mesh is achieved by using specialized software – Geomagic Design X, which is able to capture the geometry from the mesh. It is possible to use functions for both for parametric and for freeform modelling, as for complex parts often the combination of both is needed. These products are called Scan-to-CAD software. The process of creating a solid model goes through several stages:

4.1. Dividing the mesh on regions

The first stage is related to the division of the mesh of regions. This action is necessary in order to be able to use several regions to create different surfaces (figure 7). For the purpose the feature "Auto Segment" under the menu "Region". This feature allows the separation of the geometry in primitives – planes, fillets, parts of sphere, etc. The regions are later used as a base for the construction of a surface model.

4.2. Construction of surfaces on the polygonal mesh

For the construction of a surface model of the turbine blade, Scan-to-CAD software's options are used to directly intercept surfaces on the mesh. Also, features such as "Extrude", "Revolve", "Sweep" and others are used. The first step is to create the middle part of the model using the instrument "Mesh fit" under the menu "Model". This feature intercepts the regions and creates primitives – planes. The second step consists of modelling of the "tail" of the turbine using a section sketch and a guiding path – the so-called "Sweep" feature. The next step is the creation of the turbine profile. For the purpose "Mesh fit" instrument is used. After the generation of the surfaces, "Boolean" feature is used in order to cut the unnecessary elements of the created areas. Finally, the hole is created using the "Revolve" feature. In figure 8, the stepwise construction of the surface model on the polygonal mesh and the finished surface model are shown [8].

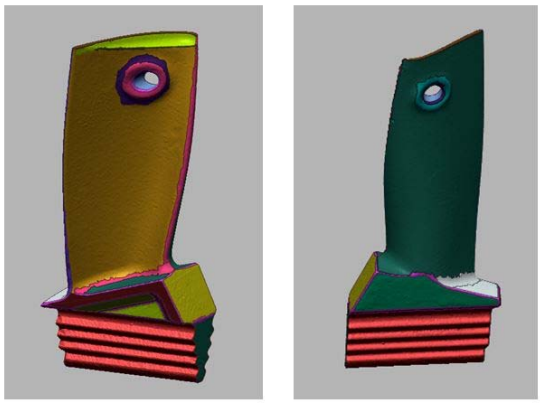

Figure 7. Result of the the regions processing.

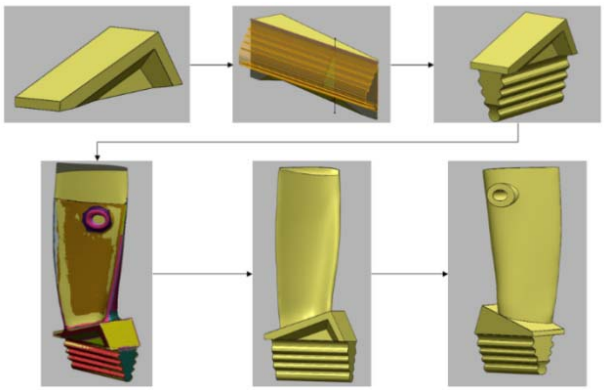

Figure 8. Stepwise surface model creating on a polygonal mesh.

4.3. Creating a solid CAD model

In order to create a solid 3D model, first it is necessary to proceed the work in another CAD software, because the Scan-to-CAD software used in the previous steps does not have the required functionality. For this purpose, the created surfaces are saved in a neutral file format – in this case "Parasolid" format is used. The next step is to open the file in CAD environment in which it is possible to transform the surface model into a solid one. For the purposes of the current study Solidworks CAD software solution was used [9]. The feature "Knit Surface" under the "Surface" menu is used. All surfaces are selected and the options "Try to form solid" and "Merge entities" are chosen. In figure 9, a cross-section view of the newly-created solid model is shown.

4.4. Placing the fillets and chamfers in the solid model

In the environment of the specialized software for reconstruction, the fillets and the chamfers are placed. In order to achieve this purpose, the mesh and the solid model are compared. In figure 10, fillets' and chamfers' placement is shown stepwise. The used features are "Fillet" and "Chamfer".

Figure 9. Cross-section of the solid CAD model.

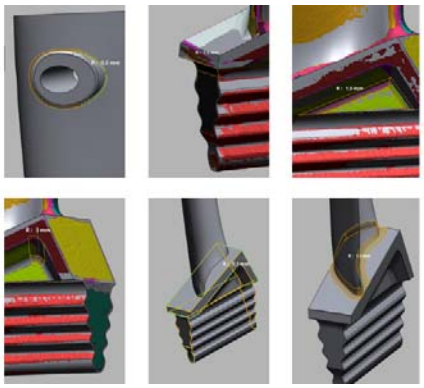

Figure 10. Stepwise fillet placing.

4.5. Accuracy analysis

One of the last steps in the reconstruction of a complex part is the accuracy analysis. For the purpose, a comparison between the polygonal mesh and the solid model is made. The characteristics of the deviations, examined under Gauss's law are presented in table 2.

Table 2. Accuracy analysis.

Parameter	Deviation
Max. negative value	-0.567 mm
Max. Positive value	0.764 mm
Average value	0.019 mm
RMS	0.115 mm
Standard deviation	0.113 mm

The data in table 2 shows the presence of relatively large maximum positive and maximum negative deviations. Due to the results a geometry analysis has been performed and it is estimated that areas with large deviations do not belong to the main working area of the turbine blade and can therefore remain unchanged (figure 11).

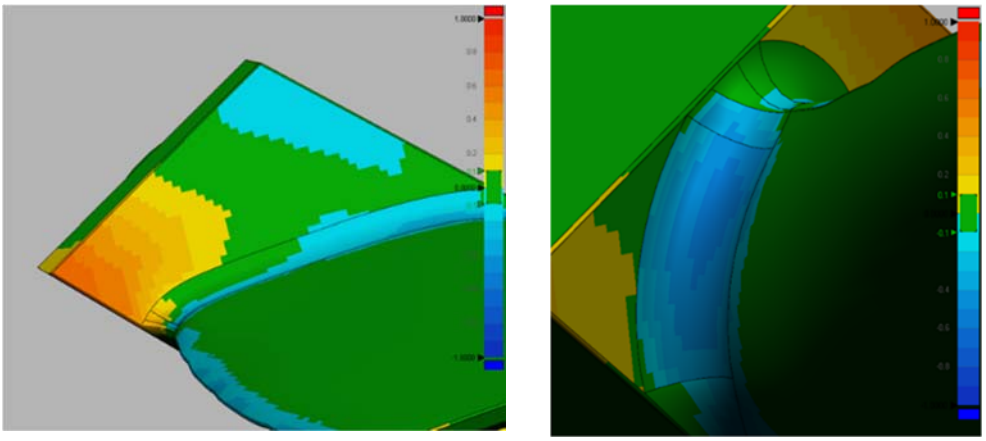

Figure 11. Zones with maximum positive and negative values.

5. Material Selection

The final stage of the reconstruction of the part is related to the material selection that should be as close as possible to the structure and properties of the original. For achieving this goal, the chemical composition of the original material (figure 12) has been determined by means of a scanning electron microscope EVO MA 10 with the CARL ZEISS EDX system (figure 13) [10].

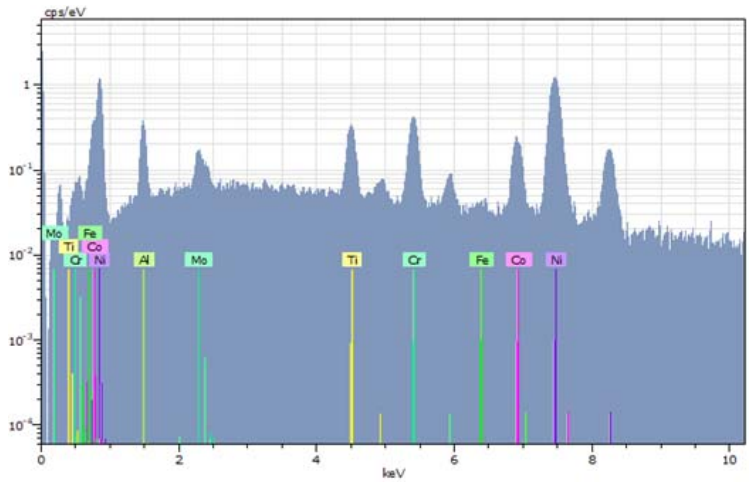

Figure 12. Graphical representation of the results.

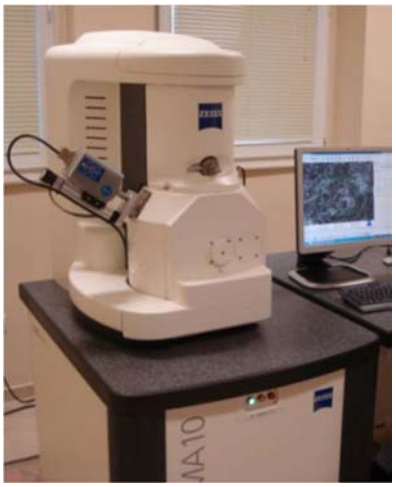

Figure 13. Scanning electron microscope EVO MA 10.

From the analysis, it is found that the material is a nickel alloy with a high content of nickel (Ni), cobalt (Co) and chromium (Cr). Such a chemical composition is particularly characteristic of the so-called "Super alloys" – specially developed materials, which are used for producing parts in turbochargers, jet engines and others. The nickel based "Super alloys" have a stable behaviour in continuous operation at high temperatures (above 500 ° C), which determines the use of similar material for the turbine blade [11].

6. Conclusion

The presented methodology facilitates the creation of a computer model of a part with complex surfaces and no available documentation, which is subsequently used for various engineering purposes. The described methods require the availability of a laser scanner and specialized software.3D scanning tools allow a component with complex geometry to be thoroughly surveyed geometrically.

Skills to handle a variety of specialized software are required.

During the model creation, mistakes are accumulated, which leads to geometry deviations of several tenths of a millimetre, which is insufficient accuracy for certain dimensions of a part and in particular, for determining the type of joining in an assembled unit.

Acknowledgments

This work has been supported by Sofia Tech Park and the National Science Fund of Bulgaria under the Project DH-17-23 "Developing an approach for bone reconstruction and implant manufacturing through virtual engineering tools".

References

[1] Kamberov K 2015 Types of analysis for reliability of mechanical products through virtual prototypes *28 Sci. Conf. Int. Part. – Faculty of Industrial Technology*, 361–8 (in Bulgarian)

[2] Galabov V, Savchev S and Nikolov N 2004 Design of functional model for specialised robot for serving die-cast machines *Sci. Conf. Int. Part. – Mechanical Engineering and Technologies*, 142–5

[3] Todorov G and Kamberov K 2017 *Virtual Engineering: CAD/CAM/CAE&PLM Technologies* (Direct Services – Sofia, in Bulgarian)
[4] Thompson W B, Owen J C, Germain H D S, Stark S R and Henderson T C 1999 Feature-based reverse engineering of mechanical parts *IEEE Transactions on robotics and automation* **15(1)** 57–66
[5] Rönnholm P, Honkavaara E, Litkey P, Hyyppä H and Hyyppä J 2007 Integration of laser scanning and photogrammetry *International Archives of Photogrammetry, Remote Sensing and Spatial Information Sciences* **36(3/W52)** 355–62
[6] Poredoš P, Povšič K, Novak B and Jezeršek M 2015 Three-dimensional measurements of bodies in motion based on multiple-laser-plane triangulation *Rev. Téc. Fac. Ing. Univ. Zulia* **38** 53–61
[7] Marjanovic M 2018 Process for converting a set of image slices into a segmented 3D surface mesh, http://artisynth.org/pmwiki.php?n=OPAL.MarkoMarjanovic, open on 17.12.2018
[8] Sofronov Y, Todorov G and Kamberov K 2014, Geometry reconstruction in CAD environment after optimization or scanning of real object by complex product development *J. CIO, CAD/CAM&GIS* **8(X)** (in Bulgarian)
[9] Todorov G, Kamberov K and Savov I 2015 Automated approach for CAD modeling of orthoses for bone implants *28 Sci. Conf. Intern. Part. – Faculty of Industrial Technology*, 391–8 (in Bulgarian
[10] Kamburov V, Dimitrova R and Kandeva M 2018 Introduction of nickel coated silicon carbide particles in aluminum metal matrix hardfaced by MIG/TIG processes on precoated flux layer *Tribology in Industry* **40(1)**
[11] Singh S 2016 *Superalloys Report* DOI 10.13140/RG.2.1.2385.0009.

Water-hydrocarbons mixture as a fuel for diesel engine

P Haller[1,3], Z Ivanov[2], L Sitnik[1] and M Skrętowicz[1]

[1] Wroclaw University of Science and Technology, Division of Automotive Engineering, 51-640 Wrocław, Braci Gierymskich 164, Poland
[2] Technical University of Varna, Faculty of Mechanical Engineering, Department Transport Engineering and Technologies, 9010 Varna, Studentska str. 1, Bulgaria

[3] E-mail: piotr.haller@pwr.edu.pl

Abstract. The aim of the work is to analyse the advantages and possibilities of using a mixture of water and diesel fuel as a fuel for combustion engines. The inspiration to choose such a topic is the constantly growing increase in demand for alternative fuels, resulting from care for the natural environment. The main problem to be solved in diesel engines is the emission of nitrogen oxides (NO_x). One of the ways to reduce it is to supply combustion engines with hydrocarbon emulsions. The article considers the possibility of using a mixture of water and diesel oil as a liquid used to power internal combustion engines. Engine tests were carried out on the engine test bench in two conditions: driven with pure diesel fuel and a hydrocarbon-water emulsion (80% diesel oil and 20% water). As a result, analysis of the characteristics of the engine parameters was performed, describing its operation in both cases. Analysis of the results of the conducted research allows to conclude that the emission level of harmful substances decreases with the increase of the amount of water in the fuel.

1. Introduction

The diesel engine is still regarded as the most efficient source of energy resulting from the combustion of fuel. For this reason, a lot of attention was paid to the development of this engine – both the construction itself and the fuel used were being worked on.

A very important factor that affects both the pace and direction of development of internal combustion engines is the emission of toxic exhaust components, including mainly nitrogen oxides NO_x. An important role in this process is also non-toxic, but affecting the greenhouse effect of carbon dioxide CO2 [1-4].

Follow to reduce emissions of the above-mentioned compounds results in more and more restrictive regulations regulating these issues. To meet the demands placed on engines, engineers are working on the fuel combustion process to improve it in the entire work cycle.

The current work presents the results of the reduction of nitrogen oxides in exhaust gases obtained using emulsion fuels.

Circulation temperatures are the decisive factor determining the intensity of nitrogen oxides formation in the combustion chamber. Reducing the formation of NO_x inside the cylinder can be achieved by affecting the process of mixing fuel with air and then its combustion, taking into account the distribution of oxygen concentrations and temperatures. A group of methods interfering with the combustion process include processes enabling the input into the combustion space of water in natural form or bound in a water-fuel emulsion [5].

The use of water additive for motor fuels is not a new solution:

- in the 1930s the engine power was increased in this way (by increasing the compression ratio);
- During World War II, water injection was widely used in aircraft and tank engines for short-term engine overloading.

Water is also used as an additive in the manufacture of fuel-water emulsions. The water content in the emulsion affects the combustion process, affecting the increase in engine efficiency in the case of increasing the compression ratio and reducing the toxicity of exhaust gases.

There are already companies in the world that manufacture and sell water-oil emulsions used to power internal combustion engines:

- The American company Lubrizol uses PuriNO_x technology. The fuel thus obtained, depending on the geographical conditions, local regulations and the needs of the consumer, may contain from 10% to 20% of water;
- Pirelli Ambiente produces fuel emulsion containing 10% water.

2. Water-oil microemulsion

Water-oil microemulsions are liquid systems composed of water phase, oil phase and reducing the tension between them surfactant. The droplets of the dispersed phase in these liquids are smaller than one micrometre, which makes them nanodispersion systems [6]. The low surface tension between the phases forming them affects their high thermodynamic stability. The task of the surfactant is the reduction of interfacial tension, which as an amphiphilic compound locates at the interface.

The basic problems associated with the production of water-diesel microemulsion are to resist the separation of two immiscible liquids. To prevent this, various types of surfactants are added [7-9].

In microemulsions, aqueous and oily fractions form mutually interpenetrating structures separated from each other by a layer of surface-active component. The most important factors determining the type of microemulsion that forms are the quantitative ratio between the individual fractions and the geometry of the amphiphilic molecules included in the film located at the interface. This gives the opportunity to obtain an alternative liquid with a water content of 5 to 20% by volume in diesel. Mechanism formation of microemulsion is shown in figure 1 [10].

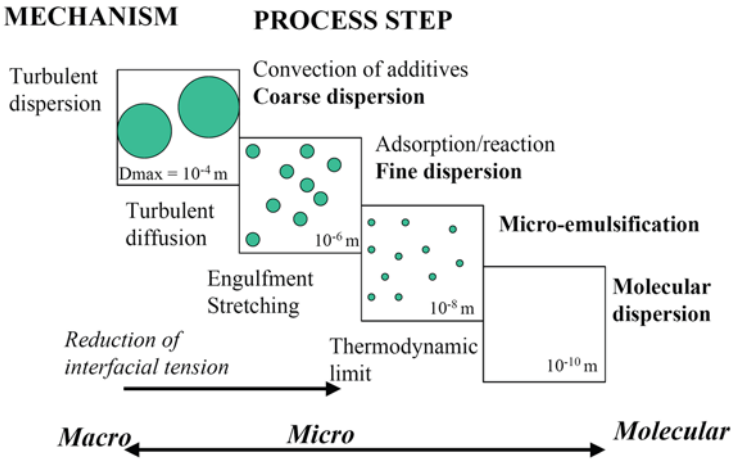

Figure 1. Mechanism formation of microemulsion.

The mechanical method of microemulsion production consists in mechanical fragmentation of water droplets to sizes appropriate for microemulsions. It is possible to obtain such an effect in devices of the cavitation type or in devices with disks rotating counter-rotating at a very high speed.

The tested fuels were provided by a company specialized in the production of fuels and the exact process of their production is not known.

3. Measurements

The aim of the study was to compare the performance characteristics of the diesel engine in the two conditions, using diesel oil and diesel oil emulsion with water. Influence of powered the diesel engine with microemulsion created from diesel oil and water on its work was determined by measuring fuel consumption and emission of nitrogen oxides NO_x in exhaust gases.

For the needs of the tests, a liquid with a water content of 20% was prepared.

The tests were carried out in Division of Automotive in the Wroclaw University of Science and Technology, on the engine test bench, using the VW 1.9 TDI engine.

Individual engine operating points at which the measurements were made were selected independently based on the ESC test, which is no longer used, and which is replaced by the WLTP test. These points have been chosen to get as close as possible to the natural operation of the vehicle in road traffic.

Schematic diagram of the research place is shown in figure 2. The test stand is shown on figures 3 and 4. The engine load characteristics were determined at selected values of rotational speed and torque.

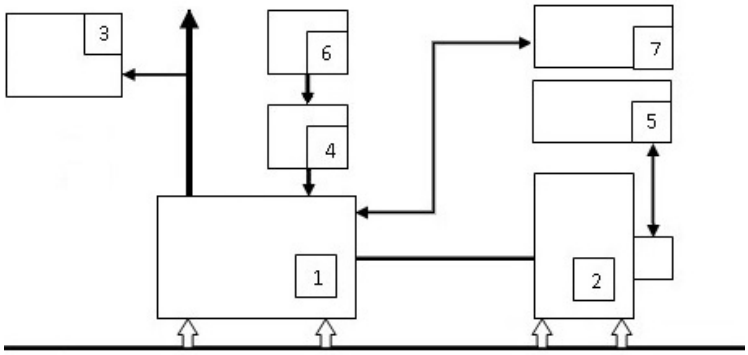

Figure 2. Schematic diagram of the research place: 1 – engine, 2 – dyno, 3 – exhaust gas analyser, 4 – fuel gauge, 5 – dyno control device, 6 – fuel tank, 7 – engine control device.

Figure 3. Test stand – engine test bench.

Figure 4. Test stand – measuring and control devices.

4. Test results

To properly assess the emission of nitrogen oxides NO_x in the exhaust and engine fuel consumption, a prerequisite is to ensure the engine's operating conditions close to the average operating conditions in normal drive cycle. Therefore, in this test, the motor load torque is 50, 100, 150 and 200 Nm and crankshaft speeds is idle speed, 1900, 2500 and 3000 rpm. The study predicted that the engine performance would vary depending on the use of diesel oil or emulsion composed of diesel oil and water. For this reason engine loads were the same for both fuels so that the measurement could be made at identical points of the characteristic, independently of the liquid used. In the case of emulsions, all fuel standards are not met. All test result are shown in Table 1, figures 5 and 6.

Table 1. Test results for Diesel oil + H_2O and Diesel oil.

		Diesel oil + H_2O		Diesel oil	
Speed, rpm	Torque, Nm	Fuel consumption, g/kWh	NO_x, ppm	Fuel c., g/kWh	NO_x, ppm
860	15	363.77	41.62	298.09	94.45
1900	50	236.95	95.89	223.03	346.04
1900	100	231.09	317.28	212.51	641.82
1900	150	225.50	600.99	202.93	906.21
1900	200	243.12	860.38	204.78	126.53
2500	50	268.76	124.92	219.48	289.38
2500	100	257.08	289.73	206.26	567.65
2500	150	251.61	510.34	203.80	950.43
2500	200	233.40	890.49	208.77	162.79
3000	100	250.54	364.48	206.76	655.07
3000	50	289.84	168.54	228.26	373.91
3000	150	246.36	610.85	211.35	934.57
3000	200	254.86	764.70	203.80	73.58

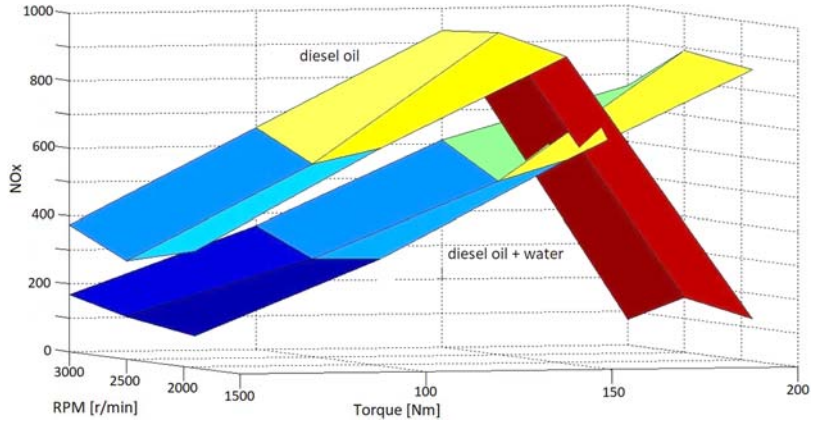

Figure 5. Values of nitrogen oxides NO_x emission in all points of the test using the both fuels.

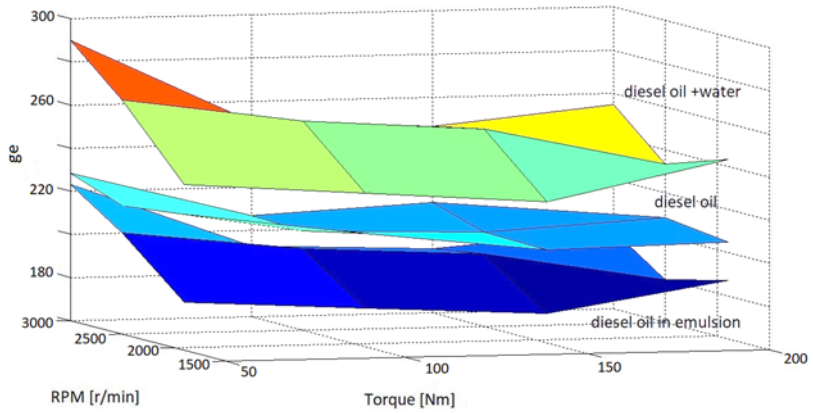

Figure 6. The values of fuel consumption in all test points.

5. Conclusions

The search for new fuels for internal combustion engines must take into account the need to reduce emissions to the environment, as well as their toxicity. Therefore, it seems reasonable to create new mixtures that can meet these requirements.

By supplying the diesel engine with water microemulsion, a reduction of the NO_x level was observed. Their content dropped by more than 10% in the test, but if you take into account the work at lower loads, this value could be up to 50% lower than the value obtained with diesel fuel. This is due to the lower temperature inside combustion chamber after using of the emulsion, caused by evaporation of water during the combustion process. The NO_x emission decreases with the use of emulsion together with the decrease of rpm and torque. The NO_x emission values become equal only at high engine torque. At high loads and emulsion powered engine, emission is constantly increasing.

As expected, consumption of emulsion fuel is higher by almost 20% due to adding of the water in it. Emulsions composed of water and diesel oil have a lower calorific value in comparison to the diesel oil itself. If we take water from the emulsion, there are no such large differences in fuel consumption. In the test, after taking into account and subtracting the weight of water added to the emulsion, a diesel oil saving of 8% was obtained in relation to the demand for diesel supplied to the engine in its pure form. The charts also show these mutual relations of the fuels studied. In the entire engine operation range studied, emulsion consumption is higher than diesel oil, but after exclusion of emulsion forming water from the calculation, a lower demand for diesel oil delivered in the form of an emulsion was obtained. During using water-diesel microemulsion, the power of the engine decreases slightly, while the consumption of the engine's liquid is increasing. The power reduction depends on the speed of rotation and the amount of water in the microemulsion. The use of microemulsion fuel causes an obvious reduction in the overall efficiency of the engine, but to a lesser extent than the share of water in the fuel.

Acknowledgements
The paper is as a result of the research project No. N N509 356134 support by Polish Ministry of Science and Higher Education in 2008-2011.

References

[1] Sitnik L J 2004 *Ekopaliwa Silnikowe* (Oficyna Wydawnicza Politechniki Wrocławskiej)
[2] Sitnik L, Dworaczyński M and Haller P 2013 Water-hydrocarbon emulsions obtained by cavitation used for the fueling of diesel engines *The Archives of Automotive Engineering (ISSN 1234-754X)* **60(2)** 21–33
[3] Jankowski A, Sowa K and Zabłocki M 2009 Some aspects using of micro emulsion fuel-water for supply of combustion engines *J. KONES 2009 Powertrain and Transport* **16(4)** 531–8
[4] Yoshimoto Y, Tamaki H 2001 Reduction of NO_x and smoke emissions in a diesel engine fueled by biodiesel emulsion combined with EGR *SAE Paper 2001-01-0649*
[5] Piaseczny L and Zadrąg R 2005 Badania wpływu dostarczania wody do cylindra na wskaźniki procesu spalania i toksyczności silnika ZS *Silniki spalinowe* **3(122)**
[6] Jankowski A 2011 Influence of chosen parameters of water fuel microemulsion on combustion processes, emission level of nitrogen oxides and fuel consumption of ci engine *J. KONES Powertrain and Transport* **18(4)**
[7] Kolanek C 1997 Ograniczenie emisji NO_x z silników o zapłonie samoczynnym przez wprowadzenie wody do procesu spalania *Ochrona środowiska (Wyd. Oddziału Dolnośląskiego PZTIS)* **1(64)**
[8] Kolanek C, Kułażyński M and Kempińska M 2007 Examination of the effects of water presece in Fuel on toxicity indices of a compression-ignition engine *J. KONES; European Science Society of Powertrain and Transport Publication*
[9] Bemert L and Strey R 2007 Diesel-Mikroemulsionen als alternativer Kraftstoff *FAD Konferenz Herausforderung – Abgasnachbehandlung fuer Dieselmotoren (7.11-8.11.2007 Dresden)*
[10] Haller P, Jankowski A, Kolanek C and Walkowiak W 2012 Microemulsions as fuel for diesel engine *J. KONES Powertrain and Transport* **19(4)**

Advanced solutions providing for safety of shipping in coastal areas

G L Dimitrov

Department of Electronics, Faculty of Navigation, Nikola Vaptsarov Naval Academy, 73 Vasil Drumev Str., Varna 9002, Bulgaria

E-mail: g.dimitrov@nvna.eu

Abstract. Europe's seas and oceans are a rich and often underestimated source of innovation, growth and employment. They provide valuable ecosystem services and resources on which all marine activities depend. Since its establishment in 2007, the Integrated Maritime Policy (IMP) aims to improve the sustainable development of the European maritime economy and better protect the marine environment by facilitating cooperation among all maritime participants crossing different sectors and borders. Investment in research should fully develop its potential for innovation in the maritime economy. As the activities in the coastal areas increase, the vessel traffic system should have alternative means for better maritime awareness. Internet of Things could offer a solution where its small transceivers interacting with a mobile device application provide information about the movement of the small leisure or fishing vessels in an area covered by a gateway in 868 MHz band. Carriage requirements for the automatic identification systems do not consider small boats and jets. This is an expensive system. The paper discusses an experimental application of an IoT device that is utilized for position reporting aid to the vessel tracking system. Such solution could be effective in the adjacent coastal area ranging from 3 to 5 km. The major contribution of the maritime sectors to the European economy and the objectives of the Europe 2020 strategy are reinforced by coordinated action to reduce costs, improve safety and resource efficiency, mitigate risks, support innovation and make better use of public funds.

1. Introduction

A plan to create effective marine safety system is envisaged as a national strategy for many countries worldwide. While providing new economic opportunities, the coasts and waterways of Europe should remain protected having in mind safety of navigation. Protection projects will be a large investment but will lead to responsible shipping and healthy coastal community and environment. Considering leisure boat accidents each year, more than 90 percent of the casualties were not wearing personal floating or alerting devices. If small vessels and leisure crafts are equipped with inexpensive trackers, accidents could be avoided and alerting could be initiated in due time. Information and communication technology developments in recent years lead to effective solutions for ship management in coastal areas and inland waterways. The modern technologies complementary to each other are the cellular network communications, the radio frequency identification techniques and the high-level communication protocols. [1].

The traditional methods include well-known GPS trackers using SIM card and sending data via the PLMN operator. Such conventional system is for example the popular tracker ST-901 which uses GPRS, 3G, 4G LTE technology. It sends data at pre-programmed regular intervals as well as messages

containing its coordinates when interrogated. These devices incorporate also an accelerometer that alerts when craft is blown or other impact is registered. Control is carried remotely via SMS or an Android smartphone application. It is also possible to interface the tracker with other restraint systems onboard [2]. The traffic normally costs 2 EUR per month for the volume of 250 MB but such device spends actually not more than 30MB for monthly position reporting. In the coastal areas, the coverage is up to 3 km from the shore. Lately, the trackers are considered as an enhancement to e-business websites, allowing to geo-locate shipment detention, monitoring and storage.

2. Proposal for utilization of LoRa device

The e-Navigation concept initiative, supported by IMO aims to secure safe ship navigation, preserve marine environment and provide security-related services during these activities. Establishing a common frameworks and standardization is under progress, so alternative ways to facilitate the exchange of marine traffic information should be sought [3].

The aim of this experiment is to demonstrate such alternative way to track vessels in the coastal areas by means of long-range low power devices (LoRa) – part of the IoT network. The device proposed in this article is based on AcSIP S76G chip and could be utilized with success to provide for safety of navigation near shore as a supplementary means to VTS operation. The equipment contains pre-programmed identification keys and operates on 868 MHz [4]. In the coastal area of Varna bay for the moment, there are two gateways in operation covering with considerably high signal strength – 117 dBm (see figure 1). In the area, there's still a small number of providers operating LoRa gateways. Customers could choose between those having contacts with The Things Network and Everynet. The test results presented in this article are coordinated with a Bulgarian company provider of Everynet as seen from the screenshots.

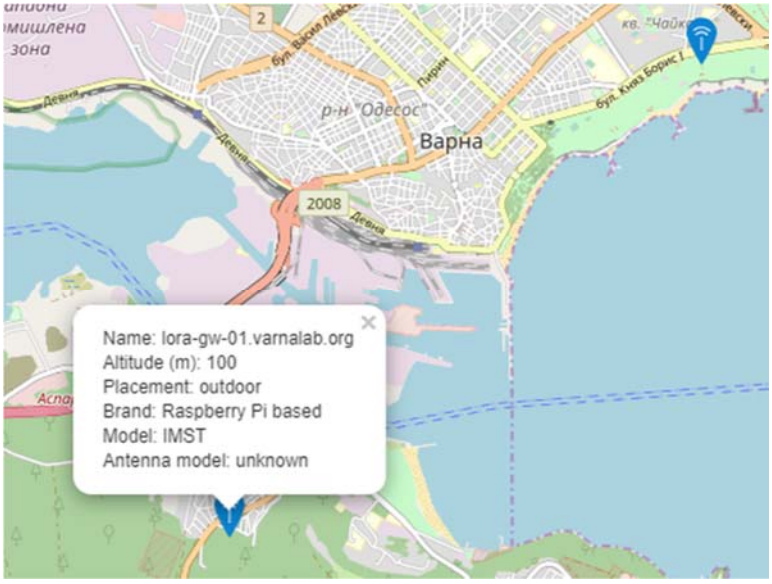

Figure 1. The LoRa operational gateways used for data transfer on the territory of Varna.

For Bulgaria, the following rules apply – EU863-870, EU433 according to CEPT Rec.70-03 [5]. As these devices operate in the ISM band, there are advantages and disadvantages. The advantage is that anyone is allowed to use these frequencies and no license fee is required. Since anyone can use these frequencies this could be considered also as a disadvantage because of the expected interference. Low data rate is also a disadvantage. Having in mind the duty cycle of the system, 1% and 0.1% are both acceptable for this project purpose. Thus, the vessels could be followed in an area between 2 and 5 km from shore. The device generates traffic costs up to 3.5 EUR per year for one-way uplink traffic sending 7-100 reports per day.

The device GAT2038 is an inexpensive LoRa sensor tracker and is a wireless remote positioning solution based on LoRA+GPS nRF52832 chip [6]. It also includes temperature and humidity sensor. The circuit uses LoRaWAN 1.0.2 protocol and supports LoRaWAN working mode, allowing customers conveniently to link to the IoT network. Figure 2 shows the appearance outlook.

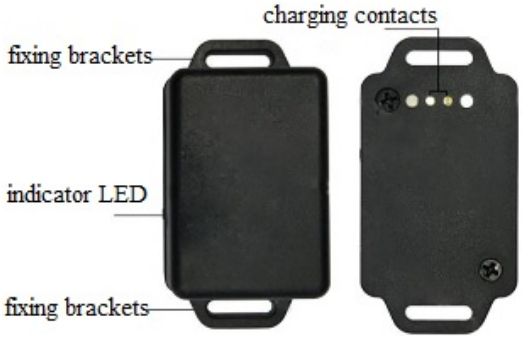

Figure 2. Device GAT2038 with the corresponding fixing elements. The case material is ABS and size is 48×32×20 mm. The device has a Bluetooth connection (BLE) option. AT commands via a laptop or smartphone could be utilized to configure it. There's a built-in 3D acceleration chip so that motion status of the object could be detected or determined if the vessel is stationary. GAT2038 is intended for industrial scenarios and can also be configured via an application.

3. Methodology for activation, registration and utilization of the IoT network

The LoRa network is based on the standard LoRaWAN architecture [7]. This includes LoRa compatible base stations, LoRa networks server and client applications for end-to-end communication with compatible devices. For testing purposes, the server could decode the data using the customer's application key and to send the data to the application in both ways – encrypted or not encrypted. The network offers public CRM applications access. Thus, any customer could register an account to test, administer, configure parameters and manage devices for a certain period of time (for example 30 days). Using ready-made public CRM applications allows the testing customers to define and put in service personal devices of already known manufacturer and type, as well as common type device if not listed. The equipment here is considered as of low power payload type.

When the customer uses commercially available devices, tables with historical data records on the server are generated. The CRM application offers an additional option the test accounts to send data back to the devices (downlink packages) in the form of raw bytes, carrying previously entered information. The network as a transport media registers the packages sent from the devices in their original format and does not affect or alter their content. There is a statistical record of the number of transferred data packages – sent and received from a registered device for a period of 14 days. The statistic information could be downloaded and presented offline. The communication between the network and the applications could be only according to the described API standards.

3.1. Conditions that should be fulfilled in order to operate the device on the IoT network

- To have a client's application integrated in the network. This means that the end user should have an identification network number as a virtual connection;
- To register and activate the device in the network to allow for normal operation.

The device registration requires the exchange of the following parameters between the item and the network:

- Address of the IoT device (DeviceAddress – *DevAddr*) between the device, the network and the application;
- Network Session Key (NetworkSessionKey – *NwkSKey*) – between the device and the network server;
- Application Session Key (ApplicationSessionKey – *AppSKey*) – between the device and the client's application.

The device offers both activation by personalization or over the air. Over-the-Air Activation (OTAA) is the preferred and most secure way to connect with The Things Network. Devices perform a join-procedure, during which a dynamic *DevAddr* is assigned and security keys are negotiated with the equipment [8]. In some cases, the user might need to hardcode the *DevAddr* as well as the security keys

in the chip. This means activating the circuit by personalization (ABP). The strategy might seem simpler, because the join procedure is skipped, but it has some downsides related to security. The parameters concerning normal operation and performance data when activated by personalization are configured directly via Bluetooth. These are *DevAddr, NwkSKey, AppSKey.* The device utilized in these tests has a firmware version that limits the joining procedure to over-the-air only.

3.2. Actual operation

The tracker sends LoRa commands using its unique identification *DevEUI*, the application identifier *AppEUI* and its personal pre-programmed recognition identifier *AppKey*. The server sends back to the LoRa device commands with the selected device address *DevAddr* and the generated *NwkSKey* as well as *AppSKey*. These are stored inside and then the parameters are used further on. It is necessary the customer's application to be integrated in the network in order to receive information from the tracker and to send back commands towards it via the internet. The client's application during integration utilizes unique identifier *AppEUI* which corresponds to the identifier configured inside after OTAA activation process or random one when configured using the APB method [9].

The data is being exchanged as standard meta-data information similar to *json* objects, surrounded by square or big brackets – parameter pairs containing names and values (in inverted commas) and the parameter pairs themselves separated by commas. The network supports additional interfaces based on HTTP or MQTT protocols, as well as specific API for direct connections with public IoT platforms – Amazon WS IOT, PubNub, Cayenne MyDevices, etc. The solution with Cayenne MyDevices supports and offers customer application simulation on a test server, where the received data packages from the corresponding equipment are sent in the original format and are monitored on the server side. The network retransmits the coded data packages from the device registered and associated with the customer's application. The application decodes the data using *AppSKey* and then additionally processes the information if necessary according to customer requirements.

4. Results and visualization

Figure 3 shows the data coming from the device after receiving a remote command to transmit with lower power (from DR0 to DR2) to preserve battery life and avoid interference. The changes in the frequency are also seen on this picture. Data uplinked from remote devices to the Everynet application are published so that one can connect also using an application of his own. The user can utilize MQTT nodes to receive the data published by Everynet. To make it even easier, Everynet has written custom nodes for Everynet integration.

Figure 3. The log showing the activity of the device, the signal strength and the channels.

As per the manufacturer's decision, there are separate channels for each "service". Channel 1 is allocated for GPS data, channel 2 is the data from the accelerometer, channel 3 is the temperature data, and channel 4 is the data coming from the humidity sensor (see table 1).

The decoding process is shown in table 2. An example is taken to consider data coming from the accelerometer as type 71 on data channel 2. The next channel 3 is selected for the temperature readings and the value could be read from the table. The tracker has been open deck mounted which explains why the reading contains such high temperature.

Table 1. Data entering the visualization platform.

Timestamp	Chan	Sensor ID	Data	Unit	Values
2019-08-08 12:55:14	3	17b8c3a0-b9b3-11e9-879f-4ff2bd1b7688	temp	c	42
2019-08-08 12:55:14	2	17cdab30-b9b3-11e9-b6c9-25dbdbf93e02	accel	g	-16.132,24.576,-24.572
2019-08-08 12:55:04	3	17b8c3a0-b9b3-11e9-879f-4ff2bd1b7688	temp	c	41
2019-08-08 12:54:43	1	9457de80-b9b0-11e9-80af-177b80d8d7b2	gps	m	43.1918,27.9215
2019-08-08 12:53:42	1	9457de80-b9b0-11e9-80af-177b80d8d7b2	gps	m	43.1912,27.921
2019-08-08 12:53:53	2	17cdab30-b9b3-11e9-b6c9-25dbdbf93e02	accel	g	-16.382,-16.384,16.638
2019-08-08 12:48:52	3	17b8c3a0-b9b3-11e9-879f-4ff2bd1b7688	temp	c	46
2019-08-08 12:45:32	1	9457de80-b9b0-11e9-80af-177b80d8d7b2	gps	m	43.1936,27.9208

Table 2. The payload 02 71 20 00 e0 ff e0 00 decoding process.

	Data Channel	Type	Value
Payload (HEX) 02 71 20 00 e0 ff e0 00	02⇒ 2	71 ⇒ Accelerometer	X:2000 = +8192 ⇒ +8.192G Y:e0ff = +57599 ⇒ +57.599G Z:e000 = +57344 ⇒ +57.344G
Payload 03 67 01 b8	03 ⇒ 3	67 ⇒ Temperature	01b8 = 440 ⇒ 44.0°C

Figure 4 contains accelerometer data from channel 2 only. The payload in base 64 format is written directly in the log.

Time	Payload Base64	B11	B10	B9	B8	B7	B6	B5	B4	B3	B2	B1	B0
09:16	AnEAAMD/4P4DZwJE	2	71	0	0	c0	ff	e0	fe	3	67	2	44
09:19	AnGg/8D/AP8DZwJi	2	71	a0	ff	c0	ff	0	ff	3	67	2	62
09:19	AnFgACD/AAADZwJi	2	71	60	0	20	ff	0	0	3	67	2	62
09:19	AnFAACAAAAADZwJi	2	71	40	0	20	0	0	0	3	67	2	62
09:19	AnEAAKAAIAADZwJi	2	71	0	0	a0	0	20	0	3	67	2	62
09:20	AnFg/+D/AAADZwJs	2	71	60	ff	e0	ff	0	0	3	67	2	6c
09:30	AnEAAOD/oP8DZwKA	2	71	0	0	e0	ff	a0	ff	3	67	2	80
09:31	AnEAAOD/AAADZwJ2	2	71	0	0	e0	ff	0	0	3	67	2	76
09:39	AnHgAOD/AAADZwKA	2	71	e0	0	e0	ff	0	0	3	67	2	80
09:39	AnEAAAD/QAADZwKA	2	71	0	0	0	ff	40	0	3	67	2	80
09:39	AnFgAEAA4AADZwKA	2	71	60	0	40	0	e0	0	3	67	2	80
09:40	AnFAACAA4AADZwKA	2	71	40	0	20	0	e0	0	3	67	2	80

Figure 4. The payload as base64 format showing the 12 bytes of data used to send information.

An online service like Cayenne makes it easy to integrate with Everynet, but one can also integrate with own software using MQTT protocol. The data from GAT2038 in this article is compatible with Cayenne Mydevices platform. Cayenne Mydevices is a solution to build applications based on platforms as Arduino, Raspberry Pi, ESP8266 and Serial devices, WiFi, LoRa devices, which also include a MQTT API client. The GAT2038 LoRa tracker utilizes AcSIP S76G and is registered as Cayenne low power payload (Cayenne LPP) [10]. Table 1 shows the data entering the visualization platform.

Figure 5 represents the result and the dashboard on the Cayenne Mydevices website. The screenshot shows the positions of the boat “Ephemerida” in the Port of Varna as well as outside temperature data and the accelerometer data readings (see figure 6).

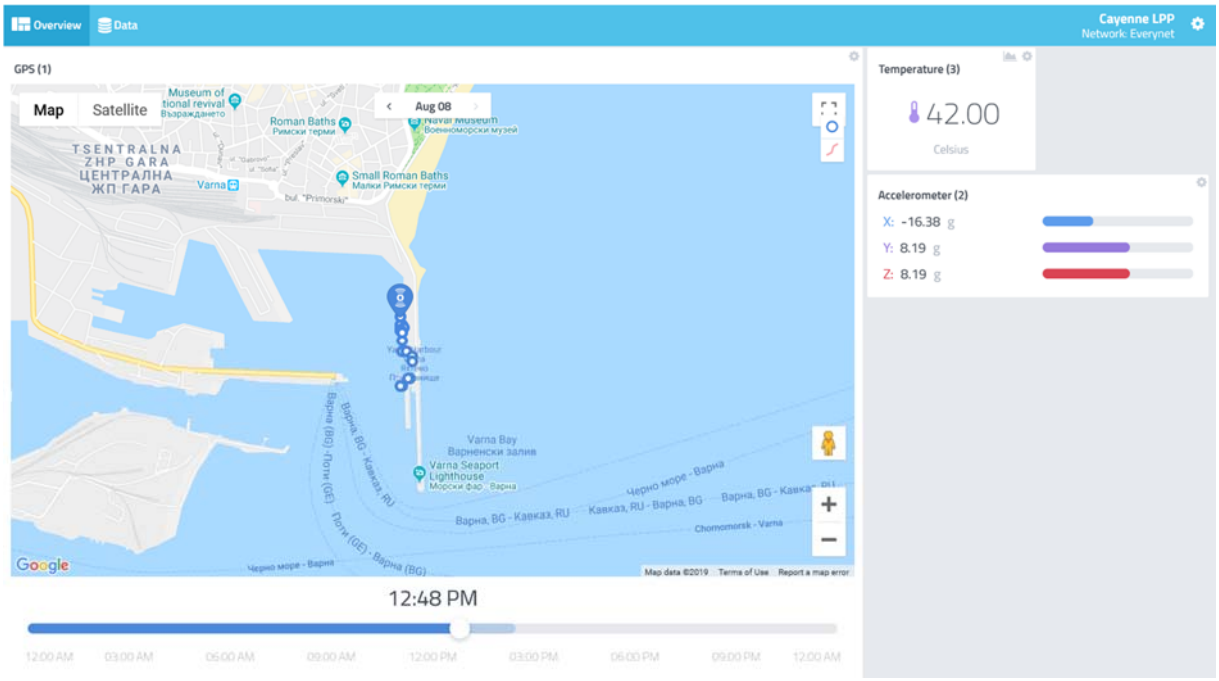

Figure 5. Visualization of the Cayenne Mydevices platform.

Figure 6. The boat "Ephemerida" that carries the LoRa tracker in the bay of Varna, Bulgaria.

5. Conclusions

LoRaWAN could definitely facilitate the sustainable development of the shipping industry and would provide for efficient marine traffic control. For the moment, the IoT gateway infrastructure could seems insufficient but the growth rate is high enough. In Bourgas area – another large Bulgarian port, the number of gateways is approaching 60. The idea to utilize inexpensive LoRa trackers in coastal areas will improve in effective way the risk evaluation process, consideration of the circumstances and predict the actions for accident prevention. Such solution is both cost effective and meets the need of waterway users, VTS and stakeholders. Furthermore, the collected measurements concerning the maritime environment – temperature, humidity and accelerator readings could be of help for the oceanographic research in Black Sea coast areas. Further study is required to determine the reliability of these devices and their utilization for disposable control.

Acknowledgements

The tracking device utilized in this experiment comes from the Chinese manufacturer GATIntelligent. Special acknowledgements are given to the Bulgarian provider IoTNET and Varna Lab for their support in data adaptation and the follow up visualization on the Internet.

References

[1] Zhuang Y and Song S 2013 Use of Internet of Things for ship management of inland rivers *InICTIS 2013: Improving Multimodal Transportation Systems-Information, Safety, and Integration* 2425–31

[2] Godavarthi B, Nalajala P and Ganapuram V 2017 Design and implementation of vehicle navigation system in urban environments using internet of things (IoT) *InIOP Conference Series: Materials Science and Engineering* **225(1)** 012262

[3] Park N and Bang H C 2016 Mobile middleware platform for secure vessel traffic system in IoT service environment *Security and Communication Networks* **9(6)** 500–12

[4] Semtech: AN1200.22 – LoRa Modulation Basics (Revision 2, May 2015) URL: https://www.semtech.com/uploads/documents/an1200.22.pdf

[5] ETSI EN 300 220-2 (V3.2.1, June 2018) URL: https://www.etsi.org/deliver/etsi_en/300200_300299/30022002/03.02.01_60/en_30022002v030201p.pdf

[6] Semtech: SX1276/77/78/79 Datasheet (Rev. 5, August 2016) URL: https://www.semtech.com/uploads/documents/DS_SX1276-7-8-9_W_APP_V5.pdf

[7] LoRa Alliance, Inc: LoRaWAN specification URL: https://lora-alliance.org/lorawan-for-developers

[8] Semtech: AN1200.13 - SX1272/3/6/7/8 LoRa Modem Design Guide (Revision 1, July 2013) URL:https://www.semtech.com/uploads/documents/LoraDesignGuide_STD.pdf

[9] Semtech SX1301 Datasheet (V2.4 - June 2017) URL: https://www.semtech.com/uploads/documents/sx1301.pdf

[10] Semtech: ANNWS.01.2.1.W.SYS – LoRaWAN Network Server Demonstration: Gateway to Server Interface Definition (Revision 1.0 - July 2015)

Preservation of macro fractographic signs of the plane of fracture of the details for expert engineering research

A Batig[1,5], P Hrytsyshyn[1,2,3], O Kovalchuck[1], A Kuzyshyn[1,4], S Dovhaniuk[4] and J Sobolevska[3]

[1]Lviv Research Institute of Forensic Expertise, 79000 Lviv, Ukraine
[2]Western centre of the Ukrainian branch of the World laboratory, 79021 Lviv, Ukraine
[3]Lviv branch of Dniprovsk National University of Railway Transport named after Academician V. Lazaryan, 79052 Lviv, Ukraine
[4]Dniprovsk National University of Railway Transport named after Academician V. Lazaryan, 49000 Dnieper, Ukraine

[5] E-mail: batigasha1992@gmail.com

Abstract. Estimates of operational reliability and durability of machine parts and mechanisms cannot be carried out without technical diagnostics of the presence or absence of fatigue cracks, which are the cause of destruction. In some cases, the object of investigation, which is a material proof in the execution of expert engineering studies, may be accidentally or deliberately damaged or destroyed. This leads to the loss of specific signs of the presence of fatigue cracks and the inability to identify patterns that led to their appearance. Ultimately, this affects the reliability of the results. For example, such circumstances in the future significantly complicate the identification of the true causes of accidents and disasters on the railway. Preserving the plane of fracture of the object of research at the scene of the incident and in the process of its transportation to a research institution is an important factor in increasing the reliability of expert engineering and technical opinion taking into account the requirements of the European Union technical specifications (TSI).

1. Introduction

The stability of the development of the national economy depends on the degree of development of each of its branches and infrastructural components. European integration is one of the main priorities of Ukrainian state policy. The development of the railway industry of Ukraine is a prerequisite for stable development and recovery of the economy, strengthening its competitiveness, expanding its foreign economic activity in providing European integration vector for the development of the state. In this context, railway traffic safety remains one of the most important factors in the development of the industry, since without an adequate level of safety, the efficient operation of the entire railway segment is impossible.

Usually, the level of safety operation of the railway transport system depends, to a large extent, on the successful development of socio-economic programs of the state. But at the same time, along with the development of the railway system, the number and level of accidents and disasters, the death toll and the number of wounded people, and material losses to citizens and the state as a whole are increasing. In the investigation of rail-transport accidents (RTA) one of the main sources of evidence is the conclusion of the court rail-transport expertise.

Investigation of railway accidents is impossible without solving the problems of identification causal relationship between breakage (surface or internal) or destruction of a structural element and the time when the threat to safety movement on the railway transport occurs. Such tasks fall within the competence of experts with specialty "Research of vehicle parts".

A number of recent studies have been devoted to the investigation of the causes of rolling stock derailments [1-3]. The development of track deformations and defects in its elements are outlined among the possible reasons the derailments. The initiation and the development of the track deformations are primarily associated with the residual settlements of ballast layer. A mathematical modelling of track unevenness development and calculations of rolling stock loading on ordinary track and turnouts is carried out in the studies [4-5]. The influence of the maintenance works and their influence on the quick initial deformations are studied in [6].

The study of the behaviour of the rolling stock and the railroad after the moment of derailment is presented in the papers [7-9]. One of the objectives of these studies is to establish the causes and the mechanism of railway traffic accidents by the help of tracking the superstructure destruction and the damages in track and rolling stock.

A series of papers [10-12] is devoted to preventing and forecasting the destruction of especially loaded track elements – the crossings of turnouts. These studies deal with an experimental observation of the rolling stock dynamic loading and appearing of cracks in the common crossing rails during its lifecycle. Both on-board and track monitoring systems of dynamic loads are used for this purpose.

A fractography study of metal surfaces in the destruction areas of rolling stock and railway track is presented to a number of studies [13-16]. The results of the studies allow to determine the conditions of the elements operation and the causes for the destruction as well as the defect prevention. An analysis of the cracks development in the rail rolling surface and the prediction of its development depending on the size and shape of cracks, is studied in [17-20].

The task of the forensic railway expert examination, in this case, is to identify technical conditions of systems and elements of railway transport in case of their loss of strength, studying the actions of participants of the railway transport accident (RTA).

2. Formulation of the problem

The practice of carrying out engineering and transport research at L'viv Research Institute of Forensic Expertise of the Ministry of Justice of Ukraine indicates that in certain cases, upon removal, the destroyed objects of investigation may have unintentionally or deliberately damaged planes of breakage, which leads to the loss of their specific features and inability to detect regularity, which led to the occurrence of damage and destruction, and hence the reliable identification of the causes of an accident or disaster is impossible. As a result, these circumstances, in the future, substantially complicate the establishment of actual causes of traffic accident occurrence, and in some cases, may lead to erroneous conclusions.

3. The purpose of the work

Provide recommendations for material evidence preservation as objects of engineering and technical research for the performance of court rail-transport expertise.

4. Main research material

From the theory of materials resistance it is known that the destruction of rolling stock parts is most likely due to the following reasons:

- if the quality of the metal which they are made of does not ensure mechanical properties provided by the design, such as the strength limit, hardness, impact strength, etc.;
- if their geometrical parameters do not meet the requirements of the working drawings (mismatch and distortion of linear dimensions, radii of quirks of parts, the presence of dints and scratches on the surface of the loaded parts, etc.);

- if the forces acting on the corresponding element of the moving mechanism of the vehicle exceed the maximum load that it can withstand.

However, it is also known from the expert practice in the research of machine parts and mechanisms of the railway industry that destruction occurs when the qualitative parameters of the metal which the part is made of, its geometric parameters correspond to the requirements of the normative documents, and the forces acting on the part do not exceeded the maximum load that this part can withstand. In such cases, it is necessary to apply the mechanics of destruction of solids with cracks. [21-25].

The criteria and approaches for assessing the strength of materials and structures formed at the beginning of the last century come from the fact that the calculation model of a real solid is a continuous medium with given rheological properties (for example, elastic continuum), and the deformable body element is located in one of these states: solid (*S*-state) or destroyed (*D*-state) (figure 1). The transition of a material element from the state *S* to the state *D* (the process of destruction) is carried out instantaneously as soon as the stress-strain state, calculated within the framework of the adopted rheological model, reaches some critical value (for example, if the tensile stress at the given point of the deformed solid reaches strength limits σ_B).

Such a classical approach to materials in a fragile state, which have sharpened defects such as cracks, cannot solve the task of their strength, because this approach does not take into account special stress-deformed state of the material in the vicinity of the peak of the acute defect that is a crack in the process of body deformation. This is due to the fact that the radius of peak rounding of such a concentrator is comparable to the parameters of the structure of the material itself.

The most important postulate in the mechanics of solid destruction is the interpretation of destruction as the process of origin and spread of a crack, which (in comparison with classical approaches) already involves the mechanism of destruction itself, and the crack becomes the instrument with which the destruction is carried out. This implies the importance of evaluating the extremely equilibrium state of solids with deformable cracks, as well as the development of a crack under the short-term or long-term impact on the body of the given workload and environment and determining the characteristics of the material resistance to spreading cracks in it, that is the crack-resistance of the material.

The main idea of the neoclassical approach (mechanics of material destruction) is reduced to the following (figure 1). It is believed that the transition of an element of a deformed body from the state *S* to state *D* is accompanied by an intermediate state *I*, which must be taken into account when solving the problem of body strength with defects such as cracks. The most important feature of a deformable solid, where the state *I* (area before deformation) arises is that its material is always deformed beyond the limits of elasticity, and precisely there the most intense plastic deformation, diffusion processes, material damage and other phenomena, which ultimately lead to local destruction of the material, that is, $S \rightarrow I \rightarrow D$ transition takes place. Thus, the neoclassical destruction scheme involves allowance of *I*-state of near-sharp defects in a deformed body and, first of all, stress concentrators of crack type whose radii of curvatures are comparable to the typical linear size of the structural element of the material.

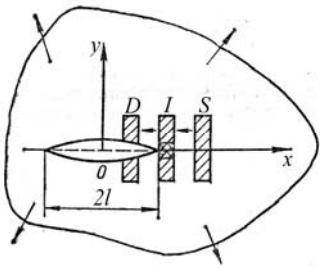

Figure 1. Neoclassical destruction scheme.

The direct task for engineering practice is to find effective factors for increasing the index of friction resistance. However, in expert practice, there is a need to study the inverse problem – what coursed the problem and how actually the process of destruction took place.

In analysing the causes of fatigue destruction of machine parts, mechanisms and elements of steel structures, the forensic expert practice investigates the structure of fracture planes. Also, for the analysis of reasons of cracks origin, metallographic methods of research are used to determine the size, shape and mutual placement of crystals, structural features, as well as non-metallic inclusions, cracks, shells, pores, etc. They distinguish macroscopic and microscopic methods of investigating the structure of surfaces of fracture planes.

The macroscopic method is a study of the structure of metals with the naked eye or with the use of a magnifier or microscope with magnification of 5-30 times; it makes it possible to detect holes on the fracture planes of shells, slag inclusions, damage of the structure continuity (macro- and microcracks), and other defects of the metal structure, which product is made of. They show chemical, structural heterogeneity of a metal and deviations from the regulatory requirements.

If macrofractographic studies do not show visible defects in a metal product, then the microscopic analysis of the structure is used, which consists in using optical or electronic microscopes on specially prepared samples, to determine the cause of the destruction. These samples are cut from fragments of destroyed parts, which have already entailed the destruction of the object of research, which, as a rule, is a real evidence of the case. Therefore, ensuring the safety of detected planes of fracture parts of rolling stock at the place of railway accident and in the process of their transporting to an expert institution is an important factor in increasing the reliability of expert judgment as an instrument of evidence and objectivity of engineering and technical expert research.

5. Experimental data

If, during derailment, in the pile of carriages, breakage of rails, sidewalls or other parts were revealed, even in the presence of old fatigue cracks, such breakage should not been unconditionally accepted as the cause of a disaster and accident, which is often manifested in the texts of technical statement on the event drawn up by members of the commission on official investigation of the causes of the railway accident. First of all, it is necessary to determine why supercritical power could occur, which led to the breakdown of elements of the construction of the railway transport, for example, the use of emergency braking of a train (figure 2). In most cases, such breakdowns can be both a cause and a consequence of derailment.

Therefore, a detailed study of fracture plane of part fragments gives important information about:

- whether static load exceeding limits of flow (so-called plastic fracture) affected the part (figure 3);
- whether significant impact loads, which were applied at a high speed (fragile fracture), affected the part;
- whether prolonged cyclic loading (fatigue breakdown) (figure 4) affected the part.

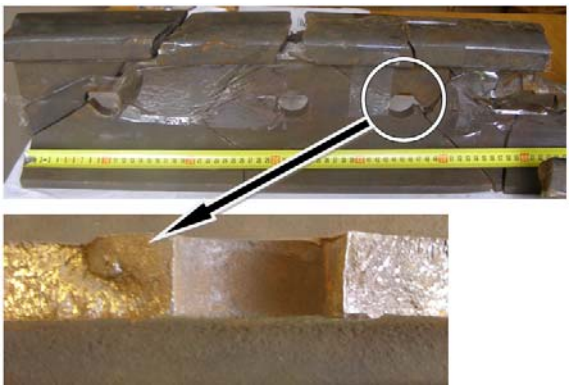

Figure 2. Rail fracture due to emergency braking of a train.

In addition, the investigation of fracture planes also gives information to the expert about the location, direction of the applied load and the grounds for choosing the method for estimating causes and time of destruction.

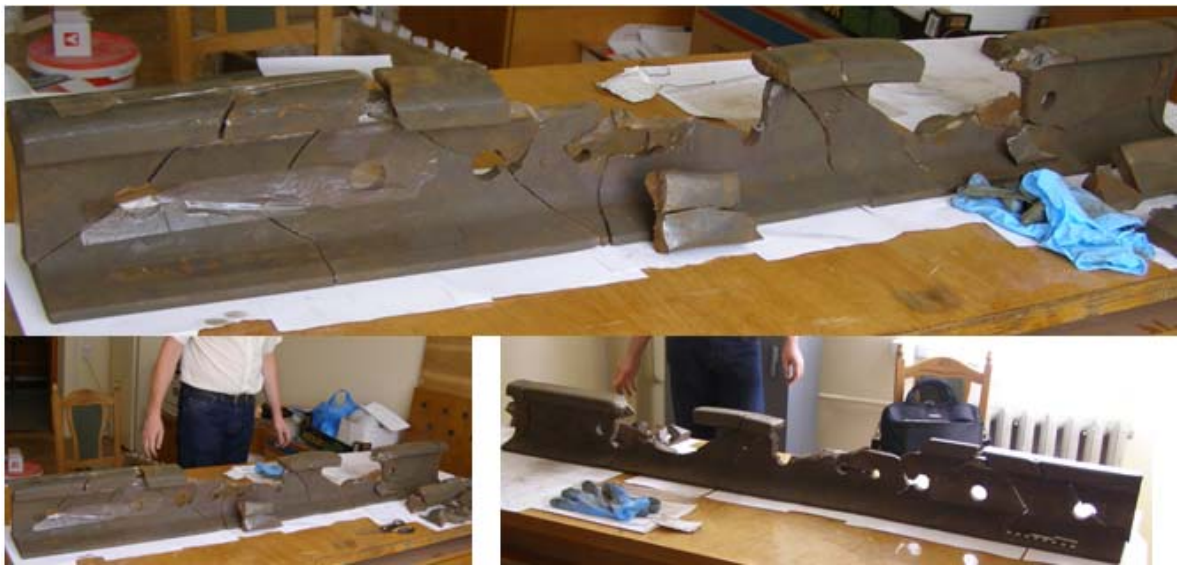

Figure 3. Fragments of plastic breakage of rail track due to the use of emergency braking of a train.

Fatigue destruction (figure 4) is characterized by the presence of the zone of origin (pos.1), the zone of gradual (fatigue, pos.2, 3) and spontaneous (uneven, pos.4, 5) crack development, and the zone of complete fracture (pos.6). Also, there is a source of destruction on the breakdown planes, which includes the microzone of the crack origin (pos.1). In turn, the zone of fatigue destruction consists of areas of selective and accelerated (catastrophic, spontaneous) crack development. The presence of such several zones indicates the change in operating conditions or change in the angle of direction of load force effect.

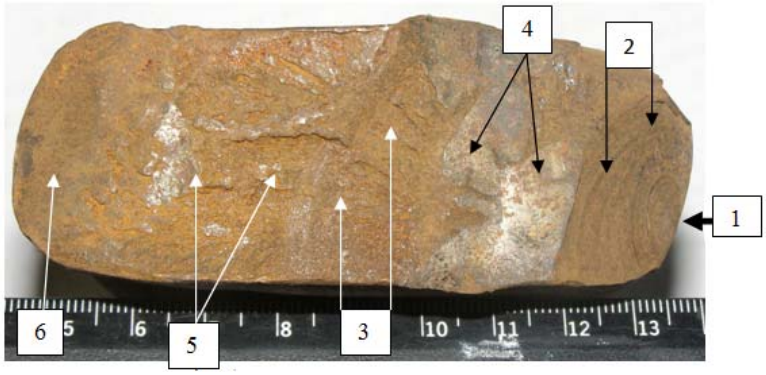

Figure 4. Fatigue fracture of the drawbar due to cyclic loading.

It is clear that non-recorded traces of damage during inspection (dints, burrs) or not saved fracture planes can be simply lost for further research. Therefore, the survey and description of the condition of the destroyed parts must be started with detailed review and recording of the entire part or a unit, considering them in the relationship as an integral element of the object of research. Particular attention should be paid to surfaces adjacent to the fracture plane, because subsequent correct and accurate expert interpretation of them depends on how far the contingent factors are eliminated that could change the characteristics of the surface of destruction. This can lead to erroneous conclusions when performing research.

Each structure has a large number of cracks of different sizes: from microscopic to macrocracks. The development of cracks takes a considerable amount of time, and the rate of crack development is very slow at the beginning of its origin and is approaching the speed of sound at the final stage. The strength of a part or a structure decreases with the development of a crack.

At the same time, during the manufacture of parts and their operation, cracks may occur, especially in areas of local tension increase, and with variable loads, in the presence of aggressive environments, temperatures and other factors that contribute to brittle fracture. The need to record all operations carried out at on-site inspection is also necessary in view of the impact on accuracy of subsequent studies. If destruction is not cut-through and further transportation is assumed, it is necessary to remove the destroyed part or unit in order to prevent damage of the fracture surface. In this case, the urgent need is to photograph objects that are related to damaged and destroyed parts, their deformation changes of the shape (figure 5).

Figure 5. Railway accident due to the breakage of the side frame of the bogie.

In view of the fact that fracture will be subject to further laboratory metal graphic analysis, a number of appropriate steps should be undertaken to obtain maximum information on the specific features of the destruction plane. The need for the committee to carry out an official investigation of the causes of a railway accident is based on the recognition that the surface of the fracture carries much valuable information about the causes of destruction. The destruction of such information by ignorance (for example, during disassembly, unskilled mapping of the fracture plane, subsequent transportation or for other reasons) may complicate or lead to an incorrect interpretation of destruction regularity or even the impossibility of conducting further reliable studies (figure 6).

Figure 6. Mapping of fracture plane of the side frame of the bogie.

Since the surface of the fracture is subject to intense corrosion, a good way of preserving the surfaces of the breakages and their protection against corrosion is the use of coatings (preservative lubricants or plastic coatings through which the surface and the fracture profile are clearly visible) that are eliminated with trichlorethylene (acetone) during further laboratory studies (figure 7). To prevent corrosive damage to the fracture plane, it is recommended to use solvents based on petroleum products, which are easily removed from the surface. It is not recommended to use a sticky tape to protect the fractures as it is difficult to remove it, and as a result of moisture adsorption, the fracture surface undergoes corrosion under it.

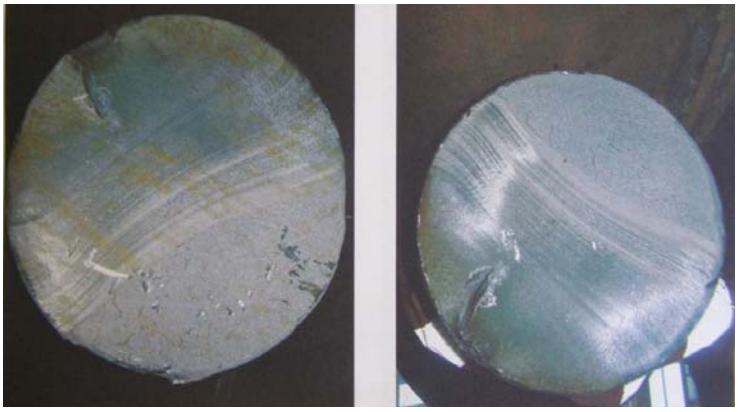

Figure 7. Fracture plane of the part, which is stored with the use of special protective coatings.

During inspection, it is important, along with identification of mechanical damage of rolling stock components, to obtain information about its general state in order to:

- differentiate defects that could exist before RTA or arise during further transportation and storage of the part of rolling stock;
- fixation of the location and size of primary or secondary damage (caused during transportation), as well as comparing it with the damage of other components of rolling stock;
- identification of traces indicating contact with other parts of rolling stock.

6. Conclusion

The proposed ways of preservation of destroyed objects directly at the scene are a set of specific knowledge that gives the persons responsible for providing destroyed objects from the scene for expert engineering and technical research, with a direct precautionary measure to avoid false conclusions and partial expert judgment.

References

[1] Magel E, Mutton P, Ekberg A and Kapoor A 2016 Rolling contact fatigue, wear and broken rail derailments *Wear* **366-367** 249–57

[2] Ju S H 2016 Study of train derailments caused by damage to suspension systems *J. Computational and Nonlinear Dynamics* **11(3)** 031008

[3] Jin Z, Pei S and Qiang S 2014 Study on derailment of railway vehicles on bridges during earthquakes based on IDA analysis *Tumu Gongcheng Xuebao/China Civil Engineering Journal* **47** 234–9

[4] Nabochenko O, Sysyn M, Kovalchuk V, Kovalchuk Yu, Pentsak A and Braichenko S 2019 Studying the railroad track geometry deterioration as a result of an uneven subsidence of the ballast layer *Eastern-European Journal of Enterprise Technologies* **7(97)** 50–9

[5] Sysyn M, Gerber U, Gruen D, Nabochenko O and Kovalchuk V 2019 Modelling and vehicle based measurements of ballast settlements under the common crossing *European Transport / Transporti Europei - International Journal of Transport Economics, Engineering and Law* **71** 1–25

[6] Sysyn M, Gerber U, Kovalchuk V and Nabochenko O 2018 The complex phenomenological model for prediction of inhomogeneous deformations of railway ballast layer after tamping works *Archives of Transport* **46(3)** 91–107

[7] Kim J H, Bae H U, Kim J W, Song I H, Lee C O and Lim N H 2018 Post-derailment behavior of casting bogie by full scale test *J. Korean Society for Railway* **21(8)** 815–29

[8] Kaewunruen S, Wang Y and Ngamkhanong C 2018 Derailment-resistant performance of modular composite rail track slabs *Engineering Structures* **160** 1–11

[9] Mirza O and Kaewunruen S 2018 Resilience and robustness of composite steel and precast concrete track slabs exposed to train derailments *Frontiers in Built Environment* **4** 60

[10] Sysyn M, Gerber U, Nabochenko O, Li Y and Kovalchuk V 2019 Indicators for common crossing structural health monitoring with track-side inertial measurements *Acta Polytechnica* **59(2)** 170–81
[11] Sysyn M, Kovalchuk V and Jiang D 2019 Performance study of the inertial monitoring method for railway turnouts *Int. J. Rail Transportation* **7 (2)** 103–16
[12] Sysyn M, Gruen D, Gerber U, Nabochenko O and Kovalchuk V 2019 Turnout monitoring with vehicle based inertial measurements of operational trains: A machine learning approach *Communications - Scientific Letters of the University of Zilina*, **21(1)** 42–8
[13] Li Q, Huang X and Huang W 2019 Fatigue property and microstructure deformation behavior of multiphase microstructure in a medium-carbon bainite steel under rolling contact condition *Int. J. Fatigue* **125** 381–93
[14] Wang Z, Han J, Domblesky J P, Li Z, Fan X and Liu X 2019 Crack propagation and microstructural transformation on the friction surface of a high-speed railway brake disc *Wear* 45–54
[15] Masoudi Nejad R, Shariati M and Farhangdoost K 2019 Prediction of fatigue crack propagation and fractography of rail steel *Theoretical and Applied Fracture Mechanics* **101** 320–31
[16] Masoudi Nejad R, Farhangdoost K and Shariati M 2018 Microstructural analysis and fatigue fracture behavior of rail steel *Mechanics of Advanced Materials and Structures* 1–13
[17] Daves W, Kráčalík M and Scheriau S 2019 Analysis of crack growth under rolling-sliding contact *Int. J. Fatigue* **121** 63–72
[18] Maneesh Kumar M, Murali M S, Saranya M, Arun S and Jayakrishnan R P 2018 A Survey on Crack Detection Technique in Railway Track *Proc. IEEE Conf. Emerging Devices and Smart Systems* 269–72
[19] Kim S, Sung D, Kang Y and Park Y 2018 Fracture mode analysis according to inclination angle of rail internal crack *J. Korean Society for Railway* **21(7)** 671–8
[20] Sysyn M, Gerber U, Nabochenko O, Gruen D and Kluge F 2019 Prediction of rail contact fatigue on crossings using image processing and machine learning methods *Urban Rail Transit* **5(2)**
[21] Panasyuk V V 1988 Fracture mechanics and strength of materials: Ref. manual: 4 tons *Science. Dumka Kiev* 225
[22] Khyl V, Rudavskyi D, Kanyuk Yu and Sas N 2018 Determination of the period of subcritical growth of internal cracks in the rail head under operating loads *Materials Science* **53(6)** 80–7
[23] Datsyshyn O 2005 Service life and fracture of solid bodies under the conditions of cyclic contact interaction *Materials Science* **41(6)** 709–33
[24] Kaminsky A 2014 Mechanics of the delayed fracture of viscoelastic bodies with cracks: Theory and experiment (Review) *International Applied Mechanics* **50(5)** 485–548
[25] Guz A, Guz I, Men'shikov A and Men'shikov V 2013 Three-dimensional problems in the dynamic fracture mechanics of materials with interface cracks (review) *Appl. Mech.* **49(1)** 1–61

Problems of interaction of contact wire and current collectors of electric transport with different contact materials

M Babyak

Lviv branch of Dnipro National University of Railway Transport named after Academician V. Lazaryan, 79052 Lviv, Ukraine

E-mail: mobabjak@gmail.com

Abstract. The reliability of the current transfer process depends on the reliable sliding contact between the current collector and the contact wire; the value of the resistance of the contact element of the current collector; the value of the contact wire's contact and the contact element. Graphite inserts for operation on electric transport of railways of alternating current operate at low values of current, on electric trains of a direct and an alternating current at high speeds, and on electric locomotives of a direct current at large values of a current. They are good lubricate the contact wire, but have a high resistivity and are rapidly mechanically erased. Copper and metal-ceramic lining have relatively less resistance, but due to the high hardness of the material, they quickly wipe off themselves and the contact wire. When using all materials in open and closed mines, dust and dirt on contact plates, high temperature and the presence of gas, which is dangerous when the spark is in contact, must be considered additionally. It is proposed to use the new contact material of BRZG from bronze, graphite and iron. The effectiveness of this material is confirmed by the operation of electric locomotives and electric trains of direct and alternating current on railways and trolleybuses.

1. Introduction

Reliability of electric transport, which receives electric energy from the contact network, depends primarily on the reliability of the electricity supply system. The main problems arising in the operation of the electric transport of the railways are not enough reliable contact in the "pantograph-contact wire" sliding contact, and the contact wire hanging system is not always properly selected or not adjusted according to the requirements. Providing electric rolling stock with high-quality current-drawing is one of the most difficult tasks [1].

The problem of reliable contact on current collectors is important for railroad electric transport, and for the electric transport of the city – the tram and trolleybus. Even more complicated problems exist in electric transport, which works in open and closed mines, where, in addition to large currents, there is gunpowder and dirt on contact elements of the current collector. When operating high-speed lines it is confirmed that ensuring reliable interaction pantograph and contact wire is even more difficult technical task than ensuring the reliable interaction of the rolling crew with rails [2-5].

2. Purpose and objectives of the research

The purpose and tasks of the research is to analyse the work of pantographs on various types of electric transport and to find a solution to the problem of contact between the contact wire and current collectors of electric transport by using modern contact material.

3. Analysis of pantograph work on various types of electric transport

To determine the dynamic characteristics that are included into the indices, with help of which the dynamic properties of the mechanical part of the diesel train are estimated, the analysis of the car design and its spatial mechanical model should be carried out [6, 7].

Reliability and the required quality of current-picking are determined by the velocity of the rolling stock and the structural parameters of the contact pendant and current collector, and their interaction is a complex oscillatory process that causes different intensity of mechanical and electrical wear of the contact wire and current-drawing elements [8]. In the process of oscillation various vibrational systems participate. Special influence on this process is made by oscillations of the locomotive and self-oscillation of the contact wires caused by the air flow.

Most researchers in their studies to improve the interaction of contact pairs "current receiver - contact wire" are considering different directions: improving the systems of hanging contact network; tension adjustment of the contact wire; changes in the type of compensation of contact hanging; replacement of conductor materials of the contact network. The research of individual scientists is aimed at the invention of new structures of current collectors of electric transport. However, in the operation of the railroad main and industrial transport, there are only two main types pantographs – symmetrical heavy type, Figure 1, symmetrical light type, Figure 2, and pantograph asymmetric, or semi-pantograph, Figure 3.

Figure 1. Heavy symmetric pantograph, electric locomotive.

Figure 2. Light symmetrical pantograph, electric locomotive.

Figure 3. Asymmetrical pantograph, electric locomotive.

Sometimes different models of current collectors are used depending on the conditions of the electric locomotive – for example, the speed (Figure 4), or the energy supply system – one phase, or three phases at different levels (Figure 5). Pantographs of electric pushers may have several sections (Figure 6). In industrial electric locomotives, when loading in the carriages from above, side current collector is used, and in the main section the upper pantograph is used (Figure 7).

For rail electric transport in cities use symmetrical pantographs (Figure 8), asymmetrical pantographs (Figure 9), and bugeli (arcs) (Figure 10).In some cities, a current collector is used in the form of a rod (Figure 11). To protect against wandering currents, two rods were used instead of a rail (Figure 12). There are various types of current collectors on trams – pantograph and rod (Figure 13).

Figure 4. Different types of pantographs, one electric locomotive.

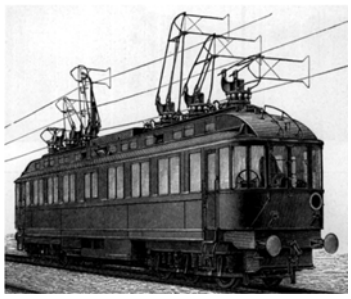

Figure 5. Three-phase current collectors.

Figure 6. Multi-sectional current collector for pusher carriages.

Figure 7. The upper pantograph and the lateral half-pantograph, industrial electric locomotive.

Figure 8. Symmetrical pantograph, tram.

Figure 9. Asymmetrical pantograph, tram.

Figure 10. Bugle (arc) current collector, tram.

Figure 11. Tram current collector – rod.

Figure 12. Two rods of the tram.

Figure 13. Various current receivers, tram.

Figure 14. Two current tram receivers.

For the reversal of the bore current collector, a special network of air arrows and contact wires is developed, which allows the trolley to unfold without lowering the current collector (Figure 14). If only one track is used to work in different directions of motion, use two rods (Figure 15), or two arcs (Figure 16).

Some cities have experience sharing the contact network for different modes of transport. For example, tram and trolleybus used common contact wires and rod current collectors (Figure 17). Together with passenger trolleybuses, cargo trolley buses (Figure 18) and trolley bus trucks (Figure 19) worked.

Figure 15. Two bugle current tram.

Figure 16. Contact wire for turning current collector.

Figure 17. Tram and trolley bus network.

Figure 18. Cargo trolleybus.

On the lines of the trolleybus trucks were used, which used a barge current collector (Figure 20). On heavy duty trucks, the bore current collectors are coupled and replace the contact heads on the skis (Figures21 and 22). The painted pantographs were replaced by semi-pantographs (Figure 23).

Figure 19. Trolley car.

Figure 20. Diesel-trolley car.

Figure 21. United pantograph.

Figure 22. Pantographs.

Figure 23. Semi-pantographs.

Figure 24. Carbon car inserts.

Figure 25. Hybrid bus collector.

At the moment, special contact networks have been created for use by their cars. At the same time, pantographs (Figure 22) and semi-pantographs (Figure 23) with copper, composite and coal strips and inserts remain in the structure of current collectors (Figure 24). Modern is the use of a hybrid bus with current collectors. At the end stops, the tumbler automatically raises to the contact wire (Figure 25).

Certain companies produce current receivers made of aluminum tubes to ease weight and reduce the weight of pantograph, which improves the process of screw-in. But the cost of such a pantograph is large. Most manufacturers use steel pipes, which makes the pantograph heavier, but its cost is lower. This causes the static and dynamic characteristics of the pantograph to deteriorate. The process of transferring electrical current from the mains to the electrical equipment becomes worse. As a result, we get worse traction characteristics of electric transport. Some scholars try to combine different designs of pantographs (Figure 28). Leading manufacturers make an asymmetrical current collector with two rows of contact elements made of graphite (Figure 29).

Figure 26. Contact roller current collector.

Figure 27. Trolley contact element.

Figure 28. Hybrid pantograph by tram.

Figure 29. Modern pantograph.

In current collectors there should be minimal friction in the hinged knots, stable pressure on the contact wire, the minimum moving weight. They should provide minimal abrasion of the contact wire and contact elements. Qualitatively selected dynamic indicators characterize quality, reliability and profitability.

Contact elements should be reliable, environmentally friendly, and ensure long-term operation of the pantograph. Qualitative and reliable work is possible only with reliable contact of current collector and contact network. Minimize short-circuiting current collector from a contact network can lead to negative consequences. First of all, tearing leads to damage to the contact element and its rapid wear and contact wire. The poor contact between the contact wire and the current collector in the closed mines not only leads to the wear of not only contact elements but can cause sparking on the pantograph, which is a threat of explosion and a danger to life. The sparking of the contact elements indicates the unsatisfactory condition of the contact inserts, and worsens the current removal rates, and as a result, the traction characteristics of the electric transport deteriorate, and the consumption of electricity increases (Figures30-32).

Figure 30. Spark on pantograph trolley bus.

Figure 31. Spark on an electric train.

Figure 32. Spark on electric locomotive in mine.

The main problem with the AC system is the rapid action of the carbon insert, which during operation leads to a reduction in electrical contact and the emergence of an electric arc. This causes intense wear of the contact wire both on the railroad and on the city electric transport. As a result, there is a breakdown of wires, breakage of current receivers and other damage that violates normal movement.

At present, most of the locomotive depot for contact areas of DC uses copper-based contact materials. In this case, there is a major problem of the mutual wear of copper wire and contact element. To reduce the harmful effects of frictional forces between the pantograph pad, the dry graphite oil is pressed and baked, and in the course of operation to reduce the wear, the lining is greased with a graphite-based liquid lubricant [9] (Figure33).

Comparing contact elements on the basis of copper and graphite, it is evident in their electrical properties. It is known that the specific electrical resistance of copper is 1.75×10^{-5} Ohm × m, and the specific electrical resistance of graphite is 10^{-6} ... 10^{-4} Ohm × m [10]. Since we do not use either pure copper or pure graphite in the form of contact elements of the current collector, we are creating the problem of using contact materials in the contact lens of the pantograph. By placing graphite on copper, we worsen the electrical properties of the sliding contact. That is, using the expensive material for the contact wire and the contact plate, we increase the electrical component of the transient resistance, which complicates the problem of the use of the overlays.

For the depot, which operate the electric transport of alternating current railways, the main material for inserts of current collectors is graphite. Here again the question arises - which graphite inserts is better to use? If you look at the problem from the point of view of electrical engineering, then it is necessary to use those inserts, which have less specific electrical resistance. According to manufacturers, the specific resistance of coal inserts should be within 4.5 ... 22×10^{-5} Ohm × m. In practice, these values range from 8×10^{-5} to 30×10^{-5} Ohm × m [10].

The European Union regulations [3-5] contain requirements and recommendations for the use of contact inserts and overlays on different models of current collectors of electric locomotives and electric trains. If we consider the main problem of the resource of work, it is better to take carbon inserts with the smallest hardness to not rub the contact wire. For example, in the contact inserts of the sign “A” (coke), the hardness is 70 HS. In the most common contact inserts of artificial “B” graphite hardness should be 50 HS. They should be washed faster than the contact wire. But in reality, the insertion of

wear occurs too quickly, which leads to the formation of zones of local wear, or the degree of wear of the inserts (Figure 34).

Figure 33. Lining of pantograph on the basis of copper with graphite lubricant.

Figure 34. Carbon inserts of the pantograph of the electric locomotive.

As a result of such a quick and improper work, there are cases of piercing pantographs with the help of a contact wire (Figure 35); hacking the pantograph (Figure 36); department of pantograph from the roof of the electric locomotive (Figure 37); and breakage of the contact wire (Figure 38).

Figure 35. Sawing the pantograph with a contact wire.

Figure 36. Hacking the pantograph of the electric locomotive.

Figure 37. Disruption of pantograph.

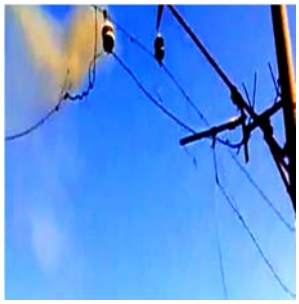

Figure 38. Break of the contact wire.

The most dangerous is the drop in the contact wire on the body of electric transport, which may be the cause of death of people (Figure 39). A similar situation is possible with the breakdown of current receivers of the tram and the trolleybus. When the contact wire of the tram or trolleybus contact network breaks, the traffic of the city electric transport stops, which leads to the accumulation of passengers, the failure in the schedule of traffic or individual routes, or the whole area (Figure 40).

It is obvious that the best in terms of maintaining the contact wire would be the use of contact inserts of artificial graphite mark "O", hardness of which should be 25 HS [10]. They also satisfy the electrical part of wear because they have a specific electrical resistance of 5×10^{-5} Ohm × m.

For urban electric transport – trolleybus and tram, graphite contact inserts are used, which have a high specific resistance of 8 ... 30×10^{-5} Ohm × m, and significantly less work life, compared with the coal inserts of rail transport. This is especially noticeable in the case of significant precipitation, sticking wet snow (Figure 41), and large ice on the contact wire and in areas where energy recovery is used [11] (Figure 42).

Worst of all, when the influence of the dynamics of the rolling stock is added to the question of a stable electrical contact [12, 13]. Due to the poor contact between the contact elements of the current collector and the contact wire, an electric arc arises which, during a certain time of combustion, warms the contact wire, it stretches under the influence of temperatures and ruptures. If on a railway rolling stock you can move from a place to burn a thin layer of ice, then on trolleybus lines it almost fails (Figure 43). Since the voltage level in the contact network is only 600 Volts, and with significant transient resistance and with a high specific resistance of the carbon inserts, there is not enough current to move

from place. This is especially true for trolley buses of new models, in which static converters are sensitive to voltage drop [14]. Under such difficult operating conditions, the insertion of the current collector is eroded sharply, as well as the elements of the contact network are spoiled.

Figure 39. Fall of the contact wire on the body.

Figure 40. Drop current receiver tram.

Figure 41. Sticking wet snow.

Figure 42. Ice on the contact network.

Figure 43. Electric arc on the trolley bus network.

4. Presentation of new material

Increasing the speed and weight of trains requires the use of electric transport of higher power, which corresponds to world trends. The main requirements for current collectors and contact elements are reliability and durability. To ensure high-quality current formation, it is necessary to use contact elements with high load capacity and wear resistance. Unfortunately, at present, none of the known contact elements guarantees full safety in the operation of electric transport and does not have large operating resources within the cost of material contact.

Most manufacturers in the European Union have focused on carbon contact elements. Some manufacturers add copper to carbon. In the manufacture of metal-ceramic contact elements, various metal compositions are used. But the main contact material is copper.

In order to comprehensively evaluate the problem of interaction of receivers of electric transport currents with different contact materials and contact wire in different conditions of operation of railway and industrial transport, contact elements were most often used: contact inserts of type of pantographs “A” and “B”; carbon inserts of pantographs of trams; copper tire for current collectors; metal-ceramic plates; copper contact plates with graphite inserts NMG-1200; copper-graphite contact plates MG-487; PCD-4-2 copper-based contact plates; Contact plates BRZG (Figure 44) [15].

For such studies, the most common carbon contact inserts, metal-ceramic inserts, contact plates BrzG-Tr (Figure 45) [16] were used in the conditions of trolley operation.

Figure 44. Contact inserts of type BRZG.

Figure 45. Contact inserts of trolleybus type BRZG-Tr.

Figure 46. Patent for the invention of the composition of the BRZG.

Having considered the problems that are common in the process of wear of contact elements of pantographs of electric trains and locomotives, electric transport of the city, industrial enterprises, we

have improved Brzg contact plates on the basis of bronze, iron and graphite. They provide reliable work on a constant and alternating current. After all laboratory tests, the effectiveness of the new Brzg material has been confirmed during operation on electric locomotives and electric trains of direct and alternating current on railways and trolleybuses. Inventions are provided with patents (Figure 46).

Compared to copper-graphite inserts, which use DC in electric locomotives, the lifetime of the inserts of the BRZG is greater 1.7-2.5 times.

Compared with graphite inserts used in trolley buses and electric trains and locomotives on AC, the lifetime of the inserts of the BRZG is greater 21-26 times.

5. Conclusions

On the reliability of a moving electrical contact pantographon the contact network is affected by many factors. The main material is the contact element, the kinematic circuit of the current collector, its dynamics and the mobile mass.

For rail, industrial and urban transport, there is a big problem with the choice of contact materials for current collectors. Given the problems of contact between contact and current collectors of electromotive transport, it is necessary to choose the contact material for the elements only after the test.

When using all materials in open and closed mines, dust and dirt on the contact plates, the high temperature and the presence of gas that is dangerous when contact with the spark should be taken into account additionally. The contact material should be strong but not destroy the contact wire.

The article proposes to use the new BRZG contact material in bronze, graphite and iron. The efficiency of this material is confirmed by the reliable operation on pantographs of electric locomotives and on electric trains of direct current and alternating current, as well as on current receivers of trolleybuses.

References

[1] Vologin V 2006 Interaction of current receivers and contact network *Moscow Intext* 256

[2] Zinkivsky A andBelyakov M 2016 An analysis of constructive solutions and the choice of current collectors for rolling stock for use in conditions of high-speed motion *Collection of scientific works of UkrDUZT* **164** 202–211

[3] EVS-EN 50318:2018 Railway applications. Current collection systems. Validation of simulation of the dynamic interaction between pantograph and overhead contact line.

[4] EVS-EN 50119:2009 Railway applications. Fixed installations. Electric traction overhead contact lines.

[5] EN 50206-1:2010 Railway applications Rolling stock Pantographs: Characteristics and tests – Part 1: Pantographs for main line vehicles.

[6] Myamlin S, Neduzha L and Urbutis Ž 2016 Research of Innovations of Diesel Locomotives and Bogies *ProcediaEngineering***134** 469–474

[7] Klimenko I, Kalivoda J and Neduzha L 2018 Parameter optimization of the locomotive running gear *TransportMeans: Proc. 22nd Int. Sci. Conf.*1095–98

[8] Babyak M 2019 Modeling of interaction of contact wire and pantograph with resource-saving contact pads *Bulletin of East-Ukrainian National University named after Volodymyr Dahl* **2(250)** 16–23

[9] Babyak M 2018 Resource-saving technology for the use of overlays of current collectors, taking into account their interaction with the contact wire *Bulletin of the East-Ukrainian National University named after Volodymyr Dahl* **2(243)** 32–37

[10] Bolshakov Y and Antonov A 2015 Increase of the resource of coil current inserts of current collectors of high-speed electromotive equipment under exploitation *Science and progress of transport* **4(58)** 57–70

[11] Sablin O, Bosyi D, Kuznetsov V, Babiak M, Kosariev Y and Hubskyi P 2016 The efficiency of recuperation the electric power in electric transport system with inverter DC traction substations *Visn. Vinnic'k. politeh. inst.* **2** 73–79

[12] Myamlin S, Dailidka S, Neduzha L 2012 Mathematical Modeling of a cargo locomotive *Proc. 16th Int.Conf.Transport Means* 310–312
[13] Klimenko I, Černiauskaite L, Neduzha L, Ochkasov O 2018 Mathematical simulation of spatial oscillations of the "Underframe-Track"system interaction *Intelligent Technologies in Logistics and Mechatronics Systems – ITELMS'2018: Proc. 12th Int. Conf.* 105–114
[14] Babyak M 2019 Analysis of exploitation of resource-saving contact elements of BRZH-TR of urban electric transport *IXth Int. Sci. and Practical Conf. Transport and Logistics: Problems and Solutions. Severodonetsk - Odessa - Vilnius - Kiev / East Ukrainian National University V Dahl, Odessa National Maritime University* 253
[15] Babyak M 2019 Simulation of interaction of contact wire and pantograph with resource-saving contact pads *Visnik of the Volodymyr Dahl East Ukrainian national university* **2(250)** 16–23
[16] Babyak M, Horobets V, Sychenko V, HorobetsY 2018 Comparative tests of contact elements at current collectors in order to comprehensively assess their operational performance *Eastern-European J.Enterprise Technologies –Kharkov* **6 12(96)** 13–21

Анализ на повредите на цилиндровите глави на локомотивен дизелов двигател 5Д49

Кирил Велков[1], Олег Кръстев

Катедра Железопътна техника, Технически университет – София, България

[1] E-mail: khvel@tu-sofia.bg

Резюме. Докладът е посветен на повредите, появяващи се по цилиндровите глави на локомотиви серия 07, от парка на „БДЖ – ТП“ ЕООД. Анализирана е честотата на поява на повредите през последните три години, както и влиянието на някои особености на експлоатацията. Акцентът е върху пукнатините и влиянието им върху охладителната система на дизеловия двигател. Разгледано е влиянието на допълнителните температурни датчици. Разгледана е възможността за изменение системата за управление на дизеловия двигател с цел намаляване случаите на прегряване. Разгледани са възможните методи на ремонт за отстраняване на повредите.

1. Въведение

Дизеловите локомотиви серия 07 (фигура 1) са с електрическа предавателна система и мощност 2210 kW. Те са произвеждани в локомотивостроителните заводи в гр. Луганск – Украйна. Локомотивите са с конструктивна скорост 100 km/h. Пригодени са за обслужването на пътнически и товарни влакове. Локомотивите са проектирани за средноевропейския габарит и се доставят също така в Германия и Унгария. Първите локомотиви са доставени и пуснати в експлоатация в у нас в началото на 1972 г. Те и до днес остават най-мощните дизелови локомотиви в България и освен от БДЖ се експлоатират от някои частни жп превозвачи – ДБ-Карго, ПИМК и др.

Дизеловите двигатели 5Д49, използвани в локомотиви серия 07, са доставяни от гр. Коломна, Русия. Двигателят е V-образен, 16-цилиндров, със свръхпълнене, като в локомотива работи съвместно с генератор за променлив ток.

Фигура 1. Дизелов локомотив серия 07.

Извършването на настоящия анализ има за цел установяване на причините за появата на пукнатини по цилиндрови глави на локомотиви серия 07, експлоатирани в локомотивно депо Русе, собственост на „БДЖ Товарни превози“ ЕООД. Спукването на цилиндрови глави при този тип двигатели е често срещана, типична повреда. В случая става въпрос за една партида от 32 броя ремонтирани цилиндрови глави. При 25 от тях, в кратък период от време, отново се появяват пукнатини.

2. Състояние на проблема

2.1. Фактология

През лятото на 2016 г. „БДЖ Товарни превози” ЕООД сключва договор за извършване ремонт на 32 броя спукани цилиндрови глави за дизелови двигатели на дизел-електрически локомотиви серия 07. Възстановяването на главите се извършва чрез заваряване на спуканите участъци и от месец декември 2016 г. те поетапно са въвеждани в експлоатация чрез монтирането им на локомотиви. За период от пет месеца са монтирани 25 броя от ремонтираните цилиндрови глави. В различни периоди от началото на експлоатацията, при тях се появяват повторни спуквания в областта на направените заварки. Повторните дефекти са констатирани след монтажа на главите, като срокът на експлоатацията е от 5 до 157 дни или средно – 36.96 дни. Експлоатационният срок на цилиндровите глави, след датата на монтажа, е показан на фигура 2.

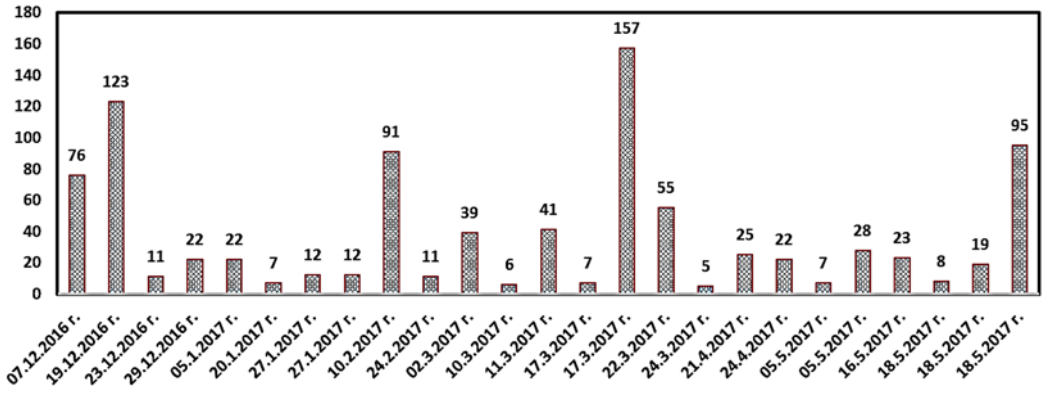

Фигура 2. Експлоатационен срок на цилиндровите глави, след датата на монтаж.

2.2. Основни технически характеристики и условия на работа на цилиндровите глави

Локомотивните дизелови двигатели от фамилията 5Д49, монтирани на локомотиви серия 07, имат следните основни технически данни:

- ефективна мощност – 2200 kW;
- брой на цилиндрите – 16;
- честота на въртене – 1000 min^{-1};
- диаметър на цилиндъра – 260 mm;
- ход на буталото – 260 mm;
- средно ефективно налягане $12{,}23.10^5$ Pa.

Цилиндровите глави на двигателите 5Д49 (фигура 3) са индивидуални за всеки цилиндър и са произведени от високояк чугун ВПЧ-НМ-П [1]. Както всички цилиндрови глави, тези също са силно термично и механично натоварени – от налягането на газовете в цилиндъра и от монтажните напрежения. Термичното натоварване е показано на фигура 4.

За разлика от останалите глави на локомотивни дизелови двигатели, тези са от окачен тип. т.е. цилиндровата втулка е „окачена“ на цилиндровата глава с четири шпилки, а тя от своя страна е свързана с блока на двигателя с още четири шпилки. Тази особеност на конструкцията допринася за допълнително механично натоварване върху цилиндровата глава [1].

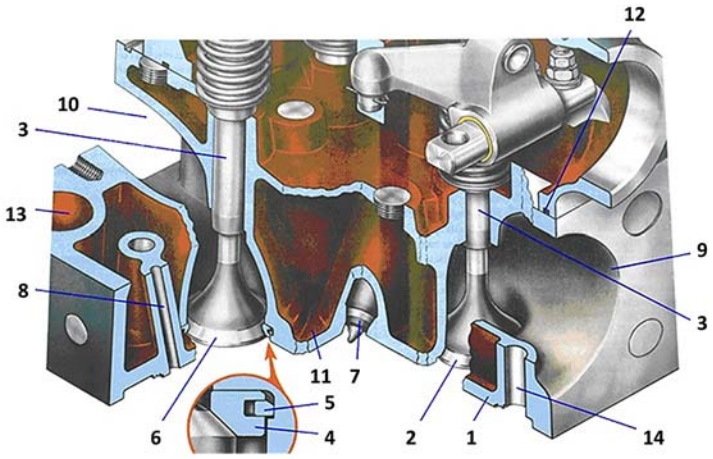

Фигура 3. Цилиндрова глава на локомотивен дизелов двигател 5Д49:
1 – цилиндрова глава; 2– пълнителен (всмукателен клапан); 3 – водач на клапаните;
4 – легло на изпускателния клапан; 5 – фиксатор; 6 – изпускателен клапан;
7 – горивовпръскваща дюза; 8 – индикаторен отвор; 9 – пълнителен (всмукателен) канал;
10 – изпускателен канал; 11 – охладителна (водна) кухина (риза); 12 – уплътнение;
13 – отвор шпилките за свързване към цилиндровия блок.

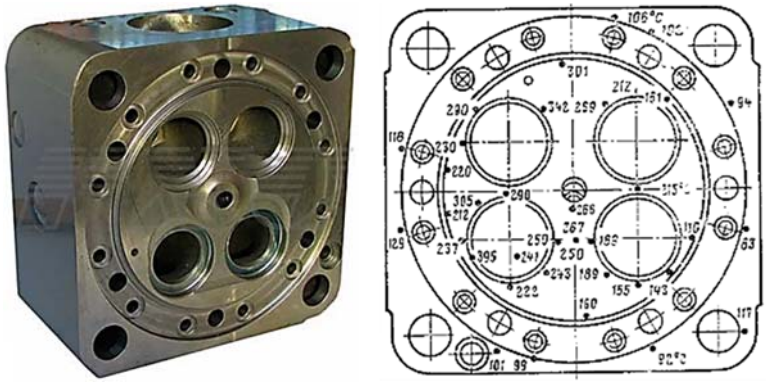

Фигура 4. Общ вид и термично натоварване на цилиндровите глави.

2.3. Причини за появата на пукнатини

Различни изследвания [1-8] са установили, че основната неизправност на цилиндровите глави при дизелови двигатели от серията Д49 е появата на пукнатини в долната част на главата. Най-често те се образуват между отворите за клапаните, в резултат на рязкото повишаване на температурата и появяващите се в следствие на това термични напрежения. Установено е, че основните причини за появата на пукнатини са:

- Нарушена циркулация на охлаждащата течност;
- Стартиране на двигателя при ниски температури на околната среда, без предварително подгряване на охлаждащата течност;
- Натоварване на дизеловия двигател преди достигане температура на охлаждащата течност от 40 °C;
- Спиране на дизеловия двигател при температура на охлаждащата течност по-висока от 70 °C.

В конкретния случай причините за появата на повторните пукнатини могат да се търсят и в технологията на ремонта. Тъй като регистрираните пукнатини са предимно в областите, където е извършвано възстановяването, възможни причини за появяването им са:

- Недобра предварителна подготовка (непълно отстранени пукнатини преди пристъпване към възстановяване);
- Неправилна технология за възстановяване (недостатъчно и/или неравномерно предварително подгряване и/или поддържане на температурата по време на заваряване, или неподходящи: метод за наваряване, използвани консумативи за заваряване, режими на заваряване);
- Недобра обработка след заваряване (неподходящи: метод и режими за термообработка).

2.4. Технология за ремонт на пукнатините по цилиндровата глава

Ремонт на пукнатините на цилиндровите глави се извършва чрез заваряване, като се вземат предвид някои особености при заваряване на чугун, тъй като той се числи към групата на труднозаваряемите материали. Получаването на качествени заварени съединения се затруднява поради следните причини:

- Високите скорости на охлаждане на метала на шева и зоната на термично влияние водят до избелване на чугуна, те. до възникването на участъци, в които се отделя цементит под една или друга форма в различни количества;
- Поради местното неравномерно нагряване, в метала възникват заваръчни напрежения, които поради нищожната пластичност на чугуна водят до образуването на пукнатини в шева и околошевната зона;
- Интензивното отделяне на газове, продължаващо и през време на кристализацията, може да доведе до образуването на пори в метала на шева.
- Присъствието на силиций, а понякога и на други елементи в метала на заваръчната вана спомага за образуването по повърхността на труднотопими окиси, водещи до образуването на непровари.

Най-силно влияние върху структурата на метала на шева и околошевната зона при заваряване на чугун оказва химичният състав и скоростта на охлаждане. При много малка скорост на охлаждане в метала на шева и зоната на термично влияние се получава винаги сив чугун със структура ферит + графит, независимо от състава на чугуна. При междинни скорости на охлаждане може да се получи сив или бял чугун със структура перлит + цементит, в зависимост от съдържанието на графитизаторите (силиций и въглерод). При по-голяма скорост на охлаждане се получава винаги избелване на чугуна, независимо от химичния състав.

Най-добрият начин за контролиране на скоростта на охлаждане при заваряване е прилагането на предварително и съпътстващо нагряване.

Най-доброто средство за борба с образуването на избелени участъци в шева и в зоната на термично влияние е загряването на изделието до температура 600-650 °C и бавното му охлаждане след заваряване. Това загряване спомага и за избягване на пукнатините и газовите пори.

Технологичният процес на горещото заваряване включва следните елементи:

- подготовка на изделието за заваряване;
- предварително нагряване;
- заваряване и следващо охлаждане.

3. Изследване на причините за възникване на пукнатините

За установяване причината/причините за много бързото повторно спукване след ремонтиране на цилиндровите глави, е извършено следното:

3.1. Оглед на главите

Извършен е визуален оглед, с помощта на лупа с двукратно и четирикратно увеличение. По всички цилиндрови глави са установени пукнатини. Пукнатините най-често се срещат в зоната между изпускателните клапани и в зоните на заварките. Снимки на характерни места на повторните спуквания са показани на фигура 5.

Фигура 5. Места на повторни спуквания на цилиндровите глави.

Същото становище е дала и фирмата MULTITEST ООД, която е извършила изследване на пукнатините на заварените цилиндрови глави по метода на магнитно-праховата дефектоскопия. В техните протокол и становище е дадена подробна информация за размерите на пукнатините.

3.2. Статистическа обработка

С цел установяване на евентуална зависимост на възникналите повреди от датата на монтаж на ремонтираните цилиндрови глави и от датата на установяване на повторното им спукване, а така също и от номера на цилиндъра, на който са монтирани, бе извършена обработка на предоставената ни информация.

Обобщената информация е представена в графичен вид на фигури 2 и 6-8. Вижда се, че сезонна и конструктивна корелация няма.

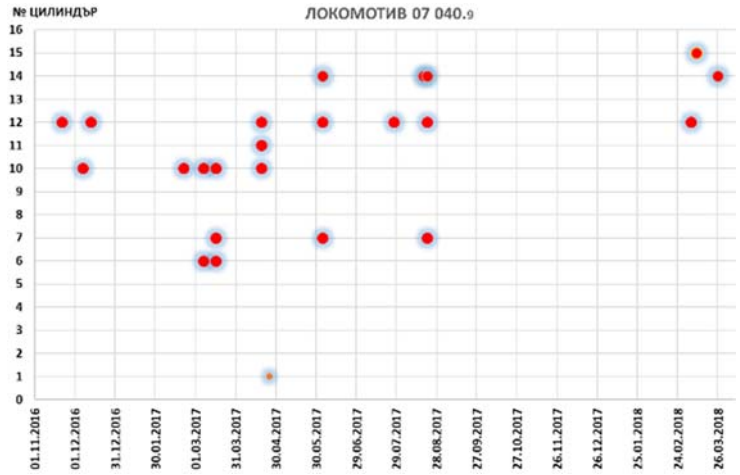

Фигура 6. Цилиндри на локомотив 07 040.9, на които са монтирани ремонтираните глави и дати, на които е станало повторното спукване.

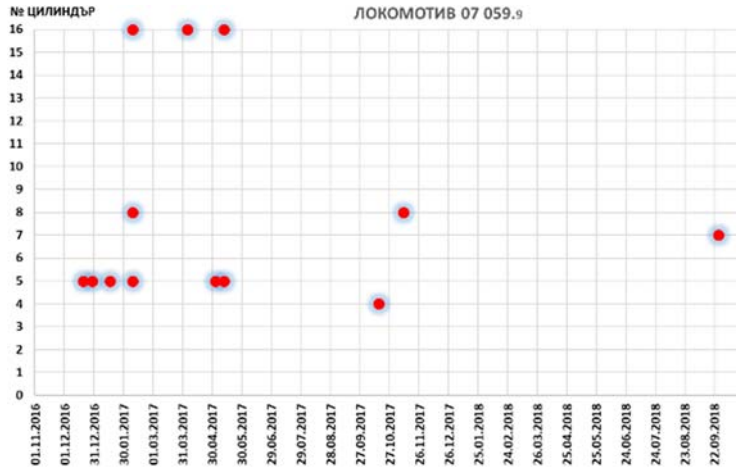

Фигура 7. Цилиндри на локомотив 07 059.9, на които са монтирани ремонтираните глави и дати, на които е станало повторното спукване.

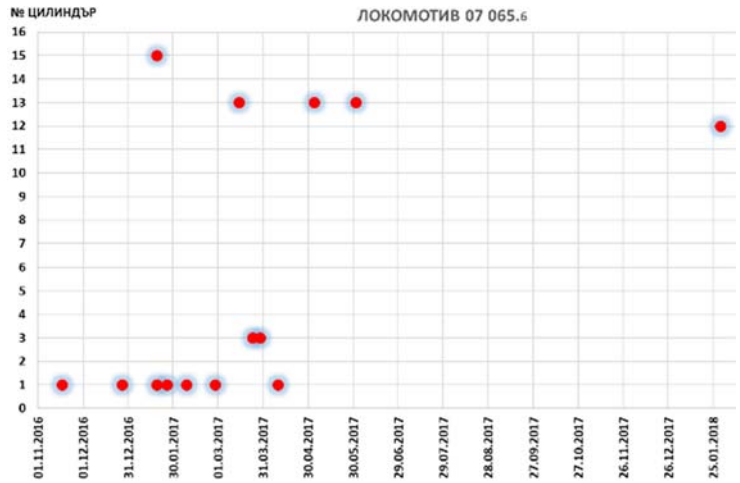

Фигура 8. Цилиндри на локомотив 07 065.6, на които са монтирани ремонтираните глави и дати, на които е станало повторното спукване.

3.3. Защитни механизми

В локомотива стандартно са монтирани четири сензора (датчика) за температура. Те са настроени, както следва:

- при температура на охлаждащата течност +70 °C първият сензор отваря жалузите на охлаждащия блок;
- при температура +72 °C се включва електродвигателят на първия вентилатор за охлаждане на течността;
- при +76 °C се включва вторият вентилатор;
- при +80 °C се включва третият вентилатор.

На локомотивите серия 07 допълнително е монтиран датчик, който не допуска локомотивът да работи на по-висока от първа позиция при температура на охлаждащата течност по-ниска от +45 °C, фигура 9.

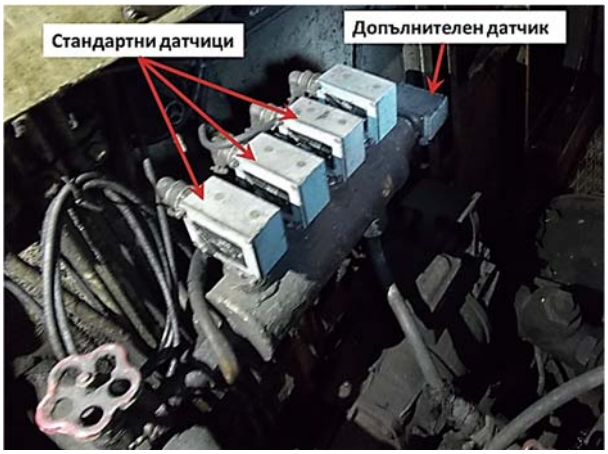

Фигура 9. Датчици (сензори) за температурата на охлаждащата течност.

При смяна на една или повече цилиндрови глави, охлаждащата течност в по-голямата си част е източена, т.е. локомотивът е отводнен. Поради това, в нормативните документи е предвидено след извършването на такъв ремонт, охладителната система да се зарежда преди запалване на двигателя отново с предварително подгрята течност, с температура ≈ +45 °C.

При спадане нивото на охлаждащата течност под допустимото, се задейства защита за ниско ниво и чрез датчик, монтиран в компенсационния резервоар, двигателят се спира.

В нормативните документи е заложено при ниски температури на околната среда, с цел температурата на охлаждащата течност в двигателя да не спадне под +40 °C, да се прилага т.нар. „горещ престой“. Той се изразява в работа на двигателя на празен ход за определено време. За серия 07, както и за другите е разработена схема за работа, в зависимост от околната температура. Липсва обаче надеждна схема за контрол дали това се изпълнява.

Когато локомотивният дизелов двигател бива угасен при температура на охлаждащата течност по-висока от +70 °C, циркулационната електрическа помпа е необходимо да бъде включена ръчно от ключ на пулта за управление. Помпата трябва да работи около 10 min, като целта е чрез тази циркулация на охлаждащата течност да се отстранят т.нар. локални прегрявания по различните части на двигателя. Това е задължение на локомотивните машинисти. Липсва обаче система за надежден контрол.

След дългогодишната експлоатация, първите симптоми за нарушена работоспособност вследствие на спукване на цилиндрова глава на двигателя на локомотива се констатират от локомотивните машинисти по време на път и от инструкторите/механиците в локомотивното депо.

Проверките за пукнатини се извършват при загасен двигател и приведен в покой локомотив, от минимум 15 минути. Чрез отваряне крана на ревизионния отвор на всеки цилиндър и завъртане на коляно-мотовилковия механизъм чрез стартера, без да се стартира двигателя, се оглежда за поява на охладителна течност от ревизионние отвори. При наличие на спукване и постъпване на достатъчно количество охладителна течност в цилиндъра, тя трябва да излезе през индикаторния (ревизионния) отвор – фигура 3, позиция 8.

При направена проба на цилиндрова глава от локомотив серия 07 с минимална пукнатина се установи, че за период от 20 (двадесет) минути охлаждащата течност само навлажни пукнатините без да се отделят капки и ли да се образува теч на охладителна течност. Това показва, че при такива обстоятелства не може да се констатира спукване на глава и локомотива ще бъде пуснат на път. При натоварването по време на експлоатация размера на пукнатината ще се увеличи, от налягането в работния цилиндър ще започне появата на въздушни кухини и ще се образуват локални прегрявания на местата, където те се задържат, докато циркулационната помпа заедно с охлаждащата течност успеят ги избутат до изравнителния резервоар. Когато локомотивната бригада забележи рязко повишение на температурата на охлаждащата течност на контролните уреди, проблемът вече ще е възникнал и ще е необратим. Това може да доведе до спукване на още една или няколко цилиндрови глави.

4. Изводи

На базата на извършените огледи, изследвания и анализи е установено:

- Местата на повторните спуквания на цилиндровите глави са: през средата на заварката, напречни спуквания в области, където не е извършван ремонт (заваряване). Спукванията се появяват както по едно и също време, така и на един и същи цилиндър на локомотивите, на които са били монтирани ремонтираните глави;
- На локомотивите серия 07 са предвидени няколко защити, които предпазват дизеловия двигател от прегряване – основни и допълнителни;
- Няма достатъчно добра и надеждна система за контрол на някои експлоатационни изисквания, залегнали в нормативните документи и касаещи повишаване работната температура на дизеловия двигател.
- Липсва система за ранно диагностициране на микропукнатини по цилиндровите глави.

Характерът, мястото и времето на появилите се в хода на експлоатация спуквания на възстановените цилиндрови глави водят до извода, че най-вероятно тези спуквания с висока за този възел честота, се дължат на особеностите на използвания технологичен процес при заваряването. Той се състои от няколко основни етапа: предварителна обработка на пукнатината; предварително подгряване до определена температура; заваряване; последваща температурна

обработка. Параметрите на всеки от един от тези етапи е от значение за крайния резултат. Неточност в някой от тях би довела до недостатъчна дълготрайност на заварката.

Необходимо е да се предприемат допълнителни мерки за ранно диагностициране на микропукнатините и за засилване контрола по изпълнение на някои от предписанията, залегнали в нормативните документи.

Използвана литература

[1] Симсон А, Хомич А и Куриц А 1980 Двигатели внутреннего сгорания (тепловозные дизели и газотубинные установки) *(Москва, Транспорт)*

[2] Тимохин Ю, Савенков В, Гущин А, Рябко Е и Тимохина В 2017 Напряженно-деформированное состояние крышки цилиндра дизеля тепловоза 2017 *Украйна, вестник ИрГТУ* **21(4)**

[3] Линьков О, Пылев В и Кравченко С 2016 Оценка влияния нагара на температурное состояние днища головки цилиндров среднеоборотного дизеля *Двигатели внутреннего сгорания, Украйна, ISSN 0419-8719* **1'2016**

[4] Инструкция за експлоатация на тягов подвижен състав, собственост на „БДЖ-Товарни превози" ЕООД, 2013 г.

[5] ПЛС 282/92 Инструкция за охлаждащите води на дизеловите двигатели и водите за котли за влаково отопление при дизеловите локомотиви и МВ на БДЖ, 1992 г.

[6] ТП_ПЛС 200/18 Предписания за междуремонтните пробези и цикличността на плановите прегледи и ремонти на дизеловите локомотиви на „БДЖ-Товарни превози" ЕООД, 2018 г.

[7] ТП-ПТО-486/14 Предписания за приложение и контрол на смазочни материали и горива в локомотиви на „БДЖ-Товарни превози" ЕООД, 2014 г.

[8] Приложение 7 от ТП_ПЛС 490/17 Инструкция за техническо нормиране разхода на дизелово гориво от влаковите и маневрени локомотиви на „БДЖ-Товарни превози" ЕООД, 2017 г.

Damage Analysis Of Locomotive Diesel Engine Type 5D49 Cylinder Heads

Kiril Velkov[1], Oleg Krastev

Department of Railway Engineering, Technical University – Sofia, Bulgaria

[1] E-mail: khvel@tu-sofia.bg

Abstract. The paper is dedicated to the damages which appear on the diesel engine heads of the diesel locomotives series 07 of the BDZ – Cargo Ltd., locomotive fleet. Analysis of the appearing frequency is carried out, including last three years and specific features of the service are estimated. The stress is on the cylinder head cracks and their impact on diesel engine cooling system. The impact of the additional temperature sensors is shown. The possibility of changing control system of the diesel engine in order to decrease cases of high temperature also is shown. The proper repairing ways are shown in the paper.

Determination of railway infrastructure capacity in context of automation of selected transport processes

Matúš Dlugoš[1], Lukáš Čechovič[1] and Jozef Gašparík[1]

Department of Railway transport, University of Zilina, Univerzitná 8215/1, 010 01, Zilina, Slovakia

E-mail: matus.dlugos@fpedas.uniza.sk

Abstract. The article describes the extent of railway infrastructure, its quantitative and qualitative characteristics, the method of capacity allocation and its calculation itself. Moreover, the article deals with the determination of throughput and the method of calculating throughput using Methodology of infrastructure manager. Mentioned are not only current methods of calculating permeability in Slovakia, but also experience from abroad. The main principles and methodology of capacity determination in the conditions of the Slovak infrastructure manager are described in detail, specifically, theoretical and practical permeability and their method of determination. At the same time, the article addresses the issue of introducing automation and its impact on throughput. The European train safety system ETCS and its 3 levels are mentioned. The conclusion is devoted to a specific case study in which the infrastructure manager methodology is applied and where the outputs are presented before and after the introduction of optimization measures.

1. Introduction

The extent of railway infrastructure is an important part in the railway transport system. Its qualitative characteristics in the form of capacity that depends on the way the service is provided. The allocation of capacity, that is to say, the sale of train routes located in space and time, is the main activity of the infrastructure manager and is a comprehensive infrastructure manager product consisting of several sub-services. In addition to capacity allocation, we can include capacity assessment, capacity assessment, capacity application processing, and so on. The Infrastructure Manager is obliged to publish the "Conditions of use of the railway network" (so-called network statement) and to determine the free capacity of the individual railway sections. Consequently, it is intended to allow non-discriminatory access to railway infrastructure managed by it for railway undertakings from all Member States.

The technical renaissance in rail transport brings innovation in the automation of rail transport through the introduction of autonomous trains and innovative intelligent information systems that communicate with each other and monitor the current situation, sending location data, delays or other restrictions to infrastructure managers, carriers and least, informing passengers themselves. They also provide continuous monitoring of rolling stock and infrastructure.

The aim of the paper is to prove that by automating traffic, or by gradually introducing innovative systems into operation, it is possible, even in the current way of calculating the performance of individual line sections, to achieve improvement and ultimately increase the actual throughput of the lines, thereby rapidly improving the actual operation of the equipment and this will allow new routes to be extended to the current range of transport.

2. Capacity of railway infrastructure and its efficiency

In the process of allocating train path capacity to railway undertakings, it is important for the infrastructure manager to know the infrastructure capacity. Defining the capacity of the railway infrastructure (transport route) is quite difficult and there are many different approaches to its determination. This widely used term gradually replaces the term "permeable efficiency" in our conditions, although in a sense it extends the meaning of the term permeable efficiency. Permeability is defined as the efficiency that is expressed by the number of trains, which can be realized on the railway without reducing the required quality of the train service. The capacity of the railway infrastructure is given by the number of train paths that can be planned for a certain period of time on a certain part of the railway infrastructure with regard to the heterogeneity of the train types and the required quality of the train transport.

3. Current trends for determining the capacity in the world

Many methodologies for determining railway infrastructure capacity are currently used worldwide. Historically, a relatively way of analysing the capacity of railway infrastructure has spread across Europe, which is still used in many countries today. Within Europe, however, the International Railway Union has come up with a decree on the capacity to unify the national methodologies used so far on individual European rail networks, so that the results of the assessment on each part of the corridors are comparable [1]. UIC Decree 406 does not have a direct but recommended character, thus enabling infrastructure managers to use national methodology for their own use.

4. Main principles and methodology of capacity assessment in Slovakia

Efficiency is to be understood as the performance expressed by the number of trains that can still be carried on the railway without reducing the required quality of the train service [2, 3]. Permeable efficiency therefore indicates the number of trains for a period of time, but it is incomplete indication of the spatial relationship. Therefore, the permissible efficiency must be indicated for a particular track section, or most often for a particular intermediate station. When examining and determining the capacity options, and thus also in investigating and determining the capacity of railway infrastructure, it is necessary to bear in mind the operational conditions in which the line operation will be realized. However, since the operation will usually be carried out under stochastic conditions, it cannot be excluded that the operating conditions will be deterministic on a particular line section [4, 5].

4.1. Theoretical and practical throughput efficiency

In principle, permissible efficiency can be divided into theoretical (maximum) and practical.

No time losses are taken into account when calculating the maximum throughput and it is assumed that a device whose permeability is to be determined is only for the activities for which the necessary occupancy times are determined and immediately followed without any loss of time [5].

We determine the maximum throughput based on the relationship:

$$N_{\max} = T / t_{obs}, \tag{1}$$

where $N_{\max}$ is maximum throughput, trains.min^{-1}; T – calculation time (either peak time or full day time frame), min; t_{obs} – the average time taken to carry out the observed technological operation (train ride, train set-up, shunting, etc.), min.

4.2. Permeable efficiency of railway equipment

We determine permissible efficiency on the following railway facilities: main track; station head; station main track.

The track section as a service system in the service process consists of many consecutive and sequential partial servicing operating systems, namely single-line (gap sections) and multi-line systems (switches, railway stations) [6].

As a rule, the efficiency of the individual sub-systems is different and often times it is not enough to compare the throughputs of the individual operating systems and to select the ones with the lowest value and subsequently to declare the throughput of the entire system. This is because, at the moment of the release of the restrictive sub-system, no additional train may be available to re-occupy the section. Thus, there is a time loss by which the computational time decreases, thereby reducing the throughput of the entire sequence of sub-systems. The capacity utilization will be higher the more trains will be in the system and the more station main tracks will be in the stations that limit the limiting section. The efficiency of the gap section depends not only on the operating conditions, but also on the way in which the train drives are organized in this section (parallel or non-parallel graphic, respectively, one-way or two-way Train Traffic Diagram).

4.3. Methodology of Slovak Railway Infrastructure Manager - ŽSR

Methodology can use a graphical method for designed graphics, but it is also designed to determine the throughput performance in forward-looking Train Traffic Diagram in an analytical manner, while clearly defining basic constraining factors as well as the planned range of train traffic (using similar procedures to analytical computation of throughput with probability and mathematical statistics). This is a procedure whereby a limiting intermediate section is determined first, for which the theoretical permeability will be calculated [7].

First, a maximum intermediate section is determined from the analysis of the running times of the calculated intermediate freight trains (*Pn* – category of freight train in Slovakia) in the even and odd directions according to their largest sum in the even and odd directions in the intermediate station.
Subsequently, the appropriate method of transporting the trains and the period of transporting the T_{per} shall be determined. The time period, which is the smallest, expresses the most advantageous way of transporting trains on a track section. This method of transporting trains is then graphically applied in the Train Traffic Diagram to the entire track section for which we detect capacity.

The theoretical permeability is calculated for all intermediate sections and the single train time is expressed as a simple arithmetic mean. The intermediate section with the lowest theoretical permeability becomes the limiting intermediate section for the practical permeability calculation, the value of which is subsequently declared to be the permeability of the entire selected track section.
The period time value is determined by the general relationship:

$$T_{per} = \sum \tau_{r+z}^{Pn} + t_{jN}^{Pn} + \sum \tau_{PI}^{Pn} + t_{jP}^{Pn}, \text{ min}, \tag{2}$$

where T_{per} is duration of one period, from the start of the first event to the cyclic start of the next event of the same character, min; $\sum \tau_{r+z}^{Pn}$ – sum of time surcharges for starting or stopping a running freight train, min; t_{jN}^{Pn} – running time of running freight train in odd direction, min; $\sum \tau_{PI}^{Pn}$ – sum of slots occurring in a certain period for a given train sequence, min; t_{jP}^{Pn} – running time of running freight train in even direction, min.

Average time for one train:

$$t_{obs} = T_{per} / 2, \text{ min}. \tag{3}$$

To calculate the practical throughput, a matrix of multiples of all train categories is constructed, both for the 1st and 2nd train and their possible sequences, for even and odd directions. It is important to know the final number of trains that occur in a given section.

The matrix cells form multiples of these numbers of trains for all their sequences [8].

The next step is to analyse the occupancy times by all train sequences in a similar matrix. The final step is to create a resultant matrix that, identically to the previous ones, contains multiples of the corresponding cells [9]. The sum of all the cells of the resulting matrix is given the time of T_{obs}'', which after dividing by the number of trains we get the time of occupation by all T_{obs}' trains. The total occupancy time for the method of Slovak Railway infrastructure manager is increased by a 10% reserve.

If there is inequality, then the throughput of the track section complies with the range of train traffic and the following indicators characterizing Train Traffic Diagram and infrastructure capacity can be recalculated.

To use this methodology, it is very important to have thoroughly analysed time elements of the train traffic diagram, especially slots, subsequent lap times and driving times.

5. Automation - way to increase infrastructure capacity

Achieving full-fledged automation is only possible under the conditions of modernization of railway infrastructure and safety systems themselves. On the infrastructure for the past two decades, there has been a generation replacement of the interlocking system that allows remote control and centralization of rail traffic management. And in the controlled area with remote-controlled safety equipment, computer support in the area of dispatching decision-making and plant management automation is currently being addressed.

The basic tool for traffic management automation is automatic train path building. Foreign experience clearly confirms the correctness of these steps, since the deployment of remote control equipment and the centralization of computer-aided traffic management have a synergistic effect, in particular:

- growth of permeable track efficiency, which is necessary especially for heterogeneous traffic, where fast and slow freight and passenger trains run along the same track, which is typical for Slovak railways;
- reducing the impact of a human factor on traffic management. Most train conflicts are dealt with exactly, not by the experiences of a transport employee;
- automation of routine activities. Transport employees can focus on major traffic nodes or other important processes and extraordinary traffic situations;
- increasing traffic flow. Increasing travel and section speed of trains, reducing number;
- stopping for traffic reasons, more economical economy of traction energy consumption;
- effective stabilization of the train traffic diagram while eliminating train delays and restrictions infrastructure (slow driving and track closures).

New technologies provide railway infrastructure with information that enables it to increase capacity faster while increasing operational, environmental and safety considerations.

6. Modern safety devices for railway infrastructure

Nowadays, control systems using specialized computers, computer networks and modern communication systems are used to manage railway traffic. The use of such control systems is a prerequisite for the operation of high-speed trains.

One of this system is modern safety device ERTMS comprises trackside and trainborne systems and utilises an in-cab signalling, and automatic train protection element called ETCS (European Train Control System). ETCS is the train control system and GSM-R (Global System for Mobile Communications – Railways) is the new radio system for voice and data communication.

ETCS exists in 3 levels across Europe. In Slovakia provide ETCS Level 1 and in test version Level 2. In the Figure 1, there are shown lines, where the ETCS has been installed in different levels. The main line from Bratislava to Žilina, continuing to Košice, there is level of ETCS 1 and from Žilina to Čadca, there is level 2. Nowadays, ETCS level 1 is used mainly by passenger trains, but not all the locomotives have this system installed in cab. In freight transport, there are many operators, who use locomotives with this system, but majority of them have older locomotives, without this system, they use only the national safety device.

In the Table 1, we can see the differences between the levels of ETCS and requirements to install them. If the level of ETCS is higher, it recommends more technique equipment to build and operate with them. In Slovakia, we use ETCS levels 1 and 2, but level 2 only in test.

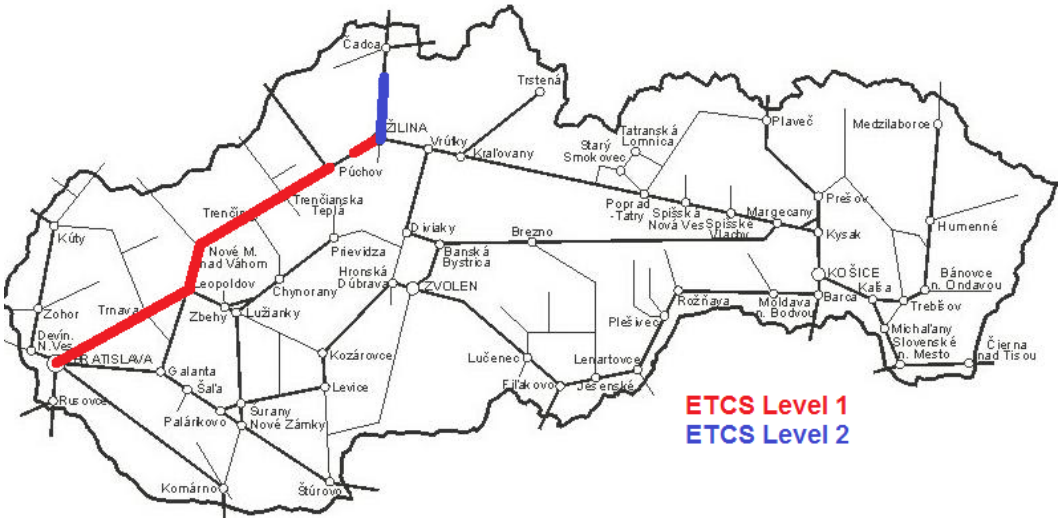

Figure 1. Map of device ETCS in Slovakia.

Table 1. Summary of ETCS Levels and their specifications [10].

ETCS Level 1	ETCS Level 2	ERTMS – regional	ETCS Level 3
Eurobalise without infill	Eurobalise	Eurobalise	Eurobalise
Overlay to existing signalling system	+ euroradio (GSM-R)	+ euroradio (GSM-R)	+ euroradio (GSM-R)
Movement authorities through eurobalise	+ radio block center	+ TCC (traffic controller center)	+ radio block center
Train integrity and position by track circuit	No more trackside Signals Required	+ object controller	Movement authorities through GSM-R
Eurobalise + infill (euroloop, radio, or extra balises)	Movement authorities through GSM-R	Movement authorities through GSM-R	Train position via eurobalise
Overlay to existing signalling system	Train position via eurobalise	Train position via eurobalise	Train integrity onboard
Movement authorities through eurobalise	Train position via eurobalise	Train integrity onboard	Moving block
Train integrity and position by track circuit	Train position via eurobalise	Additional object controller	Moving block
Train integrity and position by track circuit	Train position via eurobalise	GSM-R islands possible	Moving block

6.1. ETCS Level 3

ETCS Level 3 train (Figure 2) transmits its exact position in real time via GSM-R, which significantly helps to instantly reassess the capacity utilization of individual track sections and reduce the necessary technical equipment on the ground [10].

The application level of ETCS Level 3 is in the testing phase, because several problems have been identified in its implementation in practice. One important thing is the detection of the end of the train, which cannot be guaranteed. In the case of passenger transport using units, this doesn't appear to be a major problem, but it is worse for freight trains, where their length and number of wagons change. This is just one of several problems to solve in order to fully apply this level.

In September 2018, ETCS level 3 tests were conducted in Germany to test the functionality of ETCS equipment, both static and dynamic. A motor unit and a diesel locomotive were used for the tests. Both trains followed closely and were fully controlled by computer.

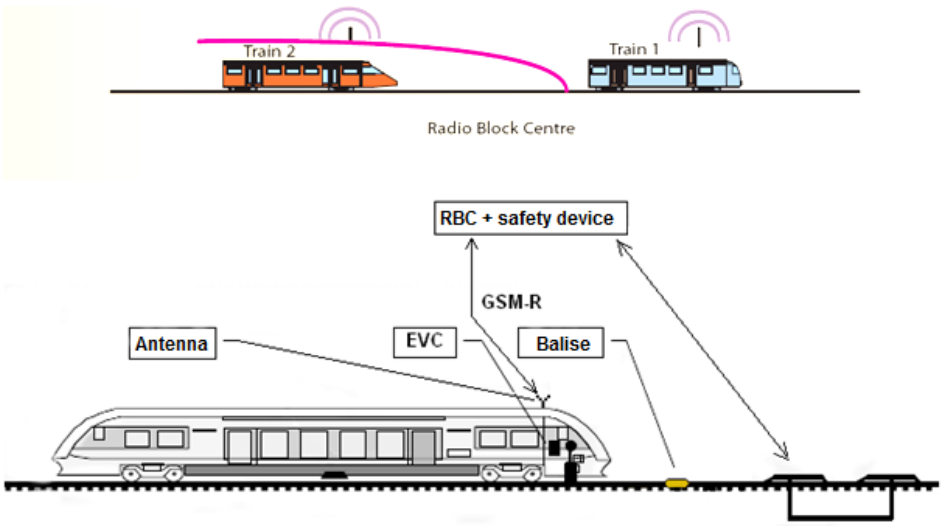

Figure 2. Principle of ETCS activity level 3.

7. Case study of permeable efficiency between Trnava-Bratislava-Rača after installing ETCS

The railway line Trnava-Bratislava Rača is part of the track Púchov-Bratislava. The line is double-track, standard gauge 1435 mm, electrified by alternating traction system 25 kV, 50 Hz. The track section is 38.855 km long; there are five railway stations (Trnava, Cífer, Šenkvice, Pezinok and Bratislava Rača), one turnout (Svätý Jur), three automatic gates (Dolina, Víšok, Vinosady) and two stops (Báhoň, Svätý Jur zast.)

The assessment of the impact of the introduction of ETCS on the performance of railways will be carried out on the mentioned line.

The calculation of the prospective practical permeability in the defined limiting intermediate section according to the ŽSR methodology consists of two calculation tables and one final table. To determine permeable performance without using ETCS, the tables contain three types of computing trains that are divided for even and odd directions. The data shall only be filled in by the first and fourth quadrants, which is the method of transporting the trains in the restrictive section on the double track. In the first quadrant there are values for the odd direction, for the direction Bratislava Rača-Trnava. The fourth quadrant represents an even direction, Trnava-Bratislava Rača.

Input data is shown in Table 2. Meanings of the abbreviations in Table 2 are Os_{ETCS} – passenger trains that pass through all the stations; Os_p – the passenger train without stopping at the station/stop; Os_z – the passenger train which stops at the station/stop; *Pn* – category of freight train in Slovakia.

Table 2. The range of transport, number of trains per day.

Type of train	Os_{ETCS}	Os_p	Os_z	*Pn*
Direction Trnava-Bratislava-Rača	4	19	20	20
Direction Bratislava-Rača-Trnava	3	21	20	20

The numbers of train in both directions were chosen from Train Traffic Diagram 2011/2012, when ETCS started to run.

In order to ascertain the throughput performance of the introduction of the ETCS, it is necessary to classify passenger trains into several types of trains. Trains under the full supervision of the ETCS operate at a specified speed of 160 km/h; they are a specific category of Os_{ETCS} passenger trains that pass through all the stations. But at this case study, we will count the number of the train of Os_{ETCS} and Os_P together in one cell, because there are minimum speed differences. We will work with this data in the Table 3, to count the train sequences.

Table 3. Train sequence counts by Methodology ŽSR.

Methodology ŽSR		Second train	Odd direction (Trnava-Bratislava-Rača)			Even direction (Bratislava-Rača-Trnava)		
First train		Number	Os_p	Os_z	Pn	Os_p	Os_z	Pn
			23	20	20	24	20	20
Odd direction	Os_p	23	529	460	460	-	-	-
	Os_z	20	460	400	400	-	-	-
	Pn	20	460	400	400	-	-	-
Even direction	Os_p	24	-	-	-	576	480	480
	Os_z	20	-	-	-	480	400	400
	Pn	20	-	-	-	480	400	400

The results in individual cells of the even and odd direction are calculated as multiplication between trains. Number of passenger train which regularly stops at the stop Os_z multiplying with number of passenger train which regularly passes the stop Os_p. For instance $20 \times 23 = 460$.

For the Tables 4 and 5 the input data are counted by manager of infrastructure, which has their own Workbook of permeability, where are the exact data for the each of railway line in Slovakia with the critical sections and their time of occupancy. It is very important to say, that time of occupancy is different in both directions. For this case, the critical section is between stations Cífer and Šenkvice. Critical section is section, where the train occupancy is the highest from the whole line.

Due to, that the traffic at this line is heterogeneous, there are several combinations of train movements in the mentioned section, so that it is important to count their time occupancy separately.

Table 4. Time of occupancy of critical section for even direction.

		Second train passes the back station				
		Os_z	Os_p	Os_{ETCS}	N_p	N_z
First train passes the front station	Os_z	6.5	7.5	7	7.5	6.5
	Os_p	3.5	4.5	4	4.5	3.5
	Os_{ETCS}	2.5	3	3	3.5	2.5
	N_p	4.5	5.5	5.5	6	5
	N_z	4.5	5.5	5.5	6	5

Table 5. Time of occupancy of critical section for odd direction.

		Second train passes the back station				
		Os_z	Os_p	Os_{ETCS}	N_p	N_z
First train passes the front station	Os_z	6	6.5	6.5	6.5	6
	Os_p	3.5	4.5	4	4	3.5
	Os_{ETCS}	3	3.5	3.5	3.5	3
	N_p	5	5.5	5.5	6	5
	N_z	5	5.5	5.5	6	5

Meanings of the abbreviations in Tables 4 and 5: Os_{ETCS} – passenger trains that pass through all the stations; *Osp* – the passenger train without stopping at the station/stop; *Osz* – the passenger train which stops at the station/stop; *Pn* – category of freight train in Slovakia; N_p – freight train without stopping at the station; N_z – freight train stopping at the station.

The each time of occupation is filling in the Table 6 according the type of train and direction and these resulting times in Table 6 are used for the making Table 7 as a result of multiplying Tables 3 and 6 together in identical positions.

Table 6. Time taken by train sequences.

Methodology ŽSR		Second train	Odd direction			Even direction		
First train		Number	Os_p	Os_z	Pn	Os_p	Os_z	Pn
			23	20	20	24	20	20
Odd direction	Os_p	23	4.5	3.5	4	-	-	-
	Os_z	20	6.5	6	6.5	-	-	-
	Pn	20	5.5	5	6	-	-	-
Even direction	Os_p	24	-	-	-	4.5	3.5	4.5
	Os_z	20	-	-	-	7.5	6.5	7.5
	Pn	20	-	-	-	5.5	4.5	6

Table 7. Calculation of occupancy time T_{obs}'.

Methodology ŽSR		Second train	Odd direction			Even direction		
First train		Number	Os_p	Os_z	Pn	Os_p	Os_z	Pn
			23	20	20	24	20	20
Odd direction	Os_p	23	2380.5	1610	1840	-	-	-
	Os_z	20	2990	2400	2600	-	-	-
	Pn	20	2530	2000	2400	-	-	-
Even direction	Os_p	24	-	-	-	2592	1680	2160
	Os_z	20	-	-	-	3600	2600	3000
	Pn	20	-	-	-	2640	1800	2400

The sequence of calculation of the performance indicators is as follows:

- Determination the occupancy time;
- Determination the average occupancy time per train;
- Determination the average actual backup time per train;
- Determination of required backup time;
- Determination of the practical throughput performance;
- Determination of the occupancy rate;
- Determination the coefficient of Practical Throughput.

7.1. Determination the occupancy time T_{obs}':

The occupancy time T_{obs}' is calculated as the sum of the fields, separately for the 1st and 4th quadrants.

The next formulas show us the principle of principle of calculation of throughput performance.

The calculated fields of the field values from the first and second tables are identical in the calculation fields.

The results are: $T_{obs1}' = 20\ 750.5$ min; $T_{obs2}' = 22\ 472$ min.

Value T_{obs}' increases by 10% as follow.

$$T_{obs}'' = 1.1\ T_{obs}', \text{ min.} \tag{4}$$

The results are: $T_{obs1}'' = 22\ 825.55$ min.; $T_{obs2}'' = 24\ 719.2$ min.

The increased time is divided by the number of trains (63 trains for odd direction, 64 trains for even direction). N describes the total number of freight trains in one direction.

$$T_{obs} = T_{obs}'' / N, \text{ min.} \tag{5}$$

The results are: Odd direction: $T_{obs1} = 362.31$ min; Even direction: $T_{obs2} = 386.23$ min.

7.2. Determination the average occupancy time per train:

The formula for average occupancy time per train is:

$$t_{obs} = T_{obs} / N, \text{ min.} \tag{6}$$

The results are: Odd direction: t_{obs1} = 5.75 min; Even direction: t_{obs2} = 6.03 min.

7.3. Determination the average actual backup time per train:

$$t_{gaps}^{real} = \frac{T - T_{con} - T_{ex} - T_{obs}}{N}, \text{ min}, \quad (7)$$

where: t_{gaps}^{real} – the actual gap time per train; T – the calculation time for which the throughput is calculated; T_{con} – the time of constant manipulation, T_{ex} – the total time at which the equipment is excluded from operation during the calculation time for the prescribed inspections, repairs and maintenance.

The results are: Odd direction: t_{gaps1}^{real}= 16.15 min; Even direction: t_{gaps2}^{real}= 15.27 min.

7.4. Determination of required backup time according to methodology ŽSR D24:

$$t_{gaps}^{req} = a + b.t_{obs}, \text{ min}, \quad (8)$$

where: t_{gaps}^{req} – the required gap time per train; the symbol a is constant and straight-line directive b is valid for t_{obs} within 5 to 16 minutes and is specified for each column at Table 8.

Table 8. Coefficients for time calculations.

	A	*B*	*C*
a	0.73625	0.420	0.6161
b	0.83147	0.564	0.3370

The time backup is recommended for operating conditions: A – difficult ratios; B – normal ratios; C – simple ratios.

For odd and even direction are fulfilled the condition $t_{gaps}^{real} > t_{gaps}^{req}$ that guarantees the feasibility of GVD.

The results are: Odd direction: t_{gaps}^{req}= 3.66 min; Even direction: t_{gaps}^{req}= 3.82 min.

7.5. Determination of the practical throughput performance of the limiting intermediate zone:

$$n = \frac{T - (T_{ex} - T_{con})}{t_{obs} + t_{gaps}^{req}}, \text{ trains/days}. \quad (9)$$

The results are: Odd direction: n_1 = 146 trains/day; Even direction: n_2 = 140 trains/day.

7.6. Determination of the occupancy rate:

$$s_o = \frac{T_{obs}}{T - (T_{ex} + T_{con})} \quad (10)$$

It doesn't have own parameter. It indicates only amount. A sufficiently busy Train Traffic Diagram is considered to have a degree of occupancy of 0.5-0.67.

The results are: Odd direction: s_{o1} = 0.26; Even direction: s_{02} = 0.27.

7.7. Determination the coefficient of Practical Throughput:

$$K_p = \frac{N}{n} 100, \%, \quad (11)$$

where K_p is coefficient of utilization of practical permeability; N – total number of trains in even and odd direction; n – number of trains in even and odd direction per day.

The results are: Odd direction: K_{p1} = 43.15 %; Even direction: K_{p2} = 45.71 %.

Table 9 shows the resulting values of the examined indicators. Permissible performance has been established for situation before installing ETCS and after installing ETCS. The situation after the introduction of the system was investigated under the conditions of Train Traffic Diagram 2011/2012, when 7 trains of the IC category run under the complete supervision of the ETCS system on the examined section of the Bratislava Rača - Nové Mesto nad Váhom line.

Table 9. Resulting performance indicators for a 24-hour calculation period.

		Before installing ETCS		After installing ETCS – current state		After installing ETCS – full use	
		Odd direction	Even direction	Odd direction	Even direction	Odd direction	Even direction
Occupancy time, min	T_{obs}	362.31	386.24	358.64	381.26	345.04	350.76
Average occupancy time, min	t_{obs}	5.75	6.03	5.69	5.96	5.48	5.48
Real backup time, min	t_{gaps}^{real}	16.15	15.28	16.21	15.61	16.43	16.08
Required backup time, min	t_{gaps}^{req}	3.66	3.82	3.63	3.78	3.51	3.51
Occupancy level, min	s_o	0.26	0.28	0.26	0.28	0.25	0.25
Coefficient of practical permeability utilization, %	K_p	43.15	45.71	42.56	45.39	41.17	41.83
Practical throughput performance, trains/days	n	146	140	148	141	153	153

8. Conclusion

Subsequently, a situation that assumes full use of ETCS has been examined. In this case, all InterCity, Fast trains and Regional Express passenger trains would travel under the full control of ETCS and their specified speed is 160 km/h. It is irrelevant for the calculation of the throughput whether the passenger trains drive under the supervision of the ETCS system, as these trains stop at all railway stations and at the stops on the track section under investigation.

For short distances between stops passenger trains continue to operate at the highest rated speed of 120 km/h.

Freight trains of all categories are running at the same speeds as before the introduction of ETCS, due to the design characteristics of freight wagons.

The limiting section was re-examined when determining throughput. After reallocating the number of passenger transport trains, the calculating train became a costly passing train to determine the limiting section. The highest occupancy time of the intermediate station is again between the railway station Cífer-Šenkvice.

The aim of modern railway signalling and safety systems is to ensure that trains can safely drive in close proximity. Their application will increase the safety of rail transport and the throughput capacity of railway lines. Significantly reduces the number of driver-related accidents, improves track performance and throughput, thereby reducing segment occupancy time and allowing trains to run in close proximity and reducing energy consumption due to better track knowledge.

Acknowledgements
The paper was supported by the VEGA Agency, Grant No. 1/0019/17 "Evaluation of regional rail transport in the context of regional economic potential with a view to effective use of public resources and social costs of transport", at Faculty of Operations and Economics of Transport and Communication, University of Žilina, Slovakia.

The paper is supported by the VEGA Agency within the Project 1/0509/19 "Optimizing the use of railway infrastructure with support of modal split forecasting“ that is solved at Faculty of Operations and Economics of Transport and Communication, University of Žilina.

References

[1] Gasparík J Abramovic B and Halas M 2015 *New graphical approach to railway infrastructure capacity analysis* (Split: Promet-Traffic and Transportation) pp 283–90
[2] Gasparík J Abramovic B and Zitricky V 2018 *Research on dependences of railway infrastructure capacity* (Osijek: Tehnickivjesnik) pp 90–95
[3] Gašparík J Blaho P 2016 *Technológia železničnej dopravy líniové dopravné procesy* (Žilina: EDIS – vydavateľské centrum ŽU) p 383
[4] Cerna L Luptak V Sulko P and Blaho P 2018 *Capacity of Main Railway Lines–Analysis of Methodologies for its Calculation* (Dubrovnik: Nase more) pp 213–17
[5] Dolinayova A Nedeliakova E 2010 *Prognózovanie pre manažérov dopravy* (Žilina: EDIS – vydavateľské centrum ŽU) p 147
[6] Buček O and coll. 2002 *Transformácia železníc vo svete* (Žilina: EDIS – vydavateľské centrum ŽU) p 159
[7] Nedeliakova E.Sekulova J 2016 *Dynamické modely kvality služieb* (Žilina: EDIS – vydavateľské centrum ŽU) p 115
[8] Lizbetin J Ponicky J and Zitricky V 2016 *The throughput capacity of rail freight corridors on the railway network* (Dubrovnik: Nase more) pp 161–9
[9] Halas M 2014 *Progressive procedures for the detection of railway infrastructure capacity*. (University of Žilina: Disertation thesis) pp 78–83
[10] Kapsch Carrier Com *European Railway Traffic Management System – ERTMS* KCC 7414-01 EN 1202 White Paper

A survey on needs and possibilities of training in acquiring "Train dispatcher" qualification

Mirena Todorova[1], Teodor Kirchev and Kostadin Trifonov

Todor Kableshkov University of Transport, 158 Geo Milev Str., Sofia, Bulgaria

[1] E-mail: mirena_todorova@abv.bg

Abstract. A train dispatcher is a person who manages and controls the movement of all trains within the dispatching section, coordinates the operation of the stations and ensures the proper regulation of the movement of trains in violation of the "Train Running Schedule", take prompt and operational measures to ensure the carriage of passengers and goods. In order to determine the need for training to occupy the position of "Train dispatcher", a questionnaire was drawn up aimed at the companies in need of such staff. The report presents the results of this survey, the questions of which are grouped into three sections. The first section "Identification" is intended for collecting general information about the place of work of the interviewed, the second "Conducting training" specifies its form and manner and the third section "Teaching content" defines the scope and timing of the topics covered in order to obtain the necessary knowledge, skills and competences. The conclusion from the analysis of the results of the questionnaire is that the training can be carried out in the form of specialization/courses or as additional courses and qualifications at the Master's degree program.

1. Introduction

The realization of trains' movement schedule is done by Direct Traffic Control System (DTCS) on traffic processes in the railway and underground network. The movement of trains and other railway vehicles is managed by train dispatchers, with the help of a power box and the on-duty signalmen in stations [1].

Department of Technology, Organization and Management of Transport (TOMT) and University of transport "Todor Kableshkov" are specialized in the training of staff for the management of different types of transport. Many projects, during the years, have elaborated on the dispatchers' management problems and have given training opportunities for signalmen and dispatchers [2-4]. The last project in this particular area: "Interactive WEB-simulator for situational environment and signalling in transport movement simulation", was developed in 2003 [5]. The means and methods for traffic management have thoroughly changed in the last 15 years, and that identifies the need of a new project – "Simulation model of underground and railway block power box – Simulator". One of the aims of the authors developing the project is to identify the need of training for the post "train dispatcher", as well as the form and contents of this training.

To achieve this goal, the project team needs feedback from the staff, of the railway infrastructure and transport companies serving the DTCS, regarding knowledge, skills and competences, as well as the need of training for the "train dispatcher" qualification. In order to acquire this information a short questionnaire was developed, aiming the examination of the staff training needs, in terms of the whole spectre of participants in the transport sector [6-8].

The questions are grouped in three sections. First section "Identification" is designed for gathering the general information for the interviewees' workplace (their position and education). The second section "Training Session" determines the form of conducting the training [9]. The third section "Learning content" determines the scope and hourly distribution of the topics listed for acquiring the needed knowledge, skills and competences. In sections two and three, the interviewees can give their opinions, proposals and recommendations [10, 11].

2. Result analysis of the questionnaire

In "Identification" section, the following data was gathered:

The number of interviewed people is 110. The interviewees are from companies executing transport management and planning, and can be summarized as follows (figure 1):

- 65% of the interviewed are employees of National Railway Infrastructure Company (NRIC), where dispatcher control is used in all railway blocks, but DTC is available only for 3 sections.
- Around 25% work in "Metropoliten Sofia" – traffic management is conducted by means of DTCS;
- The rest 6% work in railway transport companies as "BDZ passenger transport", "BDZ freight transport" and "DB Cargo Bulgaria", where they rely on planning the railway activity and operational management of train movement;
- Four lecturers from University of Transport "T. Kableshkov", training the students for the certification "Signalman".

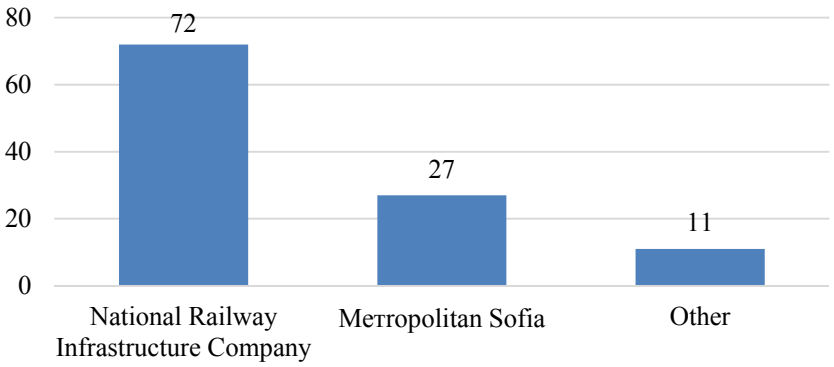

Figure 1. Companies in which the interviewed work

People employed as train dispatchers have acquired their qualification and educational level at different stages of their life. It is important to gather the data about the preferable form of training for the future trainees. The structure of the interviewed educational level is shown in figure 2.

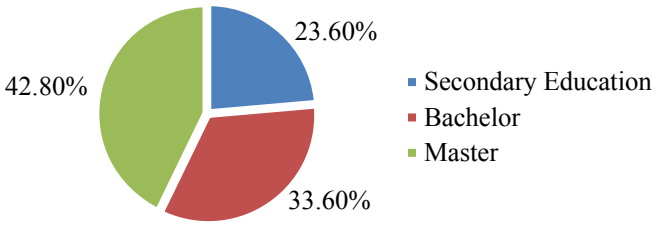

Figure 2. Educational level.

Most of the participants in the study work as train dispatchers - 46%, and 9% are mid-level managers as Senior dispatchers, Shift managers, Station master etc. 35% are on-duty managers and the rest 10% are other employees in the sphere of railway transport, having the professional qualification "Signalman" and lecturers-experts in the preparation of training programs and process (figure 3).

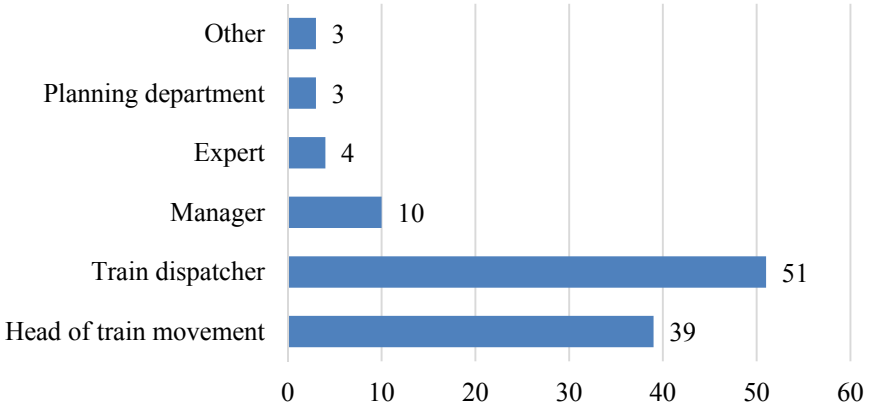

Figure 3. Position.

In the next section "Training session", to the question whether a training is needed, none of the interviewees answered that it is unnecessary and only two answered that it is needed in a particular area. Regarding the training form for the qualification acquisition, 55 people answered "specialization" which is normal for employees wanting to upgrade their competence (figure 4). Moreover, many of the train dispatchers, which does not work with DTCS want to become acquainted with this work method in the form of one week specialization. The interviewees could answer positively to this question if desired.

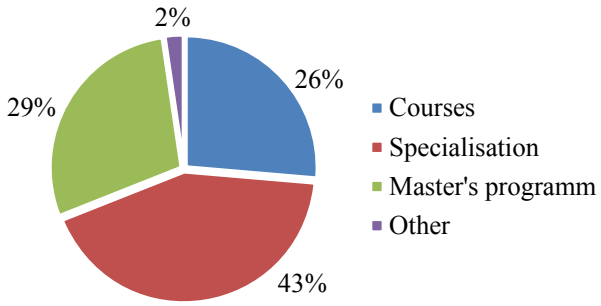

Figure 4. Organization of training for acquiring "train dispatcher" qualification.

Another important issue is the form of the training and the leading answer (51%) is full-time training – 8 hours every day. Part-time evening training is not preferable as the shifts in railroad transport are 12 hours. 15% of the interviewed chose other types of training, as the "block training" – two days a week is the most preferable among them (figure 5).

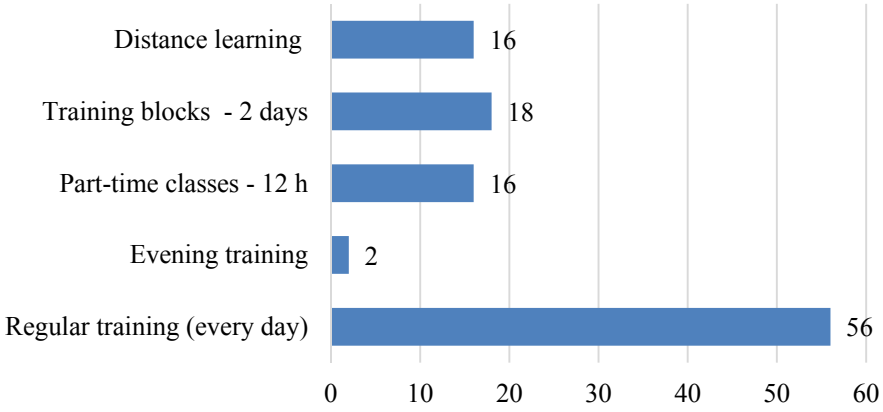

Figure 5. Method of training sessions.

The research traced in the third part the knowledge areas that is considered the most important and their distribution in the common share of learning hours (figure 6):

- Obligations of the train dispatcher to ensure the movement of the trains;
- Acceptance and submission of duty to get acquainted with the requirements and documents;
- Planning and management of train movements to ensure a safe meeting and scheduling. This topic covers the largest part of the activities and the dispatcher's workloads –control of signals and indicators, communication with the duty managers, providing monitoring and coordinating of train movements;
- Familiarization with dispatch centralization – buttons, menus, commands and mode of operation
- Actions taken to manage unexpected events and emergencies, depending on their type;
- Ensuring movement in organizing repair activities. Carrying out the preliminary planning. Prior planning shall be carried out prior to commencement of an order for manoeuvre or service train, but it is essential for efficient train management;
- Interpersonal skills and stress management (e.g. fatigue management). These skills are becoming increasingly important in the work of the train dispatcher, as dispatchers communicate with different departments and many individuals and face a wide variety of work-shift situations. In this way, it should also focus on those goals that are aimed at personal and life skills.

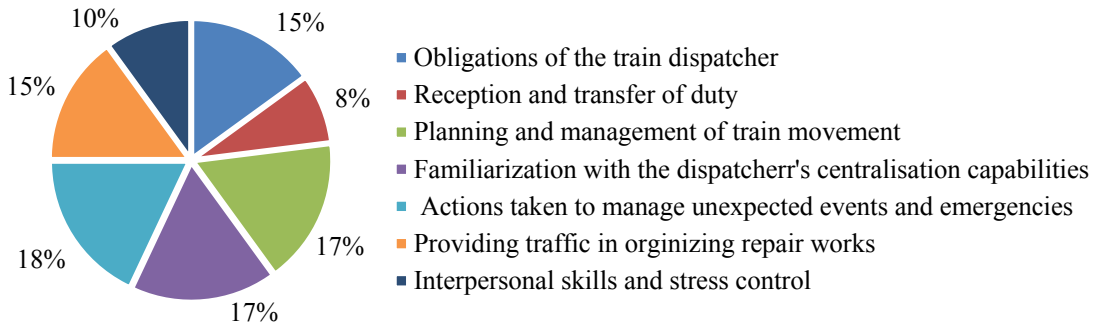

Figure 6. Main topics of training.

Some of the survey participants recommend that the following topics be included in curriculum development:

- Familiarity with the characteristics and the peculiarities of rolling stock;
- Ensuring connections at interchanges with passenger trains;
- Priority for passing trains.

It is also suggested to include psychology, but this area of study is part of the topic on "Interpersonal skills and stress management". It is recommended to increase the hours considering "Actions taken in the management of unexpected events and emergencies".

The survey identifies three types of hands-on training to achieve a good level of learner knowledge for the operation of dispatch centralization and their distribution is given in figure 7:

- Seminar exercises in which to consider the sequence of operations under predetermined traffic conditions and the state of the dispatching signalling. Case management should be developed in different traffic disruptions and emergencies;
- Gaining practical skills by operating a simulator. The simulation model for DTCS is a simulator for operational dispatching of train movement on a service section. The simulator should be a set of microprocessor equipment that provides performance of the functions of the train station automated workplace and information exchange on the activities performed;
- Work in a real workplace where the practical examination for qualification will be held. The jobs of train dispatchers are concentrated in the control room, the areas of activity are formed on a geographical basis – on dispatch circles.

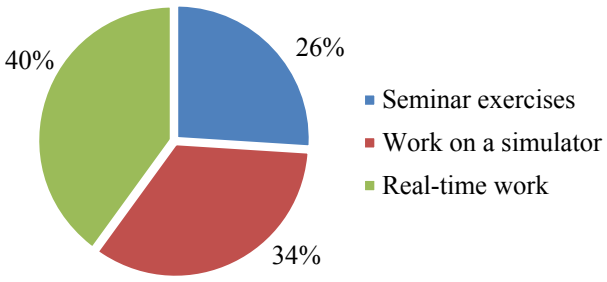

Figure 7. Distribution by type of practical training.

As an alternative to the duration of the training period are given the options 180, 240 and 300 hours. The average value for this duration is 252 hours, so it can be determined that it will be 240 hours. This means that 96 hours of full-time work placement must be ensured after pre-employment contract with the respective company – National Railway Infrastructure Company or "Metropolitan Sofia".

As a basic requirement for the trainees given in the survey, they must have experience as a movement leader. Currently, train dispatchers at the Metropolitan can become duty managers with five years of experience and level of education degree "Bachelor" TOMT.

3. Conclusion

The train movement is realized through a centralized system for dispatching and control of the transport processes in its stations and sections. The train dispatcher must know and use the control and command and control systems and manage all traffic operations in one section.

Based on the research done, it is necessary to develop a curriculum that includes a theoretical and practical part. The subjects in theory should be studied in the following subjects: duties of train dispatcher, reception and transfer of duty, planning and management of train movements, familiarization with dispatch centralization capabilities, actions performed in the management of unexpected events and emergencies, providing movement in organizing repair activities and interpersonal skills and stress management. The practice will consist of three types of exercises – seminars, work on a simulation simulator for traffic management and work in a real workplace, which will take place and the relevant State Qualification Exam for the acquisition of the professional qualification The training can be carried out in the form of specialization/courses or as additional courses and qualification in the Master's degree program "TOMT".

References

[1] Kirchev T 2017 Modelling and management of traffic in operational conditions *VTU T. Kableshkov* 134

[2] Kirchev T, Georgiev N and Stoyanov I 1992 Use of video computer systems to simulate the actions of the duty officer in ensuring the movement of trains *III Scientific and Technical Session – VTU*

[3] Raykov R, Kupenov D, Ujdrin G, Danchev A, Georgiev N, Berov T, Manchev I, Hadjiev E and Vermezov R 1994 Project for train complex for train dispatchers and trainers – computer based movement *Railway Transport Magazine* **3** 10–15

[4] Dimirova E and Dimitrov V 2013 SCADA train control system – laboratory simulator *Scientific Papers of the University of Rousse – 2013 ISSN 1311-3321* **52** 91–95

[5] Dimitrov D and Kirchev T 2002 Using a Web-oriented toolkit in training in the dispatching manual of transportation operations *Proc. XII Sci. Conf. Int. Part. TRANSPORT-2002* 475–8

[6] Trendafilov Z 2018 Perspectives on the vocational training of traffic managers and train dispatchers in rail transport *Mechanics Transport Communications Magazine* **16(3/1)**

[7] Dimitrov D and Trendafilov Z 2018 About the need for performing training and increasing the qualification of dispatchers and movement managers in railway transport *Int. J. Innovative Technologies in Economy* **5(17/2)**

[8] Corman F 2010 Real-time railway traffic management: Dispatching in complex, large and busy railway networks *TRAIL Thesis Series T2010/14 the Netherlands TRAIL Research School ISBN 978-90-5584-133-2*

[9] Gertler J and Nash D 2004 Optimizing staffing levels and schedules for railroad dispatching centers *National Technical Information Service, Springfield, VA 22161*, *DOT/FRA/ORD-04/01, www.fra.dot.gov*

[10] Lixiao H, Cummings M and Nneji V 2018 Preliminary analysis and simulation of railroad dispatcher workload *Proc. Human Factors and Ergonomics Society 2018 Annual Meeting* 691–5

[11] Reinach S, Gertler J and Kuehn G 1998 Training requirements for railroad dispatchers: Objectives, syllabi and test designs *National Technical Information Service, Springfield, VA 22161, DOT/FRA/ORD-98-08*

12th Conference Announcement

BulTrans2020

10-13 September 2020
Sozopol, Bulgaria

Conference Topics

Aeronautics
Automotive Engineering and Technologies
Dynamics, Strength and Reliability of Vehicles
Internal Combustion Engines and Alternative Fuels
Railway Engineering and Technologies
Transport Infra-Structure
Transport Management and Logistics
Water Transport

www.bultrans.org